

Responses to (in italic font):

Interactive comment on “Representing methane emissions from wet tropical forest soils using microbial functional groups constrained by soil diffusivity” by Debjani Sihi et al.

Anonymous Referee #1

Received and published: 22 August 2020

The study “Representing methane emissions from wet tropical forest soils using microbial functional groups constrained by soil diffusivity” by Sihi et al. tries to explain soil methane emission dynamics in tropical forest soils of Puerto Rico during normal and drought conditions. They combine field measurements with modelling efforts (Microbial Model for Methane Dynamics-Dual Arrhenius and Michaelis Menten (M3D-DAMM)). Overall, I think it is a really nice study that tries to combine microbial with biogeochemical data to investigate ecosystem methane dynamics. However, I have some general and some minor comments.

Thank you kindly for the positive comments and for the constructive suggestions that really strengthened our paper.

The authors should describe the concept of “microsites” more in detail. The authors focused on the top 10 or 10-30 cm of their Ultisol although methane production/consumption dynamics in the deeper clay-accumulating horizons may be more important for the overall net methane emissions from their Ultisols. The authors do not discuss that and do not compare with other soils. How does the abundance of microsites change with soil type, soil depth and other ancillary variables?

Our sampling strategy, both of soils and of soil water, are geared to accompany the greenhouse gas flux measurements which are taken on the soil surface. Past studies (Silver et al. 1999) have taken methane concentrations at depth in similar soils, and found that concentrations are higher at 10 versus 35 cm. Examination of the soils in the Luquillo mountains have found that SOC maximums are around 35 cm depth (Johnson et al. 2014). For this site, clay is abundant at shallow depths, e.g., 20-30% clay at 0 to 10 cm depth (L177). Therefore, we designed our sampling strategy for shallow depths. We added text and the Johnson citation to a revision to ensure readers also understand this concurrence of sampling strategy and past observations (L189-194). Thanks for pointing this out; adding these details helps the manuscript.

There are no specific measurements of microsites at any depth at this site; microsites are inferred because of many observations of co-occurrences of oxygen concentrations in the soil along with CH₄ fluxes; and because of the rich clay, iron oxides, and visible redox mottling, particularly evident in the valley and slope soils (papers cited in L111-134). Techniques for measuring microsite activities remain very limited to date, here or elsewhere (L134). We added this information to in a new methods section 2.4.3 devoted to microsite modeling (L457-462).

We will address the issue of comparison to other soils in response to a more detailed question below.

Minor comments: L22-25: Is it important to give this information? I would only include the most significant ones that support your guiding questions! What is the difference between “<” and “«”. The abstract should self-explanatory.

Good point thank you. We simplified the abstract and the manuscript throughout by using only < or >; it was a subjective difference between “<” and “<<”. The geochemical parameters in L23-25 were measured and are key model inputs, so we rephrased to say they were measured at the field site, but we removed the parenthetical material regarding differences in their values with respect to topographic

positions which is not germane to the abstract.

L33: write acetoclastic methanogenesis instead of “acetotrophic” and “acetoclastic” (check the whole manuscript)

Thank you for catching these typos; corrected as suggested.

L43: what are wet tropical forest soils? What are wet tropical forests and what is the difference between wet tropical forest soils and upland soils? How do you define that? *The soils are classified as wet tropical forest soils according to the Holdridge life zone system, which considers rainfall, elevation, latitude, humidity, and evapotranspiration, as described specifically regarding the Luquillo Experimental Forest (Harris et al. 2012). Upland refers only to topography. The soils in our current study (including the valley soils) could be referred to as “upland” in that they are all located in a lower montane region (~350 m elevation). We added the Harris citation and a description of what is meant by “wet” tropical forest soils to the methods (L156). See also L88 that mentions that upland tropical soils can produce methane.*

L53-65: What are the soil types in the different studies? Since methanogenesis and methanotrophy are substrate-limited, the soil type with its specific biogeochemistry is very important. The authors mention that there are several studies that report effects of drought on net methane emissions across different wet tropical forest soils. Consequently, they should mention the different soil types.

We added the soil type (below) when the studies were mentioned in L97-105 and elsewhere as relevant.

Aronson et al. 2019 (Costa Rica) Oxisols

Davidson et al. 2004, 2008 (Brazil) Oxisols

Wood and Silver 2012 (Puerto Rico) Ultisols with a similar climate and parent material

O’Connell et al. 2018 (Puerto Rico) Ultisols, same soils as current study

L66-74: Oxygen may not be the only factor for methane emissions upon rewetting. The observed rapid flush of methane in response to a wetting event may be driven by rapid depletion of other electron acceptors, as well. The major focus of this paragraph is on oxygen but what is with acetate, H₂ and CO₂?

We concur with the reviewer’s suggestions; in fact, that is part of the reason we initiated this study. We wanted additional data on acetate concentrations, and to use a predictive model to better understand the conflicting/collaborating roles of oxygen, substrate, and microbial biomass in controlling methane emissions. In the revision, we clarified the role of these different substrates in controlling methane emissions in this paragraph so it does not appear we are only focused on oxygen. We also discussed their availability in terms of soil moisture and diffusion limitations (L113-125).

L85-86: and why not H₂ and CO₂? How do you account for acetate formation during fermentation and homoacetogenesis? How do you account for syntrophic acetate oxidation? How can you explain the “contrasting patterns of observed CH₄ emissions”, when sources and sinks of acetate etc. is not measured or simply not known?

Here, we use the model to provide quantitative answers in accordance with specific hypotheses stemming from the O’Connell et al. 2018 paper. The idea of this paper is to consider a relatively simple set of mechanisms and see how well a model that quantitatively represents these mechanisms can explain the complex observations. This study used a model where the production of methane is modeled by acetoclastic and hydrogenotrophic mechanisms only, and consumption by methanotrophy. Acetate is based on measurements of soil water. There are not measurements to constrain H₂ concentrations, but CO₂ concentrations in water are estimated according to the pH. Acetate is formed by fermentation and by homoacetogenesis as defined in Xu et al. (2015) in Eq A15 and 16 in their appendix, see also our revised Fig. 1b and caption. There is a pH feedback to acetate production that affects methanogenesis (Eqn 7) that is also described in Fig 1b caption. The model is not completely comprehensive and syntrophic acetate oxidation is neglected. In modeling, we balance parsimony and mechanisms and data limitations; we have made choices here mostly following the original model design (Xu et al. 2015). We describe the impact of some neglected processes in Section 4.3. We added that homoacetogenesis is included and that syntrophic acetate oxidation is neglected in the methods Section 2.4.1 in the revision (L280-281).

L97-105: The dominant soil type in the current study is Ultisol. I guess the whole

methane cycling will be very different in other tropical soils (What is with Oxisols?) What are the soil types in the other studies mentioned in the introduction? It would be great to see a more detailed description of the soil type. How did bulk density change with depth? At what depth does clay accumulation (subsurface zone) start? How big is the eluvial horizon?

The response to this comment also includes response to the first detailed review comment (request for comparison to other soils). The soil types of the other tropical studies of methane releases from the introduction are mentioned in a reply above. The studies in Costa Rica and Brazil on Oxisols were specific in showing that methane consumption was the major effect of the seasonal El Niño cycle (Costa Rica) or imposed drought manipulation (Brazil), which was similar to here. Only the O'Connell et al. (2018) study showed the enhanced release of CH₄ during post-drought recovery. We cannot say for certain if the O'Connell observations are related to soil type. Oxisols, because of their high oxide and clay contents, may also have microsites. In particular, hematite clay minerals (found in both soil types) enhances formation of soil aggregates because of their high surface area and charge properties. Soil organic matter can also enhance aggregation and at the same time consume O₂. So we added a statement in the introduction (with the soil type mentions) to note that these mechanisms for aggregate formation might also lead to anaerobic microsites in Oxisols and Ultisols (L131-134).

We have data on bulk density up to 1 m that are in press with Ecology and Evolution (K. Cabugao et al., in press). In that manuscript we find that on the surface, bulk density ranges from 0.5 to 0.7 g/cm³. By 25 cm depth, bulk density is 0.8 to 1.1 g/cm³. These results are similar to those published by Johnson et al. (2014) and Silver et al. (1999) at nearby sites in the same forest. See L185-185.

A publication that provides a detailed soil survey in the immediate vicinity of the field site (Soil Survey Staff, 1995) lists the following soils: Zarzal, Cristol, and Prieto soils. For all soils, the litter layer is minimal due to very rapid litter decomposition rates (Parton et al. 2007, Cusack et al. 2009). For the Zarzal soil, the surface (A) horizon is usually 4 cm thick, and the B horizon is around 150 cm thick. The Cristol soil surface horizon is listed as 6 cm thick, and B horizon to around 150 cm thick. The Prieto soil surface horizon is listed as 6 cm thick, and B horizon to around 130 cm thick. We added this information and the citation to the site description (L181-183).

L107: Why was soil only sampled from the top 10 cm of the soil? I guess methane consumption dominates at the surface due to oxic conditions while in the deeper soil horizons methane production dominates due to more anoxic conditions.

These soils are very rich in clays with high NPP and high surface C inputs (Weaver and Murphy, 1990), beginning at the interface with the atmosphere, and are often very wet, and many lab- and field-scale studies by the Silver group (see various citations in the manuscript) confirm that methane production can occur in soils at shallow depths, especially in the valley soils and to a lesser extent in the slope and ridgetop soils. The soil flux chambers are on the soil surface and the sampling strategy was designed to focus on near-surface measurements that are relevant to surface monitoring, as described above and in another comment response below.

L111-114: What was the detection limit for acetate?

We assumed it was equivalent to the lowest standard by HPLC analysis, i.e., 0.5 μM.

L117-120: The chemical data (what chemical data? Only pH?) for bulk soil is from the 0-10 cm soil depth and acetate and DOC from the pore water from 10-30 cm soil depth? I do not understand how you relate this information, taken from different soil depths, to each other. Finally, where do you find or where do you assume these microsites? (only in the top 10 cm or below? Or may be even below 30 cm?)

We assume that soil flux chambers placed on the top of the soil surfaces are dominated by fluxes from relatively shallow depths. A summary of fluxchamber methods by two experts in this field states that it is usually assumed surface chambers measure fluxes from about 25 cm in depth (Rochette and Hutchinson 2005). Given this perspective, we collected soil and soil water measurements from the 0 to 30 cm depth to best relate to surface flux chamber measurements. The chemical data used in this study consisted of acetate and DOC from the lysimeters located at a minimum depth of 5-10 cm and a maximum depth of 25-30 cm (the lysimeters are 5 cm in length). The soil samples on which pH were measured were collected from 0-10 cm depth. See L189-194 and L259.

Microsites are inferred by observations such as originally presented in O'Connell et al. (2018), i.e., sudden releases of methane during post-drought recovery; and from seminal publications such as Silver et al. (1999). In the latter, co-occurrences of soil oxygen and methane in bulk soils presume the abundance of anaerobic microsites in the soils. Because the soils have abundant clay and iron oxides at all depths, it is likely that microsites are pervasive throughout. This has also been observed repeatedly in soil incubation studies using surface soils from this. See section 2.4.3.

L144-148: What is with methylotrophic methanogenesis. You should discuss about the potential contribution of methylotrophic methanogenesis (see Norrow et al. 2019). *Our model does not include methylotrophic methanogenesis. We will add this to the mention of several other processes not considered in our model in Section 2.4.1 and cite the relevant paper (L282).*

L173-174: Why not?

We believe the reviewer is asking why iron reduction and oxidation are not included in this study. As explained in L300 in the methods and in Section 4.3, we chose to take a more simplified approach to start, just focusing on substrates and microbial functional groups for methanogenesis (both acetoclastic and hydrogenotrophic) and methanotrophy. We feel that our model does a reasonable job at reproducing the data, considering "normal" and "drought" conditions, and involving two different time frames of data collection, and we consider that as confirmation of the validity of our approach. We acknowledged in Section 4.3 that iron reduction can alter the pH of the soils and soil water and enhance methane emissions; and that iron reduction can also support anaerobic methane oxidation, as well as using acetate as a substrate and thereby reducing net methane emissions. We acknowledge that our model fits are not perfect, as you can see from Fig 3, the model misses the highest methane fluxes seen during the post drought. This could be a result of not considering the pH effects of iron reduction that enhance methanogenesis. However, other processes in the iron cycle reduce methanogenesis, so the benefit of including unconstrained iron cycling processes is unclear without additional information to constrain the model. Therefore, we felt it was appropriate to focus only on the mechanisms covered in this study.

L206: Why 15 cm?

This is the average depth sampled (ranges from 0 to 30 cm).

L214: How do calculate "total microsites"? I would assume that there are way more microsites in clayey horizons below 15 or even 30 cm soil depth? Overall, I think you have to explain the concept of microsites, more in detail? You are scratching only the soil surface at the moment but in my opinion the biggest methane production potential occurs in deeper parts of the Ultisol.

A seminal study in 1999 by Silver et al (cited in our manuscript) in a nearby Ultisol soil took measurements of methane and oxygen at 10 and 35 cm depth, as well as surface chamber flux measurements. The authors found that CH₄ concentrations were higher at the shallower depths. Most of the subsequent papers from Luquillo Experimental Forest used surface chamber measurements and focused on shallow soil depths, pls see L189-193 We surmise that perhaps diffusion would be quite slow at greater depth in these rich clays, that substrate (SOC) availability which is maximum at 0-30 cm would also be lessened, and that microbial biomass would be lower (Hall et al. 2016). Therefore, we focused on shallow depths.

We assumed that size of the microsites should be at least an order magnitude lower than the bulk soil measurements we had for soil CH₄ fluxes. Using this logic, we decided that "diameter" of microsites should be in "mm" scale as the diameter of soil chambers we used are in "cm" scale (15.24 cm). Thus, we did the math to come up with the number of "total microsites" (i.e. 10000) such that the diameter of microsites below each chamber meets our criteria, following Sihi et al. 2020a. We added this to the methods Section 2.4.3.

L270-272: Why are acetate and hydrogen production decreasing when acetoclastic and hydrogenotrophic methanogenesis also decrease? Acetoclastic and hydrogenotrophic methanogens consume acetate and hydrogen, respectively. So, if there is a decrease in acetoclastic methanogens, I would first assume an increase in acetate concentration and thereafter a sharp decrease if oxygen levels further increase.

Good catch, thank you, the cause and effect in that sentence was inverted (L611). It

now reads: "Simulated decreased production of acetate and hydrogen during the 2015 drought in the ridge and slope positions resulted in decreased biomass of aceticlastic methanogens and hydrogenotrophic methanogens (Figs. S5, S6)."

L280: How do explain that?

We believe the reviewer is referring to predicted changes in the biomass of different microbial functional groups during drought, drought recovery, and post-drought. These are model predictions, that are based upon the mechanisms within the model, and the input data that constrains model behavior (pH, acetate, DOC, and CH₄ fluxes). Although we lack measurements of the microbial biomass of specific microbial taxonomies or functional groups during the events in this paper (as we acknowledged), microbes can respond rapidly to changes in their environment. It is important to distinguish that the model is predicting changes in biomass of a particular microbial functional group and is not predicting large changes of the bulk microbial biomass in the soil. Bulk microbial biomass in the soil is likely to double or perhaps quadruple in response to changes in conditions, but individuals can grow exponentially (Goberna et al. 2010; Pavlov and Ehrenberg 2013; Roussel et al. 2015; Buan 2018). Please see L866.

L286-287: Why does the increasing production of acetate lowers the pH?
Acetate production is a source of proton (Eq 7 and Fig. 1).

L301-306: If the diffusion of H₂ increases during drought, one may think that hydrogenotrophic methanogenesis should increase as well. However, it does not increase because of increasing oxygen levels. That should be made clear!
This is true, particularly for the ridge and slope soils, please see clarification in L657 in Section 3.3. It is somewhat less true for valley soils, L669, so no changes were made there.

L304-309: The diffusion of acetate increases upon rewetting but that of H₂ decreases. Why do you observe an increase in overall gross methane production. First, I would assume that under relatively acid conditions, hydrogenotrophic methanogenesis dominates. I think the overall increase of methane emissions upon rewetting is because of oxygen depletion and therefore the stimulation of methanogenesis in general and not because of increasing acetate concentrations or a shift in the methanogenic pathway of methane formation. If it is really aceticlastic methanogenesis that is stimulated, you should provide some isotopic data. There is competition for acetate between several microorganisms. In the end it could be simply stimulation or inhibition of fermentation or homoacetogenesis that drives changes in the amount of observed acetate concentrations.

The main issue is that CH₄ emissions are not normally found in the ridge and slope soils (eg, see 2016 data), so a response of a simple increase in methanogenesis cannot explain the observations. The mechanism of hydrogenotrophic methanogenesis does not well explain the observations because as the soils wetted, hydrogen gas would become less available as its diffusion rate will decrease strongly (Fig. S8). Further, the turnover rate of H₂ in shallow soils is very high, so it is less likely (than a solute) to accumulate in microsites (Xu et al. 2015). Acetate diffusion in solution, however, more readily explains the observations (Fig. S8). As wetting commenced and progressed, acetate in solution may become more available to microorganisms and can enhance methanogenesis. At the same time, wetting decreases O₂ availability, decreasing the role of methanotrophy (Fig. S8) and allowing more methane to escape the subsurface, despite limitations in gas diffusion. Methanogenesis is definitely enhanced in response to decreasing O₂ as the reviewer points out. Text in the discussion supporting this interpretation (L732): "The return to dominantly reducing conditions also was predicted to stimulate fermentation and the production of acetate through homoacetogenesis (Fig. S6). Enhanced production and diffusion of acetate during recovery (Fig. S8) triggered growth in the predicted biomass of aceticlastic methanogens (Fig. S5), which in turn, increased rates of aceticlastic methanogenesis (Fig. S9)." See also L737: "Although secondary to aceticlastic methanogenesis, simulated rates of hydrogenotrophic methanogenesis also increased in anaerobic microsites (Figs. S9, S10), mediated by increased production of H₂ and subsequent stimulation of the biomass of hydrogenotrophic methanogens during the drought recovery in 2015 (Fig. S5)." The sensitivity analysis (Fig. 8) shows a stronger control by aceticlastic methanogenesis than by hydrogenotrophic methanogenesis. Both are important, however.

Unfortunately, there were not isotopic data available for the field study; these type of data are rarely available at the field scale. Assessing patterns in isotopic fractionation or even

isotope tracing (gross rates or label chasing) would make an interesting experiment for future research.

L318: Again, how do you define the microsities?

In addition to revising the methods section 2.4.3 as suggested above, we have revised Fig. 1 caption as follows:

“Top panel (a) shows the model representation of soil microsite distribution (modified from Sihi et al., 2020a, also see Eq. 14). The cylinder refers to the volume beneath the soil chambers. The intensity of different cylinder colors figure refers to rate of a process or the intensity of a concentration inside microsities in each theoretical cylinder, e.g., a dark color means a higher rate/intensity, and a light color means a lower rate/intensity for a given process. The 2D graph on the right refers to the probability density function of the rate of the process or intensity of the concentration in the bulk soil. A wide distribution skewed to the right (dark line) implies higher bulk rates of the process or higher concentrations, and a narrow distribution skewed to the left (light line) implies lower bulk rates of the process or lower concentrations, of any of the following: solute concentration [S_i], gas concentration [G_i], soil moisture (SoilM_i), gas and solute diffusion (Diff_i), methane production (Prod_i), and methane oxidation (Ox_i).”

We have revised the figure from the original as follows: Add an arrow on the x axis pointing towards the right, denoting increasing concentrations or rates. Moved the light-colored probability-density function to the left of the dark-colored probability-density function and make it much more narrow and signify less impact on bulk rates/concentrations compared to the dark-colored function (more impact on bulk rates/concentrations).

L346-348: Again, what makes you so sure that it is acetate that drives net methane emissions and not H₂/CO₂ and a decrease in oxygen?

All of these processes are happening simultaneously. Our model simulation suggests that acetate is driving most of the CH₄ increases, and that decreases in methanotrophy due to decreases in oxygen, are both more important than hydrogenotrophic methanogenesis. Please see also the sensitivity analysis in Fig 8. Fig S5 shows that both kinds of methanogens increase during drought recovery and post-drought, but that acetotrophic methanogens are two orders of magnitude more abundant than hydrogenotrophic methanogens. Additionally, the acetate hypothesis is supported under drought condition as acetate may accumulate in microsities. During wetting, the acetate may become more available to the methanogens as solute diffusion becomes enhanced (Fig. S8), resulting in higher CH₄ production. The model simulations suggest that hydrogen diffusion is lessened under wetting conditions which is consistent with what we might expect for a gas diffusing through a liquid versus diffusing through air (Fig. S8). So, hydrogen substrate availability does not completely explain the observations of higher CH₄ production under wetting conditions, but it is a contributor. The low contribution of H₂/CO₂ is also caused by low concentration and high turnover rate of H₂ in soil; particularly in the top soil, which is where this experiment was carried out. Please see L737-752 for improved explanation.

L369-372: and homoacetogenesis?

Yes, please see L733.

REFERENCES

Buan, N.R. Methanogens: pushing the boundaries of biology: Emerging Topics in Life Science, 2, 629–646, <https://doi.org/10.1042/ETLS20180031>, 2018.

Cabugao, K. G., Yaffar, D., Stenson, N., Childs, J., Phillips, J.; Mayes, M. A., Yang, X., Weston, D. J., and Norby, R. J.: bringing function to structure: Root-soil interactions shaping phosphatase activity throughout a soil profile in Puerto Rico, *Ecol. Evol.* (in press).

Cusack, D. F., Silver, W. L., and McDowell, W. H.: Biological nitrogen fixation in two tropical forests: ecosystem-level patterns and effects of nitrogen fertilization, *Ecosystems*, 12, 1299-1315, 2009.

Goberna, M., Gadermaier, M., García, C., Wett, B., Insam, H.: Adaptation of methanogenic communities to the cofermentation of cattle excreta and olive mill wastes at 37°C and 55°C, *Applied and Environmental Microbiology*, 76, 19, 6564–6571, doi:10.1128/AEM.00961-10, 2010.

Harris, N. L., Lugo, A. E., Brown, S., and Heartsill Scalley, T. (Eds.): Luquillo Experimental Forest: Research history and opportunities, EFR-1, Washington, DC: U.S. Department of Agriculture, 152 p., 2012.

Hall, S. J., Liptzin, D., Buss, H. L., DeAngelis, K., and Silver, W. L.: Drivers and patterns of

iron redox cycling from surface to bedrock in a deep tropical forest soil: A new conceptual model, *Biogeochemistry*, 130(1-2), 177-190, 2016.

Johnson, A. H., Xing, H. X., and Scatena, F. N.: Controls on Soil Carbon Stocks in El Yunque National Forest, Puerto Rico: *Soil Sci. Soc. Am. J.*, 79, 294-304, doi:10.2136/sssaj2014.05.0199, 2014.

Megonigal, J. P., and Geunther, A. B.: Methane emissions from upland forest soils and vegetation, *Tree Physiol.*, 28, 491-498, 2008.

O'Connell, C. S., Ruan, L., and Silver, W. L.: Drought drives rapid shifts in tropical rainforest soil biogeochemistry and greenhouse gas emissions. *Nat. Commun.*, 9, 1-9, 10.1038/s41467-018-03352-3, 2018.

Parton, W., Silver, W. L., Burke, I., Grassens, L., Harmon, M. E., Currie, W. S., King, J. Y., Adair, E. C., Brandt, L. A., Hart, S. C., and Fasth, B.: Global-scale similarities in nitrogen release patterns during long-term decomposition, *Science*, 315, 361-364, doi: 10.1126/science.1134853, 2007.

Pavlov, M. Y., and Ehrenberg, M.: Optimal control of gene expression for fast proteome adaptation to environmental change, *Proc. Natl. Acad. Sci. U.S.A.*, 110 (51), 20527-20532, doi/10.1073/pnas.1309356110, 2013.

Rochette, P., and Hutchinson, G. L.: Measurement of soil respiration in situ: Chamber techniques, Publications from USDA-ARS / UNL Faculty, 1379, <https://digitalcommons.unl.edu/usdaarsfacpub/1379>, 2005.

Roussel E. G., Cragg, B. A., Webster, G., Sass, H., Tang, X., Williams, A. S., Gorra, R., Weightman, A. J., and Parkes, R. J.: Complex coupled metabolic and prokaryotic community responses to increasing temperatures in anaerobic marine sediments: critical temperatures and substrate changes, *FEMS Microbiology Ecology*, 91, 2015, fiv084, doi: 10.1093/femsec/fiv084, 2015.

Sihi, D., Davidson, E. A., Savage, K. E., and Liang, D.: Simultaneous numerical representation of soil microsite production and consumption of carbon dioxide, methane, and nitrous oxide using probability distribution functions, *Glob. Change Biol.*, 26, 200-218, <https://doi.org/10.1111/gcb.14855>, 2020.

Silver, W. L., Lugo, A., and Keller, M.: Soil oxygen availability and biogeochemistry along rainfall and topographic gradients in upland wet tropical forest soils, *Biogeochemistry*, 44, 301-328, 1999.

Soil Survey Staff: Order 1 Soil Survey of the Luquillo Long-Term Ecological Research Grid, Puerto Rico, USDA, NRCS, <https://luq.lter.network/content/order-i-soil-survey-luquillo-long-term-ecological-research-grid-puerto-rico>, 1995.

Weaver, P. L., and Murphy, P. G.: Forest structure and productivity in Puerto Rico's Luquillo Mountains, *Biotropica*, 22(1), 69-82, <https://doi.org/10.2307/2388721>, 1990.

Xu, X., Elias, D. A., Graham, D. E., Phelps, T. J., Carroll, S. L., Wulschleger, S. D., and Thornton, P. E.: A microbial functional group-based module for simulating methane production and consumption: Application to an incubated permafrost soil, *J. Geophys. Res.-Biogeo.*, 120, 1315-1333, doi:10.1002/2015jg002935, 2015.

Interactive comment on Biogeosciences Discuss., <https://doi.org/10.5194/bg-2020-222>, 2020.

Responses to (in italic font):

Interactive comment on “Representing methane emissions from wet tropical forest soils using microbial functional groups constrained by soil diffusivity” by Debjani Sihi et al.

Anonymous Referee #3

Received and published: 26 August 2020

The manuscript of Debjani Sihi and colleagues brings up a very interesting topic on disentangling gross methane emission and uptake from wet tropical forest soil using a combination of microbial functional group CH₄ model and a diffusivity module. This work clearly shows how landscape topography and climate affect net CH₄ emissions due to shift of substrate production, soil redox conditions, and diffusivity of O₂, H₂, and acetate under drought and recovery phases. The experimental work is well performed, convincing and well discussed in the context of previous literature. The manuscript is well organized and clearly written and I enjoyed reading it. I only have a few comments that should be addressed:

Thank you kindly for the positive comments and for the constructive suggestions, all of which we have adopted.

Line 54 Should it be “increased consumption of atmospheric CH₄”?

Good catch. Thank you, the manuscript is corrected as suggested (L99 in the tracked version [note: all line numbers refer to tracked version]).

Line 258 The correlation seems stronger and more negative in 2015 (-0.36) than 2016 (-0.61).

The reviewer is correct. The sentence L601 is changed to “The correlation between CH₄ emissions and O₂ concentrations was stronger and more negative in 2015 than 2016.”

Line 321-322 You defined pre-drought period from DOY 57-115 instead of DOY 200. The details in results should be checked.

Yes, we mean to say “during the drought period (DOY 200) (L688)”. We will double-check all other similar references and ensure there are no additional errors. Thank you.

Fig. 1 I appreciate the conceptual figures herein, but it looks a bit confusing and I do not well understand what means in panel a. How to relate microsite frequency with soil properties?

*We agree this figure and its description could use some revisions. Our caption says currently: **Top panel (a) shows the model representation of soil microsite distribution (modified from Sihi et al., 2020, also see Eq. 13). Different shades indicate substrate concentration [S_i], soil moisture (SoilM_i), diffusion (Diff) of solutes and gases, production (Prod_i) and oxidation (Ox_i) processes at each microsite.***

We revised the caption, extensively, as follows:

“Top panel (a) shows the model representation of soil microsite distribution (modified from Sihi et al., 2020a, also see Eq. 14). The cylinder refers to the volume beneath the soil chambers. The intensity of different cylinder colors figure refers to rate of a process or the intensity of a concentration inside microsites in each theoretical cylinder, e.g., a dark color means a higher rate/intensity, and a light color means a lower rate/intensity for a given process. The 2D graph on the right refers to the probability density function of the rate of the process or intensity of the concentration

in the bulk soil. A wide distribution skewed to the right (dark line) implies higher bulk rates of the process or higher concentrations, and a narrow distribution skewed to the left (light line) implies lower bulk rates of the process or lower concentrations, of any of the following: solute concentration [S_i], gas concentration [G_i], soil moisture (Soil M_i), gas and solute diffusion (Diff), methane production (Prod $_i$), and methane oxidation (Ox $_i$)."

We also revised the figure from the original as follows: Add an arrow on the x axis pointing towards the right, denoting increasing concentrations or rates. Moved the light-colored probability-density function to the left of the dark-colored probability-density function and make it much narrower and signify less impact on bulk rates/concentrations compared to the dark-colored function (more impact on bulk rates/concentrations).

Do substrate concentration, soil moisture, diffusivity of solute and gas present the similar pattern for one kind of microsite?

The frequency distribution for the microsities is the same for all of these, according to Eq 14. But, the diffusivity of liquids is according to Eq 11 and 12; diffusivity of gasses according to Eq 8, 9, and 10. Here is a little more information on the microsities that is included in a new methods Section 2.4.3 devoted to microsities: We assumed that size of the microsities should be at least an order magnitude lower than the bulk soil measurements we had for soil methane fluxes. Using this logic, we decided that "diameter" of microsities should be in "mm" scale as the diameter of soil chambers we used are in "cm" scale (15.24 cm). Thus, we did the math to come up with the number of "total microsities" (i.e. 10000) under each fluxchamber such that the diameter of microsities meets our criteria, following Sihi et al. 2020a. This is why the frequency of microsities is the same for both low rate/intensities (light yellow line Fig 1a) and high rate/intensities (dark line Fig 1a) (see also Fig. 7 in manuscript and Fig. S10 in SI)."

Why this figure links to Eq.13?

This figure 1 should link to Eq 14; apologies for the confusion and thank you for the catch. It is corrected in the revision.

Also in panel b, it would be more clear for readers if you could adjust it to a better shape or based on the clue of the present study. Can you try to improve the conceptual figure and clarify this in the legend?

We removed the Air/Soil diagram at the top of this figure, and the word "solute diffusion" from the figure. Panel b should only represent the geochemical pathways that the model is representing, and we should rely on panel (a) to address diffusion. We hope that makes the content of both panels more understandable.

We revised the caption from the current version: **Bottom panel (b) is the schematic of the microbial functional group-based model coupled with a diffusivity module (Microbial Model for Methane Dynamics-Dual Arrhenius and Michaelis Menten, M3D-DAMM) for simulating soil methane (CH_4) dynamics in field soils (Modified from Xu et al., 2015), where SOM = soil organic matter, CO_2 = carbon dioxide, DOC = dissolved organic carbon, H^+ is the hydronium ion, and H_2 = dihydrogen molecule.** Revised figure caption: Bottom panel (b) is the schematic of the microbial functional group-based model for simulating soil methane (CH_4) dynamics in field soils (modified from Xu et al., 2015). The schematic represents the decomposition of soil organic matter (SOM) and plant litter into carbon dioxide (CO_2) and dissolved organic matter (DOC); the production of acetate and hydronium ion (H^+) from decomposition and fermentation of DOC which also decreases pH, the production of acetate and hydronium ion (H^+) from homoacetogenesis which decreases pH; and the production of dihydrogen ion (H_2) and CO_2 from decomposition of DOC. The intermediary products then have three possible non-mutually exclusive pathways (1) acetoclastic methanogenesis, which is the production of methane from aqueous acetate found in soil solutions, (2) hydrogenotrophic methanogenesis, which is the production of methane from hydrogen, and (3) methanotrophy, which is the oxidation of methane into carbon dioxide.

Fig.3 and 4 The label of y-axis for soil moisture and oxygen should be between 0-1 rather than 0-100, as the unit is V V-1. Otherwise, the unit should change to %.

Thank you for pointing this out. We adjusted the unit of the axes in Figs 3 and 4,

S8(g)(h)(i), and S10(i)(j) in the revision.

Fig.4 and 6 The unit of CH₄ emission should be uniform. Some of them are nmol m⁻² S⁻¹, while others are nmole m⁻² S⁻¹. Also the unite of acetate (Fig. 2).

Thank you, we should use nmol and μ mol (and not "mole"). Corrections are made to figures 2,3,4,7, and S5,S6,S7,S8,S9,S10 in the revision.

Interactive comment on Biogeosciences Discuss., <https://doi.org/10.5194/bg-2020-222>, 2020.

1 Representing methane emissions from wet tropical forest soils 2 using microbial functional groups constrained by soil diffusivity

3 Debjani Sibi^{1,2}, Xiaofeng Xu³, Mónica Salazar Ortiz⁴, Christine S. O'Connell^{5,6}, Whendee L.
4 Silver⁵, Carla López-Lloreda⁷, Julia M. Brenner¹, Ryan K. Quinn^{1,8}, Jana R. Phillips¹, Brent D.
5 Newman⁹, and Melanie A. Mayes^{1*}

6 ¹Climate Change Science Institute and Environmental Sciences Division, Oak Ridge National Laboratory, Oak
7 Ridge, TN, 37831, USA

8 ²Currently employed at Department of Environmental Sciences, Emory University, Atlanta, GA, 30322, USA

9 ³Department of Biology, San Diego State University, San Diego, CA, 92182-4614, USA

10 ⁴Institute of Plant Science and Microbiology, University of Hamburg, Hamburg, 20148, Germany

11 ⁵Department of Environmental Science, Policy and Management, University of California, Berkeley, CA, 94720-
12 3114, USA

13 ⁶Currently employed at Department of Environmental Studies, Macalester College, St. Paul, MN, 55105-1899, USA

14 ⁷Department of Natural Resources and the Environment, University of New Hampshire, Durham, NH, 03824, USA

15 ⁸Department of Biology, Boston University, Boston, MA, 02215, USA

16 ⁹Earth and Environmental Sciences Division, Los Alamos National Laboratory, Los Alamos, NM, 87545, USA

17 *Correspondence to: Melanie A. Mayes (mayesma@ornl.gov)

18 **Abstract.** Tropical ecosystems contribute significantly to global emissions of methane (CH₄) and landscape
19 topography influences the rate of CH₄ emissions from wet tropical forest soils. However, extreme events such as
20 drought can alter normal topographic patterns of emissions. Here we explain the dynamics of CH₄ emissions during
21 normal and drought conditions across a catena in the Luquillo Experimental Forest, Puerto Rico. Valley soils served
22 as the major source of CH₄ emissions in a normal precipitation year (2016), but drought recovery in 2015 resulted in
23 dramatic pulses in CH₄ emissions from all topographic positions. Geochemical parameters including dissolved
24 organic carbon (C), acetate, and soil pH, and hydrological parameters like soil moisture and oxygen (O₂)
25 concentrations, varied across the catena. During the drought, soil moisture decreased in the slope and ridge and O₂
26 concentrations increased in the valley. We simulated the dynamics of CH₄ emissions with the Microbial Model for
27 Methane Dynamics-Dual Arrhenius and Michaelis Menten (M3D-DAMM) which couples a microbial functional
28 group CH₄ model with a diffusivity module for solute and gas transport within soil microsities. Contrasting patterns
29 of soil moisture, O₂, acetate, and associated changes in soil pH with topography regulated simulated CH₄ emissions,
30 but emissions were also altered by rate-limited diffusion in soil microsities. Changes in simulated available substrate
31 for CH₄ production (acetate, CO₂, and H₂) and oxidation (O₂ and CH₄) increased the predicted biomass of
32 methanotrophs during the drought event and methanogens during drought recovery, which in turn affected net
33 emissions of CH₄. A variance-based sensitivity analysis suggested that parameters related to acetoclastic
34 methanogenesis and methanotrophy were most critical to simulate net CH₄ emissions. This study enhanced the
35 predictive capability for CH₄ emissions associated with complex topography and drought in wet tropical forest soils.

36 **Copyright statement.** This manuscript has been authored by UT-Battelle, LLC, under contract DE-AC05-
37 00OR22725 with the U.S. Department of Energy (DOE). The US government retains and the publisher, by
38 accepting the article for publication, acknowledges that the US government retains a nonexclusive, paid-up,

Deleted: ²

Deleted: ³

Deleted: ⁴

Deleted: ⁶

Deleted: ⁷

Deleted: ⁸

Formatted: Font: (Default) +Body (Times New Roman), 10 pt

Deleted: ²Department

Deleted: ³

Deleted: ⁴Department of Environmental Studies, Macalester College, St. Paul, MN, 55105-1899, USA ⁴

Deleted: ⁵

Deleted: ⁶

Deleted: ⁷

Deleted: ⁸

Formatted: Line spacing: 1.5 lines

Deleted: (ridge >> slope >> valley)

Deleted: (ridge ≥ slope > valley)

Deleted: (valley >> slope >> ridge)

Deleted:),

Deleted: meteorological

Deleted: (valley > slope = ridge)

Deleted: (slope = ridge > valley)

Deleted: acetotrophic

61 irrevocable, worldwide license to publish or reproduce the published form of this manuscript, or allow others to do
62 so, for US government purposes. DOE will provide public access to these results of federally sponsored research in
63 accordance with the DOE Public Access Plan (<http://energy.gov/downloads/doe-public-access-plan>).

Formatted: Font: (Default) +Body (Times New Roman), 10 pt

Formatted: Font: (Default) +Body (Times New Roman), 10 pt

64 1 Introduction

65 Wet tropical forest soils contribute significantly to global emissions of methane (CH₄; Pachauri et al., 2014).
66 Although net emissions of CH₄ from upland soils are infrequent in temperate climates, studies show that CH₄
67 emissions are common in wet tropical forests, even in upland soils (Cattânio et al., 2002; Keller and Matson, 1994;
68 Silver et al., 1999; Teh et al., 2005; Verchot et al., 2000). Landscape topography can strongly influence the
69 proportions of CH₄ production and oxidation in mountainous tropical regions, affecting net emissions (Silver et al.,
70 1999; O'Connell et al., 2018). Climate, and specifically patterns in rainfall, also affect emissions from tropical
71 forests. Climate change may increase the frequency and severity of extreme rainfall and drought events, altering the
72 spatial and temporal dynamics of CH₄ emissions through changes in redox dynamics and substrate availability
73 (Silver et al., 1999; Chadwick et al., 2016; Neelin et al., 2006). Thus, accurately estimating CH₄ emissions under a
74 variety of climatic and topographic conditions is important for predicting soil carbon-climate feedbacks in the humid
75 tropical biome.

76 Several studies have reported the effect of drought events on biogenic CH₄ emissions across different wet tropical
77 forest soils. For example, Aronson et al. (2019) demonstrated that the lower soil moisture conditions during 2015-16
78 El Niño event increased consumption of atmospheric CH₄ in a wet tropical forest Oxisol of Costa Rica. Similarly, a
79 large-scale, 5-year throughfall exclusion experiment in a moist tropical forest Oxisol in Brazil also reported
80 increased consumption of atmospheric CH₄ under the drought treatment, followed by a recovery of CH₄ emissions to
81 pre-treatment values after the experiment ceased (Davidson et al., 2004, 2008). Using rainout shelters, Wood and
82 Silver (2012) found spatial variability in CH₄ oxidation rates, with an increase of 480% uptake in valleys in an
83 Ultisol in Puerto Rico. More recently, in a similar Puerto Rico Ultisol, O'Connell et al. (2018) reported increasing
84 consumption of atmospheric CH₄ during a Caribbean drought event, followed by increased production of CH₄ after
85 the drought was over. The post-drought net CH₄ emission rates were higher than the pre-drought emissions, such
86 that the benefits to atmospheric radiation imparted by the lowered emissions during the drought were eliminated.
87 The sharp differences between pre- and post-drought emissions suggested that drought affected the balance of
88 methanogenesis and methanotrophy in the soils, but the study lacked analysis of the microbial community's
89 contributions to these two separate processes.

Deleted: atmospheric

Deleted: soil

Deleted: soil

Deleted: R

90 The concept of "microsites" inside soil aggregates or within soil micropores can help explain the coexistence of
91 oxidative and reductive processes in soils (Silver et al., 1999; Teh and Silver, 2006), which may have occurred in the
92 post-drought period in the O'Connell et al. (2018) study. Oxygen can remain inside micropores during saturated
93 conditions and thereby maintain aerobic microbial respiration; likewise, hypoxic conditions can persist in microsites
94 under extended droughts and thereby maintain anaerobiosis. Additionally, liquid substrates for methanogenesis such
95 as acetate, can accumulate in microsites under dry conditions because their diffusion to hungry microbial

Deleted: ,

Deleted: and

Deleted: anoxic

Formatted: Font: (Default) +Body (Times New Roman), 10 pt

103 communities may be restricted. Conversely, gaseous substrates such as CO₂ and H₂ may accumulate in microsites
104 under saturated conditions because gaseous diffusion can be limited. The observed rapid flush of CH₄ in response to
105 a post-drought wetting event (O'Connell et al., 2018) suggests methanogenesis continued during the drought in the
106 Ultisol's microsites, despite low soil moisture and high O₂ supply (Andersen et al., 1998; Bosse and Frenzel, 1998;
107 Teh et al., 2005; von Fischer and Hedin, 2002). Finely-textured soils common to the humid tropics can facilitate the
108 co-existence of reduced solute and gas species with O₂ because the rate of solute and gaseous exchanges is
109 controlled by diffusion into and out of microaggregates (Hall and Silver, 2013; Liptzin et al., 2010; Silver et al.,
110 2013). In particular, hematite precipitation on clay minerals, found in both Oxisols and Ultisols, can enhance
111 formation of soil aggregates because of their high surface area and charge properties (Hall et al., 2016). Soil organic
112 matter can also enhance aggregation and at the same time consume O₂ (Six et al., 2004). However, few if any
113 measurements of microsites exist in real field soils.

114 To explain the diverse observations of CH₄ emissions during and after drought across a wet tropical forest catena,
115 we hypothesized that explicit representations of diffusion into and out of microsites for gas and solute transport
116 would be required. To account for the balance of methanotrophy and methanogenesis, separate microbial functional
117 groups for CH₄ production and oxidation would need to be defined. Therefore, a microbial functional group model
118 for CH₄ production and consumption (Xu et al., 2015) was merged with a soil diffusivity module (Davidson et al.,
119 2012; Sihi et al., 2018) to simulate the dynamics of net *in situ* CH₄ emissions from soil microsites (Sihi et al.,
120 2020a). This module considers three key mechanisms for CH₄ production and consumption: acet~~c~~lastic
121 methanogenesis (production from acetate) and hydrogenotrophic methanogenesis (production from H₂ and CO₂), and
122 aerobic methanotrophy (oxidation of CH₄ and reduction of O₂) (Fig. 1). Here we report a modeling experiment to
123 explain contrasting patterns of observed CH₄ emissions following a severe drought in 2015 and we provide new data
124 to describe CH₄ emissions under non-drought conditions in 2016. We explicitly account for changes in soil
125 moisture, O₂, acetate, and microbial functional group dynamics within soil microsites in the model.

126 2 Materials and methods

127 2.1 Study site

128 The study was conducted across a tropical forest catena near the El Verde Research Station in the Luquillo
129 Experimental Forest (LEF) in northeastern Puerto Rico in the United States (Latitude 18°19'16.83" N, Longitude
130 65°49'10.13" W). The site is part of a National Science Foundation Long-Term Ecological Research (LTER) and
131 Critical Zone Observatory (CZO) site and is also part of the U.S. Department of Energy's Next Generation
132 Ecosystem Experiment-Tropics. The mean annual temperature at the site is 23 °C and the long-term mean rainfall is
133 approximately 3500 mm yr⁻¹ with low seasonality (Scatena, 1989). Inter-annual variability of rainfall ranges
134 between 2600 mm yr⁻¹ to 5800 mm yr⁻¹, sometimes associated with extreme rainfall events (approximately 100 mm
135 day⁻¹) from Caribbean storm systems (Heartsill-Scalley et al., 2007). The LEF is classified as a wet tropical forest
136 according to the Holdridge life zone system, which considers rainfall, elevation, latitude, humidity, and
137 evapotranspiration (Harris et al., 2012).

Deleted: soil

Formatted: Font: (Default) +Body (Times New Roman), 10 pt, Not Italic

Formatted: Font: (Default) +Body (Times New Roman), 10 pt

Formatted: Font: (Default) +Body (Times New Roman), 10 pt, Not Italic

Formatted: Font: (Default) +Body (Times New Roman), 10 pt

Formatted: Font: (Default) +Body (Times New Roman), 10 pt, Not Italic

Formatted: Font: (Default) +Body (Times New Roman), 10 pt

Formatted: Not Highlight

Formatted: Font: (Default) +Body (Times New Roman), 10 pt

Formatted: Font: (Default) +Body (Times New Roman), 10 pt, Not Italic

Formatted: Font: (Default) +Body (Times New Roman), 10 pt, Not Italic, Subscript

Formatted: Not Superscript/ Subscript, Not Highlight

Formatted: Font: (Default) +Body (Times New Roman), 10 pt

Formatted: Not Highlight

Formatted: Font: (Default) +Body (Times New Roman), 10 pt

Formatted: Font: (Default) +Body (Times New Roman), 10 pt, Not Italic

Formatted: Font: (Default) +Body (Times New Roman), 10 pt

Deleted: o

Deleted: wet

Deleted: Forest

Deleted: ~

Deleted: (~

Formatted: Font: (Default) +Body (Times New Roman), 10 pt, Not Italic

Formatted: Font: (Default) +Body (Times New Roman), 10 pt

Formatted: Font: (Default) +Body (Times New Roman), 10 pt, Not Italic

Deleted: s

Formatted: Font: (Default) +Body (Times New Roman), 10 pt

Formatted: Font: (Default) +Body (Times New Roman), 10 pt, Not Italic

Formatted: Font: (Default) +Body (Times New Roman), 10 pt, Not Highlight

Formatted ... [1]

Formatted ... [2]

145 The landscape at the field site is highly dissected with short catenas, characterized by a land surface distance of < 30
 146 m from ridgetop to valley (O'Connell et al., 2018). This study partitioned sampling along a catena from ridgetop,
 147 slope, and valley topographic positions (Fig. S1). The soils are clay-rich Ultisols, which were derived from basaltic
 148 and andesitic volcanoclastic parent materials. Soils are acidic (average pH is 4.3 and 5.1 in ridge and valley
 149 topographic positions, respectively, Fig. 2). The valley soils have approximately 30% clay and approximately 15%
 150 sand, while the ridge soils have approximately 22% clay and approximately 30% sand (Brenner et al., 2019). The
 151 soils contain high concentrations of iron (Fe) and aluminum (Al) (oxy)hydroxides where their relative
 152 concentrations vary along the catena and differences in Fe speciation are associated with variable redox conditions
 153 (Hall and Silver, 2013, 2015). A detailed soil survey in the immediate vicinity lists three soil types (Zarzal, Cristol,
 154 and Prieto) with a minimal litter layer due to rapid decomposition (Parton et al. 2007, Cusack et al. 2009), surface
 155 (A) horizons 5 cm thick, and B horizons of 130 to 150 cm thick (Soil Survey Staff, 1995). The surface soil bulk
 156 density ranged from 0.5 to 0.7 g cm⁻³, and by 25 cm depth was 0.8 to 1.1 g cm⁻³ (Cabugao et al., in press), similar to
 157 previous observations (Johnson et al., 2014; Silver et al., 1999). The forest composition is relatively diverse with the
 158 mature Tabonuco (*Dacryodes excelsa* Vahl) and Sierra palm (*Prestoea montana*) trees being most dominant
 159 (Scatena and Lugo, 1995; Wadsworth et al., 1951).

160 2.2 Soil and porewater sampling

161 Previous CH₄ measurements in the LEF at the soil surface, 10 cm depth, and 35 cm depth, found the highest CH₄
 162 concentrations at 10 cm depth (Silver et al. 1999), while 30 cm depth was the location of maximum soil organic
 163 carbon (SOC) concentrations (Johnson et al., 2014). To initialize the model, soil and soil water samples were
 164 collected from depths ranging from 0 to 30 cm in accordance with these previous studies. Soil samples were
 165 collected in triplicate from a depth of 0-10 cm and on a quarterly timeframe from the ridgetop, slope, and valley
 166 positions for over two years. The soil pH was determined using a 1:2 ratio of soil:solution using a glass electrode
 167 with 0.005 M CaCl₂ as the equilibrated soil solution (Thomas, 1996; Sihi et al. 2020b). Porewater samples were
 168 collected approximately weekly for over two years using macro-rhizon soil water samplers (length = 5 cm)
 169 (Rhizosphere Research Products B.V.; Wageningen, The Netherlands) installed at both 5-10 cm and 25-30 cm depth
 170 in triplicate in the ridge, slope, and valley topographic positions (Sihi et al., 2020c). The soil water samples were
 171 analyzed for organic acid concentrations (acetate) using High Performance Liquid Chromatography (Dionex ICS-
 172 5000+ Thermo-Fisher Waltham, MA, USA) with the Dionex IonPac AS11-HC column using a potassium hydroxide
 173 eluent and gradient elution. The samples were analyzed for total dissolved organic carbon (DOC) using a Shimadzu
 174 total organic C analyzer (Shimadzu TOC-L CSH/CSN Analyzer Baltimore, MD, USA). The soil and porewater
 175 measurements were conducted in 2017-2018 (the number of samples *n* ranged between 20 to 35, Fig. 2) to initialize
 176 different model parameters for the catena, because measurements were not available for 2015-2016. To that end, the
 177 chemical data were used as the reference characteristics of the bulk soil, and the temporal evolution of DOC, acetate,
 178 and soil pH at the microsites were calculated using probability distributions of soil moisture and O₂ across soil
 179 microsites over the two-year measurement window. Soil bulk density and particle density values were taken from
 180 O'Connell et al. (2018).

- Deleted: ~
- Deleted: ~
- Deleted: ~
- Deleted: ~
- Formatted ... [3]
- Formatted ... [4]
- Formatted ... [5]
- Formatted ... [6]
- Formatted ... [7]
- Formatted ... [8]
- Formatted ... [9]
- Formatted ... [10]
- Deleted: ~
- Deleted: around ~
- Formatted ... [11]
- Formatted ... [12]
- Formatted ... [13]
- Formatted ... [14]
- Formatted ... [15]
- Formatted ... [16]
- Deleted: s
- Formatted ... [17]
- Formatted ... [18]
- Formatted ... [19]
- Formatted ... [20]
- Deleted: i
- Formatted ... [21]
- Formatted ... [22]
- Formatted ... [23]
- Formatted ... [24]
- Deleted: ,
- Formatted ... [25]
- Formatted ... [26]
- Formatted ... [27]
- Formatted ... [28]
- Formatted ... [29]
- Deleted: i
- Formatted ... [30]
- Deleted: to
- Deleted: from 0-10 cm depth
- Formatted ... [31]
- Deleted:
- Deleted: -
- Deleted: -
- Deleted: depths
- Formatted ... [32]

197 **2.3 In situ methane flux and soil driver measurements**

198 Campbell Scientific CS 655 soil moisture and temperature sensors and Apogee SO-110 O₂ sensors were co-located
199 with soil gas flux chambers at 15 cm soil depth along the catena, each with five replications along five transects
200 (Fig. S1) (O'Connell et al., 2018). Following Liptzin et al. (2011), soil O₂ sensors were installed in gas-permeable
201 soil equilibration chambers (295 cm³). Data from these sensors were collected hourly using Campbell Scientific
202 CR10000 data loggers and AM16/32B multiplexers (Campbell Scientific, Logan, UT, USA), which were processed
203 using site-based calibration equations.

204 Soil flux chambers were placed on the top of the soil surface. Soil CH₄ emissions along the catena were measured
205 during 2015 (February 26 to December 23, O'Connell et al., 2018; Silver, 2018) and 2016 (April 5 to July 18) (Sih
206 et al., 2020d) using a Cavity Ring-Down Spectroscopy gas analyzer (Picarro G2508, Santa Clara, CA, USA)
207 connected to 12 automated eosAC closed dynamic soil chambers (Pumpanen et al., 2004) using a multiplexer
208 (Eosense Inc., Dartmouth, Nova Scotia, Canada). Data for soil CH₄ emissions were processed using eosAnalyze-AC
209 (v3.5.0) software followed by a series of quality control protocols (O'Connell et al., 2018). We used daily average
210 values of drivers (soil temperature, soil moisture, and O₂ concentrations) and CH₄ emissions in the modeling
211 exercise. See O'Connell et al (2018) for more information on the soil sensor, chamber arrays, and the data analysis
212 pipeline.

213 The data from the 2015 Caribbean drought was partitioned into four distinct periods (O'Connell et al., 2018): (1)
214 pre-drought from day of year (DOY) 57 to 115 (dark gray on Fig. 3), (2) the drought from DOY 116 to 236
215 (medium gray on Fig. 3), (3) drought recovery from DOY 237 to 328 (light gray on Fig. 3), and (4) post-drought
216 from DOY 329 to 354 (white on Fig. 3). Total precipitation during the drought period was 700 mm in 2015 and
217 1088 mm during the same time frame in 2016 (Meteorological data from El Verde Field Station: NADP Tower,
218 available at <https://luq.lter.network/data/luqmetadata127>).

219 **2.4 Modelling approach**

220 **2.4.1 Microbial functional group model for methane production and oxidation**

221 An existing microbial functional group-based model for CH₄ production and consumption (Xu et al., 2015) was
222 adopted for this research (Sih, 2020). As shown in Fig. 1, acetate and H₂/CO₂ represent substrate [Substrate_{func_i}]
223 (nM, cm⁻³) for aceticlastic and hydrogenotrophic methanogenesis reactions, respectively. On the other hand, CH₄ and
224 O₂ concentrations represent substrate for the methanotrophy reaction. Acetate and CO₂ are inputs based on
225 measurements of soil water and pH described in Section 2.2. In the model, acetate is formed by fermentation and by
226 homoacetogenesis (but not by syntrophic acetate oxidation) as defined in Xu et al. (2015) in their Appendix in Eq.
227 A15 and A16 (Fig. 1b). Methylotrophic methanogenesis (Narrowe et al. 2019) is neglected in the model. The overall
228 reaction rates are represented as:

229
$$\text{Reaction}_{\text{rate}_i} = \text{Biomass}_{\text{func}_i} \times \frac{\text{GrowR}_{\text{func}_i}}{\text{Efficiency}_{\text{func}_i}} \times \frac{[\text{Substrate}_{\text{func}_{1..n}}]}{[\text{Substrate}_{\text{func}_{1..n}}] + \text{KM}_{\text{func}_{1..n}}} \times f(T) \times f(\text{pH}) \quad (1)$$

Deleted: a

Formatted ... [33]

Deleted: nmole

Formatted: Font: (Default) +Body (Times New Roman), 10 pt

Deleted: acetotrophic

Formatted ... [34]

Formatted ... [35]

Formatted ... [36]

236 where $Reaction_{rate_i}$ (in $nM\ cm^{-3}\ hr^{-1}$) is rate of CH_4 production and/or consumption under variable substrate
 237 concentrations. $Biomass_{func_i}$ ($nM\ cm^{-3}$) represents microbial functional groups: aceticlastic methanogens,
 238 hydrogenotrophic methanogens, and aerobic methanotrophs, respectively. Growth rates and substrate use
 239 efficiencies of microbial functional groups are represented as $Growth_{func_i}$ (hr^{-1}) and $Efficiency_{func_i}$ (unitless),
 240 respectively (Table 1). The substrate limitation on CH_4 production is imposed by assuming a Michaelis-Menten
 241 relationship with the half-saturation constants for CH_4 production and oxidation being KM_{func_i} ($nM\ cm^{-3}$).
 242 Although minor contributions of iron dependent anaerobic CH_4 oxidation to net CH_4 emissions can be expected in
 243 our study site (Ettwig et al., 2016), we did not represent this process here as anaerobic oxidation of CH_4 is still not
 244 fully understood and it is generally low in most ecosystems.

245 The extent of change in $Biomass_{func_i}$ ($dBiomass_{func_i}$) is controlled by the balance between $Growth_{func_i}$ and
 246 $Death_{func_i}$ following:

247
$$\frac{dBiomass_{func_i}}{dt_{func_i}} = Growth_{func_i} - Death_{func_i} \quad (2)$$

248
$$Growth_{func_i} = Efficiency_{func_i} \times Reaction_{rate_i} \quad (3)$$

249 where $Growth_{func_i}$ is calculated as a multiplicative function of $Efficiency_{func_i}$ and the $Reaction_{rate_i}$
 250 $Death_{func_i} = DeadR_{func_i} \times Biomass_{func_i} \quad (4)$

251 and $Death_{func_i}$ is a function of $DeadR_{func_i}$ (death rate, Table 1) and $Biomass_{func_i}$ (microbial biomass).

252 All rate equations were modified by the scalars for temperature, $f(T)$ and pH, $f(pH)$ functions, described below. We
 253 represented the temperature effect, $f(T)$, using a classic Q_{10} function:

254
$$f(T) = Q_{10}^{\frac{Temperature_{soil} - Temperature_{reference}}{10}} \quad (5)$$

255 We represented the pH effect, $f(pH)$, based on Cao et al. (1995):

256
$$f(pH) = \frac{(pH - pH_{minimum}) \cdot (pH - pH_{maximum})}{(pH - pH_{minimum})^2 + (pH - pH_{maximum})^2 + (pH - pH_{optimum})^2} \quad (6)$$

257 where we set the minimum, optimum, and maximum soil pH values to 4, 7, and 10, respectively. Following Xu et al.
 258 (2015), we considered the contribution of acetate to pH as follows:

259
$$pH = -1 * \log(10^{pH_{initial}} + 4.2E - 9 * Acetate) \quad (7)$$

260 Although other mechanisms to alter soil pH are present at the site, e.g., Fe reduction and oxidation (Teh et al., 2005;
 261 Hall and Silver, 2013), these are not considered in the model at this time. Calibrated values of $Growth_{func_i}$
 262 $DeadR_{func_i}$, $Efficiency_{func_i}$, KM_{func_i} , and Q_{10_i} are presented in Table 1.

263 **2.4.2 Diffusion module for gaseous and solute transport in soil profile and across soil-air boundary**

264 In order to account for the diffusion of gases across the soil-air boundary and solutes (e.g. acetate) through soil water
 265 films (Fig. 1), we added the diffusion module of the Dual Arrhenius and Michaelis Menten (DAMM) model
 266 (Davidson et al., 2012; Sihi, 2020; Sihi et al., 2018, 2020a) to the existing microbial functional group model, which
 267 we refer to as M3D-DAMM. We calculated initial concentration of gases like O_2 , H_2 , CO_2 , and CH_4 , [Gas_{conc}], (unit:

Formatted ... [37]
 Deleted: nmole
 Deleted: nmole...cm⁻³) represents microbial functional groups[39]
 Formatted ... [38]
 Deleted: between the substrates and
 Deleted: ,
 Deleted: nmole...cm⁻³). Although minor contributions of iron
 Deleted: Fe ... e
 Deleted: Fe ... e

290 V^{-1}), as a function of a unitless diffusion coefficient of gas in air (D_{gas}), volume fraction of gas in air ($V V^{-1}$), and
 291 gas diffusivity ($a^{4/3}$) as follows:

$$292 [Gas_{conc}] = D_{gas} \times \text{atmospheric concentration} \times a^{4/3} \quad (8)$$

293 where $a^{4/3}$ represents the tortuosity of diffusion pathway for gases as a function of soil water (SoilM) and
 294 temperature (SoilT):

$$295 a^{4/3} = \left(\text{Porosity} - \frac{\text{SoilM}}{400} \right)^{4/3} \times \left(\frac{\text{SoilT} + 273.15}{293.15} \right)^{1.75} \quad (9)$$

296 where the air-filled porosity (a) was calculated by subtracting the volume fraction of soil moisture ($V V^{-1}$) from total
 297 porosity. Porosity was calculated as:

$$298 \left(1 - \frac{\text{Bulk density}}{\text{Particle density}} \right) \quad (10)$$

299 The exponent of 4/3 accounts for diffusivity of gases through porous media (Davidson and Trumbore, 1995). The
 300 exponent of 1.75 represents the temperature response of gaseous diffusion (Massman, 1998; Davidson et al., 2006).

301 Following Davidson et al. (2012), the value used for gaseous diffusivity coefficient (D_{gas}) was calculated based on
 302 an assumed boundary condition such that the concentration of gaseous substrates in the soil pore space would be
 303 equivalent to the volume fraction of gases in air under completely dry conditions.

304 We assumed another boundary condition to determine the value of the aqueous diffusion coefficient, D_{liq} , such that
 305 soluble substrates like acetate would be available at the enzymatic reaction site under conditions with saturating soil
 306 water content (Davidson et al., 2012):

$$307 D_{liq} = \frac{1}{\text{Porosity}^3} \quad (11)$$

308 We represented soluble substrates (acetate) diffused through a soil water film as Aqueous – substrate ($\mu M L^{-1}$),
 309 which we calculated as follows:

$$310 \text{Aqueous – substrate}_{av} = \text{Aqueous – substrate} \times D_{liq} \times \left(\frac{\text{SoilM}}{400} \right)^3 \quad (12)$$

311 where the $\left(\frac{\text{SoilM}}{400} \right)^3$ term represents the diffusion rate of aqueous substrates to the enzymatic active site (Papendick
 312 and Campbell, 1981). Concentrations of acetate in the aqueous phase ($\mu M L^{-1}$) were obtained from the
 313 measurements across the catena averaged by depths (10 and 30 cm) of rhizon samplers.

314 We calculated CH_4 emissions, $CH_{4emission}$ (unit: $\mu mole m^{-2} hr^{-1}$), as a function of concentration ($[CH_{4conc}]$),
 315 production (CH_{4prod}), and oxidation (CH_{4ox}) of CH_4 , multiplied by the equivalent “depth” (set to 15 cm) (for cm^3
 316 volume to cm^2 area conversion) and 10^4 (for m^2 to cm^2 conversion) as follows:

$$317 CH_{4emission} = [CH_{4conc}] + (CH_{4prod} - CH_{4ox}) \times 10^4 \times \text{depth} \quad (13)$$

318 2.4.3 Soil microsites

319 [The importance of diverse microsite conditions was inferred based on many previous observations in the field and](#)
 320 [the lab of co-occurrences of oxic soil concentrations and reduced redox-active species \(Silver et al., 1999; Teh et al.,](#)
 321 [2005; Megonigal and Geunther 2008; Hall et al. 2013, 2016; Sihi et al., 2020a\). The high clay content, abundant Fe](#)
 322 [oxides, and visible redox mottling, particularly in the valley and slope soils facilitates a diversity of soil micro-](#)

Formatted	... [78]
Formatted	... [79]
Formatted	... [80]
Formatted	... [81]
Formatted	... [82]
Formatted	... [83]
Formatted	... [84]
Formatted	... [85]
Formatted	... [86]
Formatted	... [87]
Deleted: .	
Formatted	... [88]
Formatted	... [89]
Deleted: $\mu mole$	
Formatted	... [90]
Formatted	... [91]
Formatted	... [92]
Formatted	... [93]
Deleted: $\mu mole$	
Formatted	... [94]
Formatted	... [95]
Formatted	... [96]
Formatted	... [97]
Formatted	... [98]
Deleted: M	
Formatted	... [99]
Deleted: s	
Formatted	... [100]
Deleted: are	
Formatted	... [101]
Deleted: because	
Formatted	... [102]
Deleted: of	
Formatted	... [103]
Deleted: ast	
Formatted	... [104]
Deleted: O ₂	
Formatted	... [105]
Deleted: in the soil along with	
Formatted	... [106]
Deleted: ... Teh et al., 2005; ... Megonigal and Geunther ...	[107]
Deleted: CH ₄ fluxes; because of t	
Formatted	... [108]
Deleted: thick	
Formatted	... [109]
Deleted: s	
Formatted	... [110]
Deleted: iron	
Formatted	... [111]

361 environments where O₂ and CH₄ can seemingly co-occur, albeit in different microsite locations (Silver et al., 1999;
 362 Teh and Silver, 2006). Microsite diversity was also invoked to help explain the rapid CH₄ emissions following
 363 drought at the field site (O'Connell et al., 2018). Techniques for accurately measuring in-situ microsite activities
 364 remain very limited to date, here or elsewhere. Therefore, we simulated production, consumption, and diffusion
 365 processes within soil microsites using a log-normal probability distribution function of soil moisture and available C
 366 based on these previously observed relationships (Fig. 1). The average values of individual processes across
 367 simulated microsites (represented by "i") represent the reaction in the bulk soil, which we constrained using the net
 368 measured CH₄ emissions.

$$369 \text{ Bulk soil}_{\text{average}} = \frac{\sum \text{Frequency}_i \times [\text{microsite}]_i}{\text{Total microsites}} \quad (14)$$

370 We directly adopted the probability distribution function of soil moisture and C from Sihi et al. (2020a), which
 371 constrained values of Frequency_i of soil microsites. We a priori assigned the size of the microsites to be at least an
 372 order magnitude smaller than the diameter used for bulk measurements of CH₄ fluxes. Thus, the mean diameter of
 373 microsites was assumed to be at the mm-scale (the size-class of small stable aggregates in these soils), as the
 374 diameter of soil chambers was 15.24 cm. Thus, the resultant number of total microsites below each soil flux
 375 chamber was 10,000.

376 2.4.4 Sensitivity Analysis

377 We evaluated the sensitivity of model parameters with a global variance-based sensitivity analysis using the *R-*
 378 *multisensi* package. This method uses a global sensitivity index (0 < GSI < 1) to determine the sensitivity of CH₄
 379 emissions to model parameter values (Bidot et al., 2018). We conducted a multivariate technique to estimate GSI
 380 values in sequential steps. First, we implemented a factorial design on the uncertain model parameters, which is
 381 followed by a principal component analysis on model outputs. Then, we extracted GSI values by an ANOVA-based
 382 sensitivity analysis on the first principal component. To that end, parameters with high GSI values may explain high
 383 temporal variations of the observed CH₄ emissions and those with low GSI values are insignificant to reproduce the
 384 temporal dynamics of CH₄ emissions.

385 2.4.5 Statistical Analysis

386 We used R (version 3.5.1) for statistical analyses, modeling, and visualization purposes (R Core Team, 2018).
 387 Statistical analyses and figures were produced using *R-ggstatsplot* (Patil, 2018) and *R-ggplot2* (Wickham, 2016)
 388 packages. Differences in soil and porewater chemistry across the catena were compared using robust t-test.
 389 Correlograms for soil temperature, soil moisture, O₂, and soil CH₄ emissions were created using adjusted Holm
 390 correlation coefficients. All statistical analyses were conducted at the 5% significance level. We implemented the
 391 M3D-DAMM model using *R-FME* package (Soetaert, 2016).

- Formatted ... [112]
- Deleted: ... and finally because of ... [113]
- Formatted ... [114]
- Deleted: W... simulated production, consumption, and diffusion processes within soil microsites using a log-normal probability distribution function of soil moisture and available C based on these previously observed relationships (Fig. 1). The average values of individual processes across simulated microsites (represented by "i") represent the reaction in the bulk soil, which we constrained using the net measured CH₄ emissions (detailed information and equations on microsite probability distribution function can be found in Sihi et al., 2020a) ... [115]
- Formatted ... [116]
- Deleted: a
- Deleted: We also set the number of total microsites to 10,000, which represents the envelope of simulated microsites in Sihi et al.
- Moved down [1]: (2020a).
- Formatted ... [118]
- Deleted: assumed
- Formatted ... [119]
- Deleted: at...size of the microsites should be at least ... [120]
- Formatted ... [117]
- Formatted ... [121]
- Deleted: lower
- Formatted ... [122]
- Deleted: methane
- Formatted ... [123]
- Deleted: Using this logic, we decided that
- Formatted ... [124]
- Deleted: should be
- Formatted: Font: (Default) +Body (Times New Roman), 10 pt
- Deleted:
- Formatted ... [125]
- Deleted: since
- Formatted: Font: (Default) +Body (Times New Roman), 10 pt, Not Italic
- Deleted: i
- Formatted ... [126]
- Commented [WS2]: Per what area or volume?
- Moved (insertion) [1]
- Deleted: (2020a)
- Formatted ... [127]
- Deleted: 3
- Formatted: Font: (Default) +Body (Times New Roman), 10 pt
- Deleted: 4

440 **3 Results**

441 **3.1 Observational dynamics of soil biogeochemistry**

442 Soil and porewater chemistry varied along the catena (Fig. 2). Dissolved organic carbon (DOC) values followed the
443 trend of ridge > slope > valley ($p \leq 0.001$). Soil DOC concentrations (mean \pm SE) were 0.55 ± 0.10 , 0.30 ± 0.03 , and
444 0.18 ± 0.03 mg g⁻¹ in ridge, slope, and valley soils, respectively. Organic acid (acetate) concentrations were
445 significantly higher in the ridge (6.57 ± 1.48 $\mu\text{M}\cdot\text{L}^{-1}$) and slope (6.42 ± 2.19 $\mu\text{M}\cdot\text{L}^{-1}$) than in the valley (1.80 ± 0.20
446 $\mu\text{M}\cdot\text{L}^{-1}$) ($p = 0.003$). Soil pH followed the trend of valley > slope > ridge ($p < 0.001$). Average soil pH ranged from
447 4.25 ± 0.11 in the ridge, to 4.49 ± 0.08 in the slope, and to 5.05 ± 0.09 in the valley.

448 Soil moisture and soil O₂ concentrations were distinctly different in the drought year (2015) compared to 2016. The
449 drought in 2015 decreased soil moisture in the slope and ridge soils and increased O₂ concentrations in the valley
450 soils (Fig. 3) (also see O'Connell et al., 2018). Generally, average soil moisture was higher in the valley (0.47 ± 0.05
451 in 2015 and 0.51 ± 0.01 v v⁻¹ in 2016) as compared to the ridge (0.31 ± 0.12 in 2015 and 0.39 ± 0.03 v v⁻¹ in 2016)
452 and slope (0.30 ± 0.16 in 2015 and 0.41 ± 0.04 v v⁻¹ in 2016). Average O₂ concentrations were generally lower in
453 the valley (11.54 ± 5.94 in 2015 and 6.30 ± 2.96 % in 2016) as compared to the ridge (18.37 ± 0.72 in 2015 and
454 17.52 ± 0.42 % in 2016) and slope (18.09 ± 1.22 in 2015 and 16.89 ± 0.58 % in 2016). After the drought ended, the
455 recovery of soil moisture in the ridge and slope soils proceeded more quickly than the recovery of O₂ concentrations
456 in the valley soils (Fig. 3). Soil temperature ranges were averaged across the topographic gradient and were similar
457 in both years (average was 21.58 ± 1.88 in 2015 and 22.97 ± 1.04 °C in 2016).

458 In 2016, net CH₄ emissions were generally positive in the valley and were marginally negative in the ridge and slope
459 (Fig. 4). The dynamics of CH₄ were very different following the 2015 drought, resulting in net positive CH₄
460 emissions in the post-drought period for all topographic positions (Fig. 3) (as described in more detail in O'Connell
461 et al. 2018). The magnitude of CH₄ emissions was greater in the valley, followed by the slope and then the ridge.
462 The strength of the relationships between net CH₄ emissions and soil temperature, moisture, and O₂ concentrations
463 were contingent on both topographic position and year (2015 vs 2016) (Fig. 5). For example, the relation between
464 CH₄ emissions and soil moisture was stronger in 2016 (normal year) than in 2015 (drought year). The correlation
465 between CH₄ emissions and O₂ concentrations was stronger and more negative in 2015 than 2016. Correlations
466 between soil moisture and O₂ concentrations were negative and stronger in 2016 than in 2015. Correlation
467 coefficients between soil O₂ concentrations and CH₄ emissions were negative and strongest for valley soils and
468 lowest for ridge soils in 2015, but were uncorrelated in 2016 for ridge and slope soils (Fig. S2).

469 **3.2 Model simulations of methanogenesis and methanotrophy**

470 In general, there was little bias in the relationships between the observed and simulated CH₄ emissions (Fig. 6). The
471 model explained 72% and 67% of the variation in soil CH₄ emissions for 2015 and 2016, respectively, although the
472 model performance varied across the catena (Figs. 6, S3, S4). Overall, simulated CH₄ emissions captured the trend
473 of valley > slope > ridge for 2016. The model also captured the dramatically different dynamics of field CH₄

Deleted: >

Deleted: >

Formatted: Font: (Default) +Body (Times New Roman), 10 pt

Formatted: Font: (Default) +Body (Times New Roman), 10 pt

Deleted: mole

Deleted: mole

Deleted: mole

Deleted: >

Deleted: >

Deleted: 6

Deleted: 5

Formatted: Font: (Default) +Body (Times New Roman), 10 pt

Deleted: >

Formatted: Font: (Default) +Body (Times New Roman), 10 pt

Formatted: Font: (Default) +Body (Times New Roman), 10 pt

484 emissions as a function of topography during and after the 2015 drought. Net positive CH₄ emissions were simulated
485 in the drought recovery and post-drought periods in the ridge and slope in 2015, while net negative emissions were
486 simulated in the other times for these landscape positions. Additionally, simulated net CH₄ emissions were
487 decreased during the drought and drought recovery in the valley soils, as well as the strong net CH₄ emissions in the
488 valley soils in the post-drought period.

489 The ridge and slope positions were more similar to each other than to the valley soils. Simulated **decreased**
490 **production of acetate and hydrogen during the 2015 drought in the ridge and slope positions resulted in decreased**
491 biomass of **acetoclastic** methanogens and hydrogenotrophic methanogens (Figs. S5, S6). Gross CH₄ production
492 therefore decreased during these time periods (Fig. S7). Simultaneously, as soil moisture decreased, simulated
493 methanotrophic biomass increased during the drought (Fig. S5). The simulated biomass of both **acetoclastic**
494 methanogens and hydrogenotrophic methanogens increased dramatically in the ridge and slope soils during drought
495 recovery (**acetoclastic** methanogens: 3.3 and 5.3 times higher than drought period for ridge and slope, respectively;
496 hydrogenotrophic methanogens: 6.1 and 12 times higher than drought period for ridge and slope, respectively) and
497 post-drought (**acetoclastic** methanogens: 5.2 and 8.8 times higher than drought period for ridge and slope,
498 respectively; hydrogenotrophic methanogens: 12 and 24 times higher than drought period for ridge and slope,
499 respectively) period. Concomitantly, production of acetate and H₂ was much higher in the ridge and slope soils
500 during the drought recovery (acetate: 1.8 and 2.4 times **higher than the** drought period for ridge and slope soils,
501 respectively; H₂: 3.5 and 6.0 times **higher than the** drought period for ridge and slope soils, respectively) and the
502 post-drought (acetate: 2.3 and 3.2 times **higher than the** drought period for ridge and slope, respectively; H₂: 5.6 and
503 10 times **higher than the** drought period for ridge and slope, respectively) period. Together, gross CH₄ production in
504 the ridge and slope soils was significantly higher during the drought recovery (1.9 and 2.5 times **higher than the**
505 **drought period for ridge and slope, respectively**) and post-drought periods (3.4 and 4.6 times **higher than the drought**
506 **period for ridge and slope, respectively**) compared to the drought (Fig. S7). Simulated production of acetate was
507 increased that also lowered soil pH values during drought recovery (Fig. S6), with a more pronounced effect in the
508 ridge and slope soils. Additionally, simulated methanotrophic biomass and CH₄ oxidation decreased during the post-
509 drought period (Figs. S5, S7), which is the same time period during which net CH₄ production increased strongly.

510 For the valley soils, simulated values of **acetoclastic** methanogens and concomitant acetate production increased
511 during the 2015 drought (Figs. S5, S6). During the drought recovery and post-drought period, both **acetoclastic**
512 methanogens and acetate production decreased in the valley, while hydrogenotrophic methanogens and H₂
513 production were stable. Gross CH₄ production, however, remained relatively flat during the drought event in the
514 valley, and only increased during the post-drought period (Fig. S7). Simulated CH₄ oxidation and methanotrophic
515 biomass, on the other hand, increased dramatically during the drought and drought recovery period (Figs. S5, S7),
516 and then decreased strongly during the post-drought period. However, simulated methanotrophic biomass was
517 smaller in the valley soils compared to the ridge and slope soils. Methane oxidation by methanotrophs exerted strong
518 controls on simulated net CH₄ emissions, not only in the valley but in all the topographic positions.

Deleted: acetoclastic

Deleted: decreased strongly, resulting in decreased production of acetate and hydrogen during the 2015 drought in the ridge and slope positions

Deleted: acetoclastic

Deleted: acetoclastic

Deleted: acetoclastic

Deleted: than

Deleted: than

Deleted: than

Deleted: than

Deleted: acetoclastic

Deleted: acetoclastic

532 **3.3 The influence of microsites on net methane emissions**

533 Concomitant with decreased soil moisture, the simulated diffusion of gases (O₂, H₂) was enhanced during the
534 drought event in 2015, while diffusion of the solute (acetate) was dramatically decreased, particularly for the ridge
535 and slope soils (Fig. S8). However, reduction in soil moisture **and increase in O₂** can inhibit fermentative hydrogen
536 production (Cabrol et al., 2017). Consequently, simulated gross CH₄ production through hydrogenotrophic and
537 **acetoclastic** pathways both decreased during the drought event for the ridge and slope positions (Figs. S7, S9). As
538 soil moisture increased during the drought recovery and post-drought periods, the diffusion of gases decreased, and
539 diffusion of acetate increased in the ridge and slope soils (Fig. S8). Consequently, simulated values of gross CH₄
540 production increased and gross CH₄ oxidation decreased during drought recovery and the post-drought period (Fig.
541 S7). These factors likely contribute to the large pulses of net CH₄ emissions during the post-drought period for ridge
542 and slope positions (Fig. 3).

543 Overall, the valley soils were relatively insensitive to changes in the **diffusion rate** of either gases or solutes (Fig.
544 S8), most likely because soil moisture remained relatively stable, regardless of drought conditions (Fig. 3). The
545 lower sand and higher clay contents in the valley soils (Brenner et al., 2019), as well as the lower topographic
546 position, likely caused the valley soils to remain wetter than the slope and ridge soils. Therefore, simulated values of
547 gross CH₄ production were fairly stable in the valley soils (Fig. S7) during the drought and drought recovery period.
548 Simulated production, oxidation, and net flux of CH₄ was further modified by reactions occurring within soil
549 microsites. For example, during the drought (~DOY 200 in 2015), gross CH₄ production was more frequent in soil
550 microsites in the valley compared to the slope and ridge (Fig. 7). Simulated values of CH₄ oxidation were much
551 greater in microsites in the slope and ridge positions, so the net CH₄ emissions were positive in the valley soils and
552 negative in the ridge and slope positions. During the 2015 post-drought period (DOY 345), the frequency of CH₄
553 production was much greater in all topographic positions compared to **the** drought period (DOY 200), and it was
554 also more enhanced in the valley soils compared to the slope and ridge. Thus, net positive CH₄ emissions were
555 observed in all topographic positions in the post-drought period (Fig. 3). Methane oxidation at DOY 345 was much
556 greater in the ridge and slope compared to the valley, similar to predictions at DOY 200. Therefore, the prominent
557 CH₄ emissions from all three topographic positions were primarily due to increased production (CH₄ production on
558 DOY 345 was 150, 248, and 80 % higher than DOY 200 in ridge, slope, and valley, respectively) rather than
559 decreased oxidation (CH₄ oxidation was 32, 31, and 43 % lower on DOY 345 than DOY 200 in ridge, slope, and
560 valley, respectively), which agrees with previous studies in our site (Teh et al., 2005, 2008; von Fischer and Hedin,
561 2002).

562 Diffusion into microsites strongly affected the concentrations of gases and solutes experienced by microbes, and
563 differences as a function of topographic position were again predicted. Acetate production and diffusion were
564 enhanced in valley soils during the drought, when compared to the slope and ridge soils (Fig. S10). The H₂
565 production was also enhanced in the valley soils during the drought, but the wetter valley soils experienced lower
566 rates of H₂ diffusion compared to the ridge and slope soils. Increases in O₂ diffusion were also apparent in the ridge
567 and slope soils during the drought, and those increases were greater than in the valley soils. During the post-drought

Formatted: Font: (Default) +Body (Times New Roman), 10 pt, Subscript

Formatted: Font: (Default) +Body (Times New Roman), 10 pt

Deleted: acetoclastic

Deleted: rate of

Formatted: Font: (Default) +Body (Times New Roman), 10 pt

Deleted: pre-

571 period, however, the frequency of H₂ and O₂ diffusion was much greater for the ridge soils compared to the valley
572 soils (Fig. S10).

573 Of all parameters, the most sensitive ones were those that controlled CH₄ production through the ~~acetoclastic~~
574 pathway, followed by the parameters related to CH₄ oxidation (Fig. 8). The GSI values for parameters related to
575 ~~acetoclastic~~ methanogenesis and methanotrophy ranged between 0.25 - 0.75, whereas the corresponding GSI values
576 for hydrogenotrophic methanogenesis were always < 0.1.

577 4 Discussion

578 4.1 Mechanisms governing net methane emissions

579 Although the initial concentrations of available C for fermentation (i.e. DOC) and substrate for ~~acetoclastic~~
580 methanogenesis (i.e. acetate) in the bulk soil followed the trend of ridge > slope > valley (Fig. 2), the pattern of net
581 CH₄ emissions across the catena was opposite (valley > slope > ridge), especially in 2016 (Fig. 4). The seemingly
582 counterintuitive relations of substrate concentrations in the bulk soil versus net CH₄ emissions can be explained by
583 modeling the differing redox conditions across soil microsites. Diffusion promoted the availability of the acetate
584 substrate through more connected soil water films in the wetter valley soils and caused higher gross CH₄ production
585 in 2016, as compared to the relatively drier slope and ridge soils (Figs. S7, S8). In contrast, diffusion of gaseous
586 methanotrophic substrates (CH₄ and O₂) was promoted in the air-filled pore spaces in the drier ridge and slope soils
587 (Fig. S8), resulting in reduced net CH₄ emissions for these two topographic positions in 2016 (Fig. 4). Further,
588 reduced diffusion of O₂ in the wetter valley soils decreased gross methanotrophy compared to the slope and ridge
589 soils (Figs. S7, S8). Consequently, in 2016, net CH₄ emissions dominated the valley soils but were minimal in the
590 ridge and slope soils.

591 On the other hand, the drought event in 2015 decreased the simulated CH₄ emission in the slope and ridge soils by
592 decreasing H₂ production, and both production (Fig. S6) and diffusion of acetate (Fig. S8). The drought increased
593 the CH₄ sink strength of both ridge and slope soils as the observed net CH₄ emissions became more negative during
594 the drought compared to the pre-drought period (Fig. 3). Contributing factors predicted by the model include
595 enhanced O₂ diffusion into the drier ridge and valley soils (Fig. S8), as well as enhanced methanotrophic biomass
596 (Fig. S5). In the valley, the primary impact of the drought appeared to be due to increased methanotrophy (Fig. S7),
597 since acetate, H₂, and gross CH₄ production were predicted to continue unabated (Fig. S6, S7). This suggests that
598 drought enhanced consumption of atmospheric CH₄ in our site, which is consistent with findings from natural
599 droughts and throughfall exclusion experiments in other wet tropical forest soils (Aronson et al., 2019; Davidson et
600 al., 2004, 2008; Wood and Silver, 2012).

601 However, simulation of observed CH₄ emission during drought recovery in 2015 required explicit representations of
602 the complex interaction of the diffusive supply of solute and gases, dynamics of the microbial functional groups, and
603 the associated acetate-pH feedback loop across the distribution of soil microsites (Fig. 3). The drought recovery
604 increased soil moisture which likely prompted anaerobiosis across all topographic locations by significantly
605 reducing gas diffusivity in a fraction of the simulated microsites (11, 17, and 21 % in ridge, slope, and valley,

Deleted: acetoclastic

Deleted: acetoclastic

Deleted: acetoclastic

Deleted: >

Formatted: Font: (Default) +Body (Times New Roman), 10 pt

Formatted: Font: (Default) +Body (Times New Roman), 10 pt

Deleted:

611 respectively) (McNicol and Silver, 2014; Sihi et al., 2020a; Teh et al., 2005). The return to dominantly reducing
612 conditions also ~~was~~ predicted to stimulate fermentation and the production of acetate ~~through homoacetogenesis~~
613 (Fig. S6). Enhanced production and diffusion of acetate during recovery (Fig. S8) triggered growth in the predicted
614 biomass of ~~acetoclastic~~ methanogens (Fig. S5), which in turn, increased rates of ~~acetoclastic~~ methanogenesis (Fig.
615 S9).

616 ~~Simulated rates of hydrogenotrophic methanogenesis also increased in anaerobic microsites (Figs. S9, S10),~~
617 ~~mediated by increased production of H₂ and subsequent stimulation of the biomass of hydrogenotrophic~~
618 ~~methanogens during the drought recovery in 2015 (Fig. S5). Overall, the absolute values of simulated gross CH₄~~
619 ~~production through hydrogenotrophic and acetoclastic pathways (Fig. S9) outweighed the simulated gross CH₄~~
620 ~~oxidation rates (Fig. S7), resulting in net soil CH₄ emissions across the catena during the post-drought period (Fig.~~
621 ~~3).~~

622 ~~Acetate-driven CH₄ increases, decreases in methanotrophy due to decreasing O₂ and increasing hydrogenotrophic~~
623 ~~methanogenesis all contributed to the post-drought pulses of CH₄ (Fig. 8). Both kinds of methanogens increase~~
624 ~~during drought recovery and post-drought, but acetoclastic methanogens were two orders of magnitude more~~
625 ~~abundant than hydrogenotrophic methanogens. Additionally, acetate may accumulate in microsites during drought,~~
626 ~~and then become more available with drought recovery due to enhanced solute diffusion (Fig. S8). The model~~
627 ~~simulations suggest that hydrogen diffusion was lessened under the drought recovery, which is consistent with~~
628 ~~decreasing rates of gas diffusion through saturated soils (Fig. S8). Further, H₂ has a faster turnover rate compared to~~
629 ~~acetate (Xu et al. 2015) and therefore accumulation in soils, especially shallow soils which are the subject of this~~
630 ~~study, is minimized. So, acetate versus hydrogen substrate availability, in microsites, better explains the observations~~
631 ~~of higher CH₄ production under the post-drought conditions.~~

632 Additionally, acetate is a source of proton and should reduce soil pH (Amaral et al., 1998; Conrad and Klose, 1999;
633 Jones et al., 2003). Previous studies (Xu et al., 2015; Xu et al., 2010) demonstrated that acetate-driven soil pH
634 reduction can reduce net CH₄ production by as much as 30%, especially in systems with low initial soil pH like our
635 study site. Given that optimal pH for biological activities peaks near neutral pH, the relatively higher soil pH in the
636 valley versus ridge and slope soil further enhanced the topographic patterns of CH₄ emissions (Conrad, 1996; also
637 see Figs. 2, 3, and 4). Note that the initial soil pH across the landscape was already in the acidic range (Fig. 2),
638 consequently, the simulated acetate production and concomitant decrease in soil pH during the 2015 drought
639 recovery further suppressed gross CH₄ production in ridge soils in comparison to the valley soils (Figs. S6 and S7).
640 Iron reducing bacteria can also suppress CH₄ production either by competing with ~~acetoclastic~~ methanogens for
641 acetate substrate or controlling the flow of acetate to both hydrogenotrophic and ~~acetoclastic~~ methanogens by
642 dissimilatory iron reduction (Teh et al., 2008). Additionally, Fe reduction can increase soil pH either by proton
643 consumption and colloid dispersion, while Fe oxidation can lead to more acidic conditions (Hall and Silver, 2013;
644 Thompson et al., 2006). None of the ~~Fe-associated~~ mechanisms are currently represented in the M3D-DAMM
645 model.

646 Hence, high temporal resolution field-scale measurements of CH₄ emissions and soil and porewater chemistry
647 facilitated evaluation of the combined effects of soil redox conditions (moisture and O₂ concentrations) and

Deleted: ere

Formatted

... [128]

Deleted: acetoclastic...ceticlastic methanogens (Fig. S5), which in turn, increased rates of acetoclastic

... [129]

Formatted

... [130]

Deleted: et al.... 1996; also see Figs. 2, 3, and 4). Note that the initial soil pH across the landscape was already in the acidic range (Fig. 2), consequently, the simulated acetate production and concomitant decrease in soil pH during the 2015 drought recovery further suppressed gross CH₄ production in ridge soils in comparison to the valley soils (Figs. S6 and S7). Iron reducing bacteria can also suppress CH₄ production either by competing with acetoclastic...ceticlastic methanogens for acetate substrate or controlling the flow of acetate to both hydrogenotrophic and acetoclastic...ceticlastic methanogens by dissimilatory iron reduction (Teh et al., 2008). Additionally, Fe reduction can increase soil pH either by proton consumption and colloid dispersion, while Fe oxidation can lead to more acidic conditions (Hall and Silver, 2013; Thompson et al., 2006). None of these

... [131]

Deleted: iron

Deleted: Although secondary to acetoclastic methanogenesis, simulated rates of hydrogenotrophic methanogenesis also increased in anaerobic microsites (Figs. S9, S10), mediated by increased production of H₂ and subsequent stimulation of the biomass of hydrogenotrophic methanogens during the drought recovery in 2015 (Fig. S5). Overall, the absolute values of simulated gross CH₄ production through hydrogenotrophic and acetoclastic pathways (Fig. S9) outweighed the simulated gross CH₄ oxidation rates (Fig. S7), resulting in net soil CH₄ emissions across the catena during the post-drought period (Fig. 3). ¶

718 associated pH feedbacks on underlying processes occurring across soil microsites, while accounting for variation
719 along the catena as a result of changing climatic drivers over time. The M3D-DAMM model captured the Birch-type
720 effect by quantifying the pulses in soil CH₄ emissions as a function of increases in soil moisture following a strong
721 drought (Birch, 1958). Specifically, the model coupled with microsite diffusivity explained CH₄ emissions common
722 to wet valley soils and rare in comparatively drier ridge and slope soils and predicted the net release of CH₄
723 emissions from all topographic positions following a strong drought.

724 4.2 Sensitivity analysis

725 The variance-based sensitivity analysis confirmed the importance of microbial functional groups and their complex
726 interactions with the surrounding biophysical and chemical environments in controlling CH₄ production and
727 oxidation. For example, the growth and death of acetoclastic methanogens and the relative efficiency of acetoclastic
728 methanogenesis were the most sensitive parameters (Fig. 8), which is consistent with another modeling effort on
729 CH₄ fluxes across the Arctic landscape (Wang et al., 2019). Although from completely different ecosystem types,
730 Wang et al. (2019) and the present study confirmed the importance of simulating soil topographies and microbial
731 mechanisms when evaluating the heterogeneities in CH₄ fluxes. Representations of both direct (methanogenic
732 substrate) and indirect (soil pH feedback) effects of acetate may have contributed to higher GSI values for
733 parameters representing acetoclastic methanogenesis, which is similar to a previous study (Xu et al., 2015). The
734 sensitivity of CH₄ emissions to the parameters representing methanotrophy were secondary to those representing
735 acetoclastic methanogenesis, which is consistent with the increase in methanotrophic biomass during the drought.
736 Our predicted changes in microbial biomass might be unacceptably large for the entire soil microbial community,
737 which may only double or perhaps quadruple in response to changes in conditions, but individuals can grow
738 exponentially (Goberna et al. 2010; Pavlov and Ehrenberg 2013; Roussel et al. 2015; Buan 2018).

739 4.3 Other processes

740 We did not completely reproduce the net emissions of soil CH₄ during the 2015 post-drought period across the
741 catena with the M3D-DAMM model. To capture the full potential of net emissions of CH₄ (white shading in Fig. 3)
742 from sesquioxide-rich soils, future modeling efforts may need to explicitly include the dynamics of redox-sensitive
743 elements such as Fe and associated pH feedback under contrasting redox conditions (Barcellos et al., 2018;
744 Bhattacharyya et al., 2018; Hall and Silver, 2013, 2015, 2016; O'Connell et al., 2018; Parfitt et al., 1975; and Silver
745 et al., 1999). Wetting events can lower soil redox potential and reduce electron acceptors like Fe(III) to Fe(II). This
746 concomitant reduction of Fe may increase soil pH, especially in anaerobic microsites, which could further increase
747 net emissions of soil CH₄ (Tang et al., 2016; Zheng et al., 2019). Accounting for these effects may allow model
748 simulations to better match the highest observed net CH₄ emissions in the post-drought period (Fig. 3).
749 Additionally, the reduction of Fe(III) to Fe(II) has supported anaerobic CH₄ oxidation in other ecosystems (Ettwig et
750 al., 2016). Within this context, a measurable amount of anaerobic oxidation of CH₄ has previously been reported at
751 our study site (Blazewicz et al., 2012). Additionally, Fe-reducing microorganisms can utilize acetate as a substrate
752 and thereby compete with methanogens and reduce net methane emissions (Teh et al., 2008). Given the gradient of

Deleted: acetoclastic

Deleted: acetoclastic

Deleted: acetoclastic

Deleted: acetoclastic

Formatted: Font: (Default) +Body (Times New Roman), 10 pt, Not Italic

Formatted: Font: (Default) +Body (Times New Roman), 10 pt

757 Fe in our study site, it is likely that biogeochemical cycling of Fe and CH₄ are coupled (O'Connell et al., 2018)
758 which should be accounted for in future modeling efforts. For example, a modeling study supported the importance
759 of Fe in simulating CH₄ cycling in an Arctic soil (Tang et al., 2016). To that end, building a comprehensive
760 framework that also includes Fe biogeochemistry will afford greater confidence in projected CH₄ emissions from
761 wet tropical forests under future climatic conditions (Bonan et al., 2008; Pachauri et al., 2014; Xu et al., 2016).

762 **5 Conclusions**

763 High-frequency CH₄ emission measurements coupled with real-time soil chemical measurements identified spatial
764 and temporal variations affecting CH₄ production and oxidation in wet tropical forest soils of Puerto Rico. Overall,
765 contrasting patterns of soil moisture between ridge and valley soils played an instrumental role in governing net CH₄
766 emissions. For example, consistently greater soil moisture likely favored methanogenesis by lowering the
767 availability of O₂ in valley soils compared to ridgetop soils, especially in microsites with high soil moisture and soil
768 C content. However, soil porewater chemistry, particularly the concentrations of acetate and associated soil pH
769 influenced the pattern of net emissions of CH₄ across the catena (valley > slope > ridge) during wetting after the
770 2015 drought. Thus, our results provide compelling evidence of the importance of both hot spots and hot moments
771 in generating and mediating CH₄ emissions in wet tropical forest soils. A microbial functional group-based model
772 coupled with a diffusivity module and consideration of soil microsites adequately reproduced both the spatial and
773 temporal dynamics of soil CH₄ emissions, although mechanisms involving Fe biogeochemistry were neglected.
774 This study suggests that representing the microbial mechanisms and the interactions of microbial functional groups
775 with the soil biophysical and chemical environment across soil microsites is critical for modeling CH₄ production
776 and consumption. To that end, explicit consideration of these underlying mechanisms improved predictions of CH₄
777 dynamics in response to regional climatic events and provided insight into differential dynamics of solute and gas
778 diffusion, different microbial functions, and gross CH₄ production and oxidation as a function of topography. Hence,
779 we contribute to the ongoing development and improvements of Earth system and process models to better simulate
780 microbial roles in CH₄ cycling at regional and global scales. However, observational data concerning the activities
781 of different soil microbial functional groups is still needed to confirm the mechanisms proposed here. Future studies
782 should integrate geochemical and microbiological information relevant for oscillatory redox conditions in wet
783 tropical forests, especially those related to the redox-sensitive elements to build a comprehensive framework for
784 modeling tropical soil CH₄ emissions.

785 **Code and data availability**

786 Meteorological data (<http://criticalzone.org/luquillo/data/dataset/4723/>) are available from the Luquillo CZO
787 repository. 2015 greenhouse gas fluxes (DOI: 10.6073/pasta/316b68dd254e353e1acfb16d92bac2dc) are available
788 from the Luquillo LTER repository. The 2016 greenhouse gas fluxes (DOI: 10.15485/1632882), soil chemistry
789 (DOI: 10.15485/1618870), and rhizon lysimeter data (DOI: 10.15485/1618869) are available from ESS-DIVE
790 repository. R scripts used for this modeling exercise are archived at the following Zenodo repository (DOI:
791 10.5281/zenodo.3890562).

Formatted: Font: (Default) +Body (Times New Roman), 10 pt

792 **Author contributions**

793 DS performed the data curation of 2016 flux data and the soil and lysimeter data, collated diffusion and microsite
794 processes into the model presented herein, interpreted and validated the model application, developed the
795 visualization, and wrote the original draft. XX provided the model code used in the investigation and assisted with
796 its modification and application. MSO collected the 2016 field flux data. CSO and WLS provided the 2015 flux data
797 and the 2015-2016 field soil measurements for temperature, oxygen, and moisture. CSO developed workflow for
798 field flux data management, cleaning and analysis. WLS acquired the funding, administered the project, and
799 supervised the research team involved with collection of the 2015 data. CLL collected the rhizon water samples and
800 soil samples from the field site, with assistance from MAM. JMB analyzed the rhizon water samples in the lab. JRP,
801 RKQ, and JMB completed the laboratory soil analyses. BDN supplied, installed, and maintained the rhizon water
802 samplers. MAM acquired the funding and administered the project that collected the 2016 data, conceptualized the
803 paper and proposed the methods, supervised the research team, and contributed to the writing, interpretation, and
804 visualization of subsequent drafts. All authors contributed to the manuscript through reviewing and editing
805 subsequent drafts.

806 **Competing interests**

807 The authors declare that they have no conflicts of interest.

808 **Acknowledgements**

809 We appreciate the site access and support facilitated by Dr. Grizelle González of the U.S. Department of Agriculture
810 (USDA) Forest Service International Institute of Tropical Forestry and by Dr. Jess Zimmerman of the University of
811 Puerto Rico at Rio Piedras (UPR). We thank Dr. William McDowell of the University of New Hampshire (UNH)
812 for logistical support. We thank Mr. Brian Yudkin, Ms. Jordan Stark, and Ms. Gisela Gonzalez for assistance with
813 field data and sample collection. This work was supported through an Early Career Award to MAM through the U.S.
814 Department of Energy (DOE) Biological and Environmental Research Program; and by grants from the US DOE
815 (TES-DE-FOA-0000749) and the National Science Foundation (NSF) (DEB-1457805) to WLS, as well as the NSF
816 Luquillo Critical Zone Observatory (EAR-0722476) to UNH and the NSF Luquillo Long Term Ecological Research
817 Program (DEB-0620910) to UPR. WLS received additional support from the USDA National Institute of Food and
818 Agriculture, McIntire Stennis project CA-B-ECO-7673-MS. This research used resources of the Compute and Data
819 Environment for Science (CADES) at the Oak Ridge National Laboratory, which is managed by UT-Battelle, LLC,
820 under contract DE-AC05-00OR22725 with the U.S. Department of Energy.

821 **References**

822 Amaral, J. A., Ren, T., and Knowles, R.: Atmospheric methane consumption by forest soils and extracted bacteria at
823 different pH values, *Appl. Environ. Microbiol.*, 64, 2397-2402, 1998.

824 Andersen, B. L., Bidoglio, G., Leip, A., and Rembges, D.: A new method to study simultaneous methane oxidation
825 and methane production in soils, *Global Biogeochem. Cy.*, 12, 587-594, <https://doi.org/10.1029/98GB01975>, 1998.
826 Aronson, E. L., Dierick, D., Botthoff, J., Oberbauer, S., Zelikova, T. J., Harmon, T. C., Rundel, P., Johnson, R. F.,
827 Swanson, A. C., and Pinto-Tomás, A. A.: ENSO-influenced drought drives methane flux dynamics in a tropical wet
828 forest soil, *J. Geophys. Res.-Biogeo.*, 124, 2267-2276, <https://doi.org/10.1029/2018JG004832>, 2019.
829 Barcellos, D., O'Connell, C. S., Silver, W., Meile, C., and Thompson, A.: Hot spots and hot moments of soil
830 moisture explain fluctuations in iron and carbon cycling in a humid tropical forest soil, *Soil Systems*, 2, 59,
831 <https://doi.org/10.3390/soilsystems2040059>, 2018.
832 Bhattacharyya, A., Campbell, A. N., Tfaily, M. M., Lin, Y., Kukkadapu, R. K., Silver, W. L., Nico, P. S., and Pett-
833 Ridge, J.: Redox fluctuations control the coupled cycling of iron and carbon in tropical forest soils, *Environ. Sci.*
834 *Technol.*, 52, 14129-14139, <https://doi.org/10.1021/acs.est.8b03408>, 2018.
835 Bidot, C., Monod, H., and Taupin, M.-L.: A quick guide to multisensi, an R package for multivariate sensitivity
836 analyses, [Available at [https://mran.microsoft.com/snapshot/2017-08-](https://mran.microsoft.com/snapshot/2017-08-06/web/packages/multisensi/vignettes/multisensi-vignette.pdf)
837 [06/web/packages/multisensi/vignettes/multisensi-vignette.pdf](https://mran.microsoft.com/snapshot/2017-08-06/web/packages/multisensi/vignettes/multisensi-vignette.pdf)], 2018.
838 Birch, H.: The effect of soil drying on humus decomposition and nitrogen availability, *Plant Soil*, 10, 9-31, 1958.
839 Blazewicz, S. J., Petersen, D. G., Waldrop, M. P., and Firestone, M. K.: Anaerobic oxidation of methane in tropical
840 and boreal soils: ecological significance in terrestrial methane cycling, *J. Geophys. Res.-Biogeo.*, 117,
841 <https://doi.org/10.1029/2011JG001864>, 2012.
842 Bonan, G. B.: Forests and climate change: forcings, feedbacks, and the climate benefits of forests, *Science*, 320,
843 1444-1449, 10.1126/science.1155121, 2008.
844 Bosse, U., and Frenzel, P.: Methane emissions from rice microcosms: the balance of production, accumulation and
845 oxidation, *Biogeochemistry*, 41, 199-214, 1998.
846 Brenner, J., Porter, W., Phillips, J. R., Childs, J., Yang, X., and Mayes, M. A.: Phosphorus sorption on tropical soils
847 with relevance to Earth system model needs, *Soil Res.*, 57, 17-27, <https://doi.org/10.1071/SR18197>, 2019.
848 Buan, N. R.: Methanogens: pushing the boundaries of biology: *Emerging Topics in Life Science*, 2, 629-646,
849 <https://doi.org/10.1042/ETLS20180031>, 2018.
850 Cabrol, L., Marone, A., Tapia-Venegas, E., Steyer, J. P., Ruiz-Filippi, G., and Trabaly, E.: Microbial ecology of
851 fermentative hydrogen producing bioprocesses: useful insights for driving the ecosystem function, *FEMS microbiol.*
852 *Rev.*, 41, 158-181, <https://doi.org/10.1093/femsre/fuw043>, 2017.
853 Cabugao, K. G., Yaffar, D., Stenson, N., Childs, J., Phillips, J., Mayes, M. A., Yang, X., Weston, D. J., and Norby,
854 R. J.: bringing function to structure: Root-soil interactions shaping phosphatase activity throughout a soil profile in
855 *Puerto Rico, Ecol. Evol. (in press)*.
856 Cao, M., Dent, J., and Heal, O.: Modeling methane emissions from rice paddies, *Global Biogeochem. Cy.*, 9, 183-
857 195, <https://doi.org/10.1029/94GB03231>, 1995.
858 Cattáneo, J. H., Davidson, E. A., Nepstad, D. C., Verchot, L. V., and Ackerman, I. L.: Unexpected results of a pilot
859 throughfall exclusion experiment on soil emissions of CO₂, CH₄, N₂O, and NO in eastern Amazonia, *Biol. Fert.*
860 *Soils*, 36, 102-108, 10.1007/s00374-002-0517-x, 2002.
861 Chadwick, R., Good, P., Martin, G., and Rowell, D. P.: Large rainfall changes consistently projected over
862 substantial areas of tropical land, *Nat. Clim. Change*, 6, 177-181, 10.1038/NCLIMATE2805, 2016.
863 Conrad, R.: Soil microorganisms as controllers of atmospheric trace gases (H₂, CO, CH₄, OCS, N₂O, and NO),
864 *Microbiol. Mol. Biol. Rev.*, 60, 609-640, 1996.
865 Conrad, R., and Klose, M.: Anaerobic conversion of carbon dioxide to methane, acetate and propionate on washed
866 rice roots, *FEMS Microbiol. Ecol.*, 30, 147-155, <https://doi.org/10.1111/j.1574-6941.1999.tb00643.x>, 1999.
867 Cusack, D. F., Silver, W. L., and McDowell, W. H.: *Biological nitrogen fixation in two tropical forests: ecosystem-*
868 *level patterns and effects of nitrogen fertilization, Ecosystems*, 12, 1299-1315, 2009.
869 Davidson, E. A., Ishida, F. Y., and Nepstad, D. C.: Effects of an experimental drought on soil emissions of carbon
870 dioxide, methane, nitrous oxide, and nitric oxide in a moist tropical forest, *Glob. Change Biol.*, 10, 718-730,
871 <https://doi.org/10.1111/j.1365-2486.2004.00762.x>, 2004.
872 Davidson, E. A., Nepstad, D. C., Ishida, F. Y., and Brando, P. M.: Effects of an experimental drought and recovery
873 on soil emissions of carbon dioxide, methane, nitrous oxide, and nitric oxide in a moist tropical forest, *Glob. Change*
874 *Biol.*, 14, 2582-2590, <https://doi.org/10.1111/j.1365-2486.2008.01694.x>, 2008.
875 Davidson, E. A., Samanta, S., Caramori, S. S., and Savage, K.: The Dual Arrhenius and Michaelis-Menten kinetics
876 model for decomposition of soil organic matter at hourly to seasonal time scales, *Glob. Change Biol.*, 18, 371-384,
877 <https://doi.org/10.1111/j.1365-2486.2011.02546.x>, 2012.
878 Davidson, E. A., Savage, K. E., Trumbore, S. E., and Borken, W.: Vertical partitioning of CO₂ production within a
879 temperate forest soil, *Glob. Change Biol.*, 12, 944-956, <https://doi.org/10.1111/j.1365-2486.2005.01142.x>, 2006.

Formatted: Font: (Default) +Body (Times New Roman), 10 pt

Formatted: Font: (Default) +Body (Times New Roman), 10 pt

Deleted: .

Formatted: Font: (Default) +Body (Times New Roman), 10 pt

Formatted: Font: (Default) +Body (Times New Roman), 10 pt

Formatted: Font: (Default) +Body (Times New Roman), 10 pt, Subscript

Formatted: Font: (Default) +Body (Times New Roman), 10 pt

Formatted: Font: (Default) +Body (Times New Roman), 10 pt, Subscript

Formatted: Font: (Default) +Body (Times New Roman), 10 pt

Formatted: Font: (Default) +Body (Times New Roman), 10 pt, Subscript

Formatted: Font: (Default) +Body (Times New Roman), 10 pt

Formatted: Font: (Default) +Body (Times New Roman), 10 pt

Formatted: Font: (Default) +Body (Times New Roman), 10 pt

881 Davidson, E. A., and Trumbore, S. E.: Gas diffusivity and production of CO₂ in deep soils of the eastern Amazon,
882 Tellus B: Chem. Phys. Meteorol., 47, 550-565, <https://doi.org/10.3402/tellusb.v47i5.16071>, 1995.

883 Etwig, K. F., Zhu, B., Speth, D., Keltjens, J. T., Jetten, M. S., and Kartal, B.: Archaea catalyze iron-dependent
884 anaerobic oxidation of methane, P. Natl. A. Sci., 113, 12792-12796, <https://doi.org/10.1073/pnas.1609534113>, 2016.

885 [Goberna, M., Gadermaier, M., Garcia, C., Wett, B., Insam, H.: Adaptation of methanogenic communities to the
886 cofermentation of cattle excreta and olive mill wastes at 37 °C and 55 °C. Appl. Environ. Microb., 76, 19, 6564-
887 6571, doi:10.1128/AEM.00961-10, 2010.](#)

888 Hall, S. J., and Silver, W. L.: Iron oxidation stimulates organic matter decomposition in humid tropical forest soils,
889 Glob. Change Biol., 19, 2804-2813, <https://doi.org/10.1111/gcb.12229>, 2013.

890 Hall, S. J., and Silver, W. L.: Reducing conditions, reactive metals, and their interactions can explain spatial patterns
891 of surface soil carbon in a humid tropical forest, Biogeochemistry, 125, 149-165, [doi:10.1007/s10533-015-0120-5](https://doi.org/10.1007/s10533-015-0120-5),
892 2015.

893 [Hall, S. J., Liptzin, D., Buss, H. L., DeAngelis, K., and Silver, W. L.: Drivers and patterns of iron redox cycling
894 from surface to bedrock in a deep tropical forest soil: A new conceptual model, Biogeochemistry, 130\(1-2\), 177-
895 190, 2016.](#)

896 [Harris, N. L., Lugo, A. E., Brown, S., and Heartsill-Scalley, T. \(Eds.\): Luquillo Experimental Forest: Research
897 history and Opportunities, EFR-1, Washington, DC: U.S. Department of Agriculture, 152 p., 2012.](#)

898 Heartsill-Scalley, T., Scatena, F. N., Estrada, C., McDowell, W., and Lugo, A. E.: Disturbance and long-term
899 patterns of rainfall and throughfall nutrient fluxes in a subtropical wet forest in Puerto Rico, J Hydrol., 333, 472-485,
900 <https://doi.org/10.1016/j.jhydrol.2006.09.019>, 2007.

901 [Johnson, A. H., Xing, H. X., and Scatena, F. N.: Controls on soil carbon stocks in El Yunque National Forest, Puerto
902 Rico: Soil Sci. Soc. Am. J., 79, 294-304, doi:10.2136/sssaj2014.05.0199, 2014.](#)

903 Jones, D., Dennis, P., Owen, A., and Van Hees, P.: Organic acid behavior in soils—misconceptions and knowledge
904 gaps, Plant Soil, 248, 31-41, 2003.

905 Keller, M., and Matson, P. A.: Biosphere-atmosphere exchange of trace gases in the tropics: Evaluating the effects
906 of land use changes, in: Global Atmospheric-Biospheric Chemistry, Springer, 103-117, 10.1007/978-1-4615-2524-0,
907 1994.

908 Liptzin, D., Silver, W. L., and Detto, M.: Temporal dynamics in soil oxygen and greenhouse gases in two humid
909 tropical forests, Ecosystems, 14, 171-182, 10.1007/s10021-010-9402-x, 2011.

910 Marshall, T.: Gas diffusion in porous media, Science, 130, 100-102, 10.1126/science.130.3367.100-a, 1959.

911 Massman, W.: A review of the molecular diffusivities of H₂O, CO₂, CH₄, CO, O₃, SO₂, NH₃, N₂O, NO, and NO₂ in
912 air, O₂ and N₂ near STP, Atmos. Environ., 32, 1111-1127, [https://doi.org/10.1016/S1352-2310\(97\)00391-9](https://doi.org/10.1016/S1352-2310(97)00391-9), 1998.

913 McNicol, G., and Silver, W. L.: Separate effects of flooding and anaerobiosis on soil greenhouse gas emissions and
914 redox sensitive biogeochemistry, J. Geophys. Res.-Biogeo., 119, 557-566, <https://doi.org/10.1002/2013JG002433>,
915 2014.

916 [Megonigal, J. P., and Geunther, A. B.: Methane emissions from upland forest soils and vegetation, Tree Physiol., 28,
917 491-498, 2008.](#)

918 Neelin, J. D., Münnich, M., Su, H., Meyerson, J. E., and Holloway, C. E.: Tropical drying trends in global warming
919 models and observations, P. Natl. A. Sci., 103, 6110-6115, <https://doi.org/10.1073/pnas.0601798103>, 2006.

920 [Narrows, A. B., Borton, M. A., Hoyt, D. W., Smith, G. J., Daly, R. A., Angle, J. C., Eder, E. K., Wong, A. R.,
921 Wolfe, R. A., Pappas, A., Bohrer, G., Miller, C. S., and Wrighton, K. A.: Uncovering the diversity and activity of
922 methylophilic methanogens in freshwater wetland soils, mSystems, 4\(6\), e00320-19,
923 doi: 10.1128/mSystems.00320-19, 2019.](#)

924 [O'Connell, C. S., Ruan, L., and Silver, W. L.: Drought drives rapid shifts in tropical rainforest soil biogeochemistry
925 and greenhouse gas emissions. Nat. Commun., 9, 1-9, 10.1038/s41467-018-03352-3, 2018.](#)

926 [Pachauri, R. K., Allen, M. R., Barros, V. R., Broome, J., Cramer, W., Christ, R., Church, J. A., Clarke, L., Dahe, Q.,
927 Dasgupta, P.: Climate change 2014: Synthesis report. Contribution of Working Groups I, II and III to the Fifth
928 Assessment Report of the Intergovernmental Panel on Climate Change, IPCC, 10013/epic.45156.d001, 2014.](#)

929 Papendick, R., and Campbell, G. S.: Theory and measurement of water potential, Water Potential Relations in Soil
930 Microbiology, 9, 1-22, <https://doi.org/10.2136/sssaspecpub9.c1>, 1981.

931 Parfitt, R. L., Atkinson, R. J., and Smart, R. S. C.: The mechanism of phosphate fixation by iron oxides, Soil Sci.
932 Soc. Am. J., 39, 837-841, <https://doi.org/10.2136/sssaj1975.03615995003900050017x>, 1975.

933 [Parton, W., Silver, W. L., Burke, I., Grassens, L., Harmon, M. E., Currie, W. S., King, J. Y., Adair, E. C., Brandt, L.
934 A., Hart, S. C., and Fasth, B.: Global-scale similarities in nitrogen release patterns during long-term decomposition,
935 Science, 315, 361-364, doi: 10.1126/science.1134853, 2007.](#)

Formatted: Default Paragraph Font, Font: (Default) +Body (Times New Roman), 10 pt

Formatted: Font: (Default) +Body (Times New Roman), 10 pt

Formatted: Default Paragraph Font, Font: (Default) +Body (Times New Roman), 10 pt

Formatted: Font: (Default) +Body (Times New Roman), 10 pt

Formatted: Line spacing: single

Formatted: Justified

Formatted: Font: (Default) +Body (Times New Roman), 10 pt, Not Highlight

Formatted: Font: (Default) +Body (Times New Roman), 10 pt, Not Highlight

Formatted: Font: (Default) +Body (Times New Roman), 10 pt

Formatted: Font: (Default) +Body (Times New Roman), 10 pt, Not Highlight

Formatted: Font: (Default) +Body (Times New Roman), 10 pt

Formatted: Font: (Default) +Body (Times New Roman), 10 pt, Not Highlight

Formatted: Font: (Default) +Body (Times New Roman), 10 pt

Formatted: Font: (Default) +Body (Times New Roman), 10 pt, Not Highlight

Formatted: Font: (Default) +Body (Times New Roman), 10 pt, Not Highlight

Formatted: Font: (Default) +Body (Times New Roman), 10 pt

Formatted: Font: (Default) +Body (Times New Roman), 10 pt, Not Highlight

Deleted: ¶

Formatted: Font: (Default) +Body (Times New Roman), 10 pt

Deleted: Ostertag, R., Scatena, F. N., and Silver, W. L.: Forest floor decomposition following hurricane litter inputs in several Puerto Rican forests, Ecosystems, 261-273, 10.1007/s10021-002-0203-8, 2003.¶

Deleted: p

Deleted: r

Deleted: s

Deleted: m

Deleted:

946 Patil, I.: ggstatsplot: "ggplot2" Based Plots with Statistical Details, [Available at [https://CRAN.R-](https://CRAN.R-project.org/package=ggstatsplot)
947 [project.org/package=ggstatsplot](https://CRAN.R-project.org/package=ggstatsplot)], <http://doi.org/10.5281/zenodo.2074621>, 2018.

948 [Pavlov, M. Y., and Ehrenberg, M.: Optimal control of gene expression for fast proteome adaptation to](#)
949 [environmental change. Proc. Natl. Acad. Sci. U.S.A., 110 \(51\), 20527-20532, doi/10.1073/pnas.1309356110, 2013.](#)

950 Pumpanen, J., Kolari, P., Ilvesniemi, H., Minkkinen, K., Vesala, T., Niinistö, S., Lohila, A., Larmola, T., Morero,
951 M., and Pihlatie, M.: Comparison of different chamber techniques for measuring soil CO₂ efflux, *Agr. Forest*
952 *Meteorol.*, 123, 159-176, <https://doi.org/10.1016/j.agrformet.2003.12.001>, 2004.

953 R Core Team.: R: A language and environment for statistical computing, Vienna, Austria, [Available at
954 <https://www.r-project.org/>], 2018.

955 [Rochette, P., and Hutchinson, G. L.: Measurement of soil respiration in situ: Chamber techniques. Publications from](#)
956 [USDA-ARS / UNL Faculty, 1379, https://digitalcommons.unl.edu/usdaarsfacpub/1379, 2005.](#)

957 [Roussel E. G., Cragg, B. A., Webster, G., Sass, H., Tang, X., Williams, A. S., Gorra, R., Weightman, A. J., and](#)
958 [Parkes, R. J.: Complex coupled metabolic and prokaryotic community responses to increasing temperatures in](#)
959 [anaerobic marine sediments: Critical temperatures and substrate changes, FEMS Microbiology Ecology, 91, 2015,](#)
960 [fiv084, doi: 10.1093/femsec/fiv084, 2015.](#)

961 Scatena, F. N.: An introduction to the physiography and history of the Bisley Experimental Watersheds in the
962 Luquillo Mountains of Puerto Rico, Gen. Tech. Rep. SO-72. New Orleans, LA: US Dept of Agriculture, Forest
963 Service, Southern Forest Experiment Station. 22 p., 72, 1989.

964 Scatena, F., and Lugo, A. E.: Geomorphology, disturbance, and the soil and vegetation of two subtropical wet
965 stepland watersheds of Puerto Rico, *Geomorphology*, 13, 199-213, [https://doi.org/10.1016/0169-555X\(95\)00021-](https://doi.org/10.1016/0169-555X(95)00021-)
966 [V, 1995.](#)

967 Sihi, D.: PR-model v1.0., 10.5281/zenodo.3890562, [available at
968 <https://zenodo.org/record/3890562#.XuOP3DpKg2w>], 2020.

969 Sihi, D., Davidson, E. A., Chen, M., Savage, K. E., Richardson, A. D., Keenan, T. F., and Hollinger, D. Y.: Merging
970 a mechanistic enzymatic model of soil heterotrophic respiration into an ecosystem model in two AmeriFlux sites of
971 northeastern USA, *Agr. Forest Meteorol.*, 252, 155-166, <https://doi.org/10.1016/j.agrformet.2018.01.026>, 2018.

972 Sihi, D., Davidson, E. A., Savage, K. E., and Liang, D.: Simultaneous numerical representation of soil microsite
973 production and consumption of carbon dioxide, methane, and nitrous oxide using probability distribution functions,
974 *Glob. Change Biol.*, 26, 200-218, <https://doi.org/10.1111/gcb.14855>, 2020a.

975 Sihi, D., López-Lloreda, C., Brenner J. M., Quinn R. K., Phillips J. R., Mayes, M. A.: Soil chemistry data across a
976 catena in the Luquillo Experimental Forest, Puerto Rico. *A Comprehensive Framework for Modeling Emissions*
977 *from Tropical Soils and Wetlands*, doi:10.15485/1618870, 2020b.

978 Sihi, D., López-Lloreda, C., Brenner J. M., Quinn R. K., Phillips J. R., Newman B. D., Mayes, M. A.: Porewater data
979 across a catena in the Luquillo Experimental Forest, Puerto Rico. *A Comprehensive Framework for Modeling*
980 *Emissions from Tropical Soils and Wetlands*, doi:10.15485/1618869, 2020c.

981 Sihi, D., Salazar-Ortiz, M., Mayes, M. A.: Soil chamber fluxes (CO₂ and CH₄) across a catena in the Luquillo
982 Experimental Forest, Puerto Rico. *A Comprehensive Framework for Modeling Emissions from Tropical Soils and*
983 *Wetlands*, doi:10.15485/1632882, 2020d.

984 Silver, W. L., Liptzin, D., and Almaraz, M.: Soil redox dynamics and biogeochemistry along a tropical elevation
985 gradient, in: *Ecological gradient analyses in a tropical landscape*, edited by: González, G., Willig, M. R., and Waide,
986 R. B., *Ecol. Bull., Wiley-Blackwell, Hoboken, NJ*, 54, 195-210, 2013.

987 Silver, W. L., Lugo, A., and Keller, M.: Soil oxygen availability and biogeochemistry along rainfall and topographic
988 gradients in upland wet tropical forest soils, *Biogeochemistry*, 44, 301-328, 1999.

989 [Six, J., Bossuyt, H., Dergryze, S., Deneff, K.: A history of research on the link between \(micro\)aggregates, soil biota,](#)
990 [and soil organic matter dynamics, Soil and Tillage Res., 79, 7-31, 2005.](#)

991 [Soetaert, K.: R Package FME: Inverse modelling, sensitivity, Monte Carlo—Applied to a dynamic simulation](#)
992 [model, \(CRAN Vignette 2\). \[Available at https://cran.r-project.org/web/packages/FME/vignettes/FMEdyna.pdf.\],](#)
993 [2016.](#)

994 [Soil Survey Staff: Order 1 Soil Survey of the Luquillo Long-Term Ecological Research Grid, Puerto Rico, USDA,](#)
995 [NRCS, https://luq.lter.network/content/order-i-soil-survey-luquillo-long-term-ecological-research-grid-puerto-rico,](#)
996 [1995.](#)

997 Tang, G., Zheng, J., Xu, X., Yang, Z., Graham, D. E., Gu, B., Painter, S. L., and Thornton, P. E.: Biogeochemical
998 modeling of CO₂ and CH₄ production in anoxic Arctic soil microcosms, *Biogeosciences*, 13, 5021,
999 <https://doi.org/10.5194/bg-13-5021-2016>, 2016.

Formatted: Font: (Default) +Body (Times New Roman), 10 pt

Formatted: Font: (Default) +Body (Times New Roman), 10 pt

Deleted: ¶

Deleted: ,

Deleted: .

Deleted: .

Formatted: Font: (Default) +Body (Times New Roman), 10 pt

Formatted: Font: (Default) +Body (Times New Roman), 10 pt

Formatted: Font: (Default) +Body (Times New Roman), 10 pt

1004 Teh, Y. A., Dubinsky, E. A., Silver, W. L., and Carlson, C. M.: Suppression of methanogenesis by dissimilatory Fe
1005 (III)-reducing bacteria in tropical rain forest soils: Implications for ecosystem methane flux, *Glob. Change Biol.*, 14,
1006 413-422, <https://doi.org/10.1111/j.1365-2486.2007.01487.x>, 2008.

1007 Teh, Y. A., and Silver, W. L.: Effects of soil structure destruction on methane production and carbon partitioning
1008 between methanogenic pathways in tropical rain forest soils, *J. Geophys. Res.-Biogeo.*, 111,
1009 <https://doi.org/10.1029/2005JG000020>, 2006.

1010 Teh, Y. A., Silver, W. L., and Conrad, M. E.: Oxygen effects on methane production and oxidation in humid tropical
1011 forest soils, *Glob. Change Biol.*, 11, 1283-1297, <https://doi.org/10.1111/j.1365-2486.2005.00983.x>, 2005.

1012 Thomas, G. W.: Soil pH and soil acidity, *Methods of Soil Analysis: Part 3 Chemical Methods*, 5, 475-490,
1013 <https://doi.org/10.2136/sssabookser5.3.c16>, 1996.

1014 Thompson, A., Chadwick, O. A., Boman, S., and Chorover, J.: Colloid mobilization during soil iron redox
1015 oscillations, *Environ. Sci. Technol.*, 40, 5743-5749, <https://doi.org/10.1021/es061203b>, 2006.

1016 Verchot, L. V., Davidson, E. A., Cattânio, J. H., and Ackerman, I. L.: Land-use change and biogeochemical controls
1017 of methane fluxes in soils of eastern Amazonia, *Ecosystems*, 3, 41-56, <https://doi.org/10.1007/s100210000009>,
1018 2000.

1019 von Fischer, J. C., and Hedin, L. O.: Separating methane production and consumption with a field-based isotope
1020 pool dilution technique, *Global Biogeochem. Cy.*, 16, 1034, <https://doi.org/10.1029/2001GB001448>, 2002.

1021 Wadsworth, F. H.: Forest management in the Luquillo mountains, I-setting, *Caribbean Forester*, 12, 114-124, 1951.

1022 Wang, Y., Yuan, F., Yuan, F., Gu, B., Hahn, M. S., Torn, M. S., Ricciuto, D. M., Kumar, J., He, L., Zona, D.,
1023 Lipson, D. L., Wagner, R., Oechel, W. C., Wullschleger, S. D., Thornton, P. E., and Xu, X.: Mechanistic modeling
1024 of microtopographic impact on CH₄ processes in an Alaskan tundra ecosystem using the CLM-Microbe model, *J.*
1025 *Adv. Model. Earth Sy.*, 11, 4228-4304, 2019.

1026 Wickham, H.: *ggplot2: elegant graphics for data analysis*, Springer-Verlag, New York, 2016.

1027 Wood, T. E., and Silver, W. L.: Strong spatial variability in trace gas dynamics following experimental drought in a
1028 humid tropical forest, *Global Biogeochem. Cy.*, 26, <https://doi.org/10.1029/2010GB004014>, 2012.

1029 Xu, X., Elias, D. A., Graham, D. E., Phelps, T. J., Carroll, S. L., Wullschleger, S. D., and Thornton, P. E.: A
1030 microbial functional group-based module for simulating methane production and consumption: Application to an
1031 incubated permafrost soil, *J. Geophys. Res.-Biogeo.*, 120, 1315-1333, [10.1002/2015jg002935](https://doi.org/10.1002/2015jg002935), 2015.

1032 Xu, X. F., Tian, H. Q., Zhang, C., Liu, M. L., Ren, W., Chen, G. S., Lu, C. Q., and Bruhwiler, L.: Attribution of
1033 spatial and temporal variations in terrestrial methane flux over North America, *Biogeosciences*, 7, 3637-3655,
1034 [10.5194/bg-7-3637-2010](https://doi.org/10.5194/bg-7-3637-2010), 2010.

1035 Xu, X., Yuan, F., Hanson, P. J., Wullschleger, S. D., Thornton, P. E., Riley, W. J., Song, X., Graham, D. E., Song,
1036 C., and Tian, H.: Reviews and syntheses: Four decades of modeling methane cycling in terrestrial ecosystems,
1037 *Biogeosciences*, 13, 3735-3755, [10.5194/bg-13-3735-2016](https://doi.org/10.5194/bg-13-3735-2016), 2016.

1038 Zheng, J., Thornton, P. E., Painter, S. L., Gu, B., Wullschleger, S. D., and Graham, D. E.: Modeling anaerobic soil
1039 organic carbon decomposition in Arctic polygon tundra: insights into soil geochemical influences on carbon
1040 mineralization, *Biogeosciences*, 16, 663-680, [10.5194/bg-16-663-2019](https://doi.org/10.5194/bg-16-663-2019), 2019.

1041

Deleted: v

Deleted: ¶

Formatted: Font: (Default) +Body (Times New Roman), 10 pt

Deleted: ¶

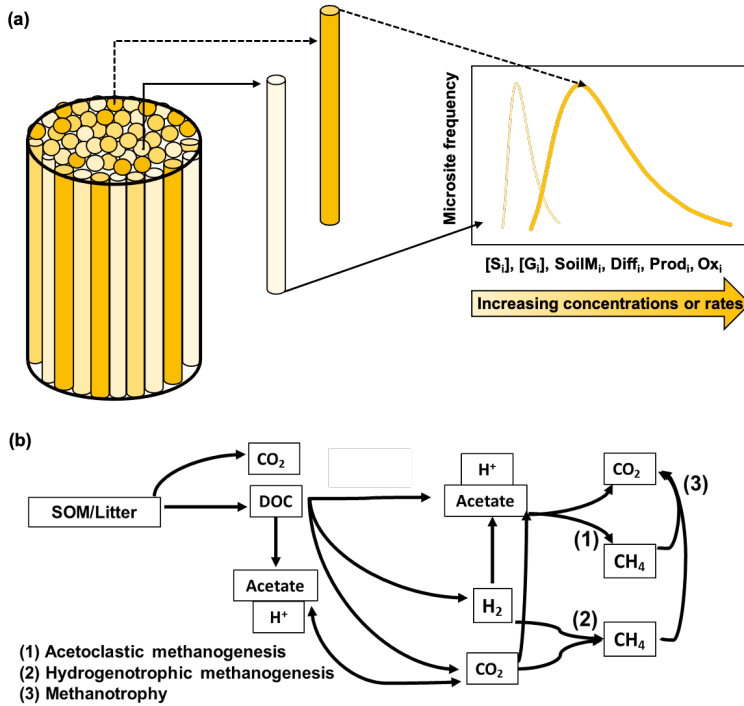
1046 **Table 1: Fitted values of M3D-DAMM model parameters.**

Parameters	Fitted values	Description	Unit	Source
GrowR_{H₂Methanogens}	0.31	Growth rates	1/day	Servais et al., 1985
GrowR_{AceMethanogens}	1.59		1/day	Servais et al., 1985
GrowR_{Methanotrophs}	0.12		1/day	Servais et al., 1985
DeadR_{H₂Methanogens}	0.03	Death rates	1/day	Servais et al., 1985
DeadR_{AceMethanogens}	0.54		1/day	Servais et al., 1985
DeadR_{Methanotrophs}	0.008		1/day	Servais et al., 1985
Efficiency_{H₂Methanogens}	0.2	Substrate use efficiencies	unitless	Grant, 1998
Efficiency_{AceMethanogens}	0.04		unitless	Kettunen et al., 2003
Efficiency_{Methanotrophs}	0.4		unitless	Kettunen et al., 2003
KM_{Ace}	16	Half-saturation constants	mmol/m3	Grant, 1998; McGill et al., 1981
KM_{H₂ProdAce}	11		μmol/m3	Conrad, 1989
KM_{H₂ProdCH₄}	2.14*10 ⁻⁵		mmol/m3	Fennell and Gossett, 1998
KM_{CO₂ProdCH₄}	9.08*10 ⁻⁹		mmol/m3	Stoichiometry theory
KM_{CH₄ProdAce}	13		mmol/m3	Kettunen et al., 2003
KM_{CH₄ProdO₂}	0.03		mmol/m3	Kettunen et al., 2003
KM_{CH₄OxidCH₄}	0.06		mmol/l	Kettunen et al., 2003
KM_{CH₄OxidO₂}	0.74		mmol/l	Kettunen et al., 2003
ACmax_{AceProd}	0.52		Maximum reaction rates	mmol/m3/h
Acemax_{H₂Prod}	1.31	reaction rates	mmol acetate/g/h	Conrad, 1989
rCH₄Prod	0.84	Rate constants	mol CH ₄ /mol acetate	Kettunen et al., 2003
rCH₄Oxid	3.06	constants	mol O ₂ /mol CH ₄	Kettunen et al., 2003
Q_{10AceMin}	1.16	Temperature sensitivities	unitless	Segers, 1998
Q_{10AceProd}	1.21		unitless	Atlas and Bartha, 1987; Kettunen, 2003; Van Hulzen et al., 1999
Q_{10H₂CH₄Prod}	1.27		unitless	Segers, 1998
Q_{10CH₄Prod}	1.13		unitless	Kettunen et al., 2003
Q_{10CH₄Oxid}	1.18		unitless	Kettunen et al., 2003

1047

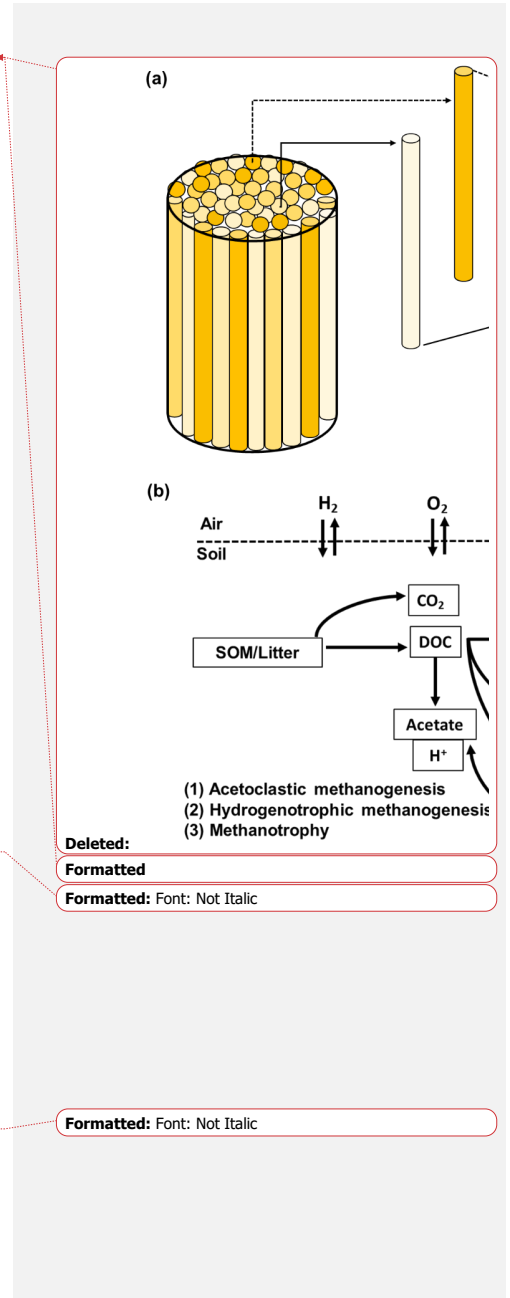
1048 Initial values of model parameters were collected from literature ("Source"). Also see Xu et al. (2015) for detailed information
 1049 on model parameters.

050



051

052 Figure 1: Conceptual figure of the modelling approach. Top panel (a), Top panel (a) shows the model representation of soil
 053 microsite distribution (modified from Sihi et al., 2020a, also see Eq. 14). The cylinder refers to the volume beneath the soil
 054 chambers. The intensity of different cylinder colors figure refers to rate of a process or the intensity of a concentration inside
 055 microsities in each theoretical cylinder, e.g., a dark color means a higher rate/intensity, and a light color means a lower
 056 rate/intensity for a given process. The 2D graph on the right refers to the probability density function of the rate of the process or
 057 intensity of the concentration in the bulk soil. A wide distribution skewed to the right (dark line) implies higher bulk rates of the
 058 process or higher concentrations, and a narrow distribution skewed to the left (light line) implies lower bulk rates of the process or
 059 lower concentrations, of any of the following: solute concentration $[S_i]$, gas concentration $[G_i]$, soil moisture (SoilM_i), gas and
 060 solute diffusion (Diff_i), methane production (Prod_i), and methane oxidation (Ox_i). Bottom panel (b) is the schematic of the
 061 microbial functional group-based model for simulating soil methane (CH₄) dynamics in field soils (modified from Xu et al., 2015).
 062 The schematic represents the decomposition of soil organic matter (SOM) and plant litter into carbon dioxide (CO₂) and dissolved
 063 organic matter (DOC); the production of acetate and hydronium ion (H⁺) from decomposition and fermentation of DOC which
 064 also decreases pH; the production of acetate and hydronium ion (H⁺) from homoacetogenesis which decreases pH; and the
 065 production of dihydrogen ion (H₂) and CO₂ from decomposition of DOC. The intermediary products then have three possible
 066 non-mutually exclusive pathways (1) acetoclastic methanogenesis, which is the production of methane from aqueous acetate found
 067 in soil solutions, (2) hydrogenotrophic methanogenesis, which is the production of methane from hydrogen, and (3)
 068 methanotrophy, which is the oxidation of methane into carbon dioxide.



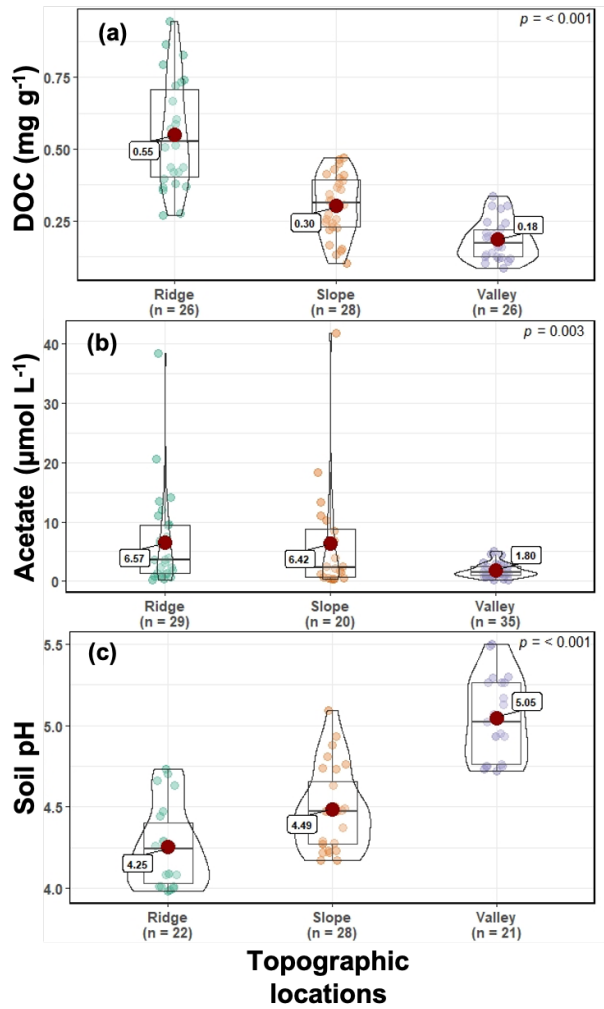
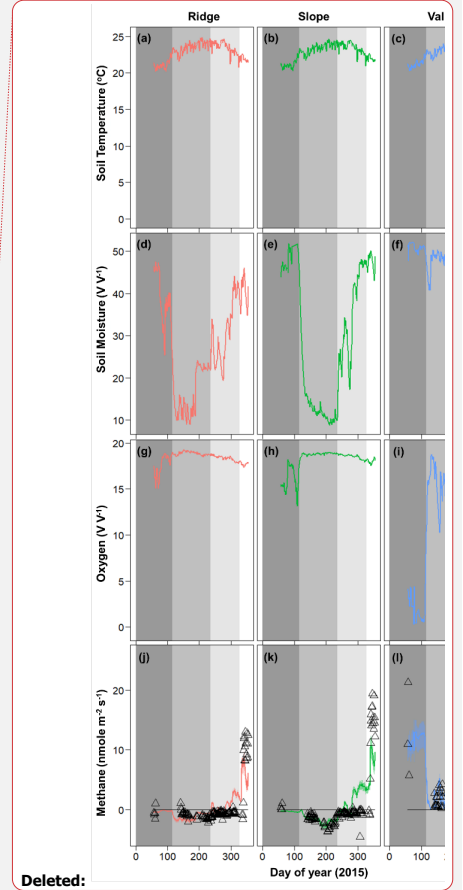
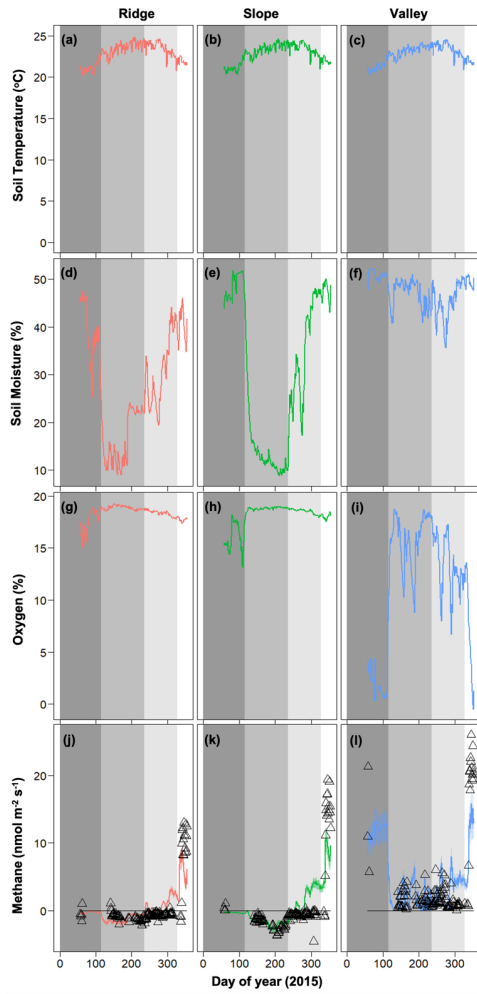


Figure 2: Soil and porewater chemistry (dissolved organic carbon [DOC] (a), acetate (b), and pH (c)) along the ridge-slope-valley topographic gradient.

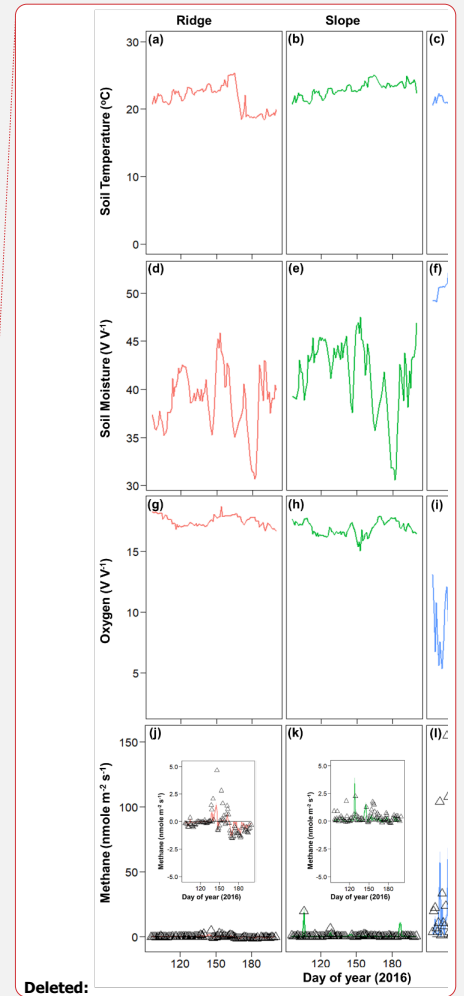
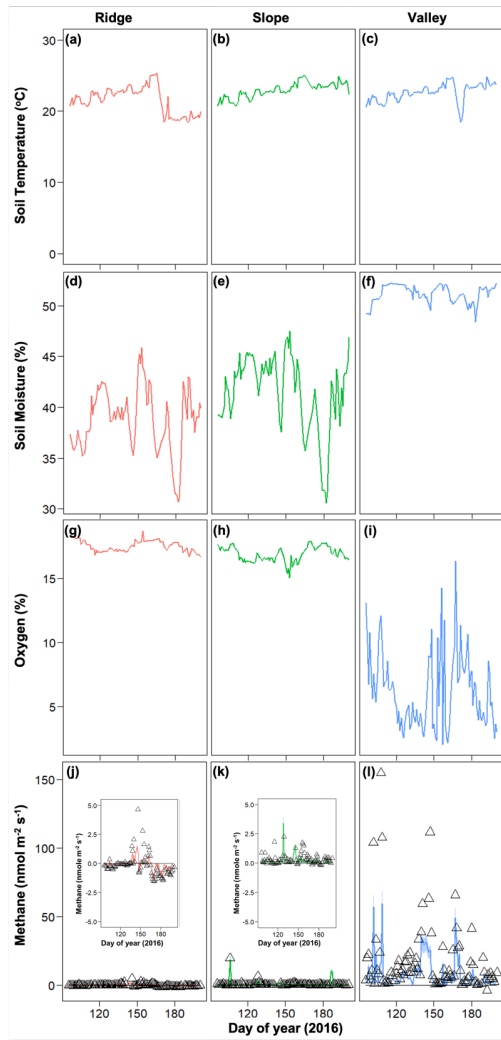
Deleted: shows the model representation of soil microsite distribution (modified from Sibi et al., 2020, also see Eq. 13). Different shades indicate substrate concentration [S], soil moisture (SoilM), diffusion (Diff) of solutes and gases, production (Prod) and oxidation (Ox) processes at each microsite. Bottom panel (b) is the schematic of the microbial functional group-based model coupled with a diffusivity module (Microbial Model for Methane Dynamics-Dual Arrhenius and Michaelis Menten, M3D-DAMM) for simulating soil methane (CH₄) dynamics in field soils (Modified from Xu et al., 2015), where SOM = soil organic matter, CO₂ = carbon dioxide, DOC = dissolved organic carbon, H⁺ is the hydronium ion, and H₂ = dihydrogen molecule. ... [132]



Deleted:

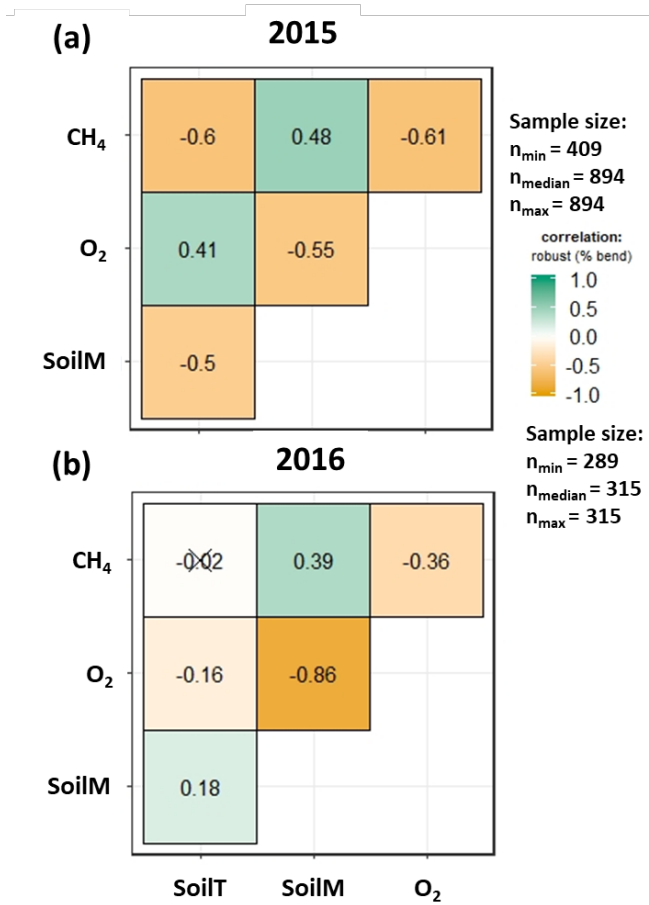
087
088
089
090
091

Figure 3: Temporal dynamics of observed meteorological drivers (soil temperature (a-c), soil moisture (d-f), soil oxygen (g-i) and net methane emissions (j-l) for 2015 (Data are taken from O'Connell et al., 2018). For methane emissions, symbols represent observed data and lines represent model simulations. Dark gray, medium gray, light gray, and white shading represent pre-drought, drought, drought recovery, and post drought events (O'Connell et al., 2018).



093
094
095
096

Figure 4: Temporal dynamics of observed meteorological drivers (soil temperature (a-c), soil moisture (d-f), soil oxygen (g-i)) and net methane emissions (j-l) for 2016. For methane emissions, symbols represent observed data and lines represent model simulations.



099
100
101
102
Figure 5: Relation between soil meteorology and methane emissions for 2015 (a) and 2016 (b). SoilM, SoilT, O₂, CH₄ represent soil moisture, soil temperature, oxygen, and methane, respectively. Numbers represent adjusted Holm correlation coefficients, and numbers with "X" indicate a non-significant correlation at p < 0.05.

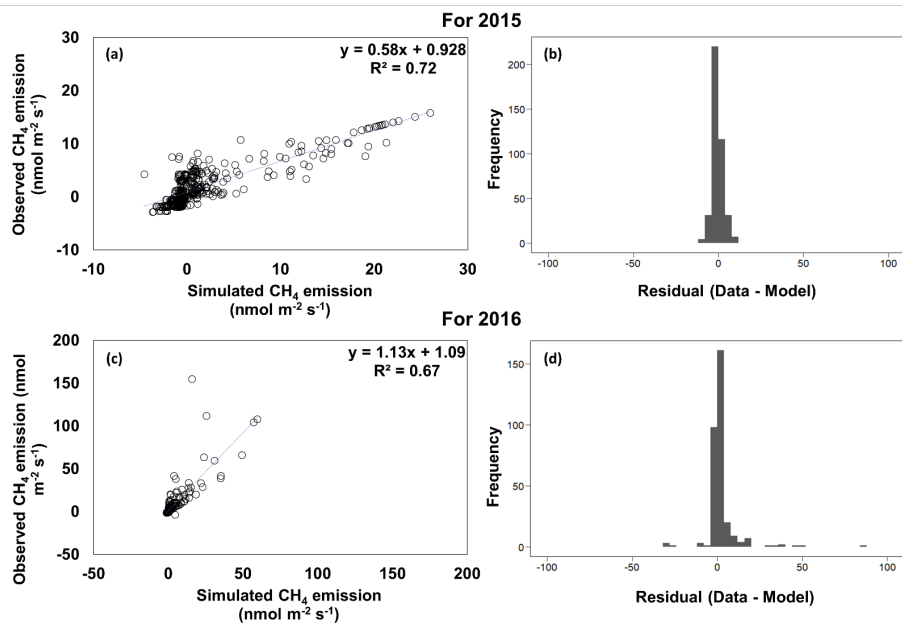


Figure 6: Observed versus simulated methane (CH_4) emissions and model residuals for 2015 (a, b) and 2016 (c, d).

103
104
105

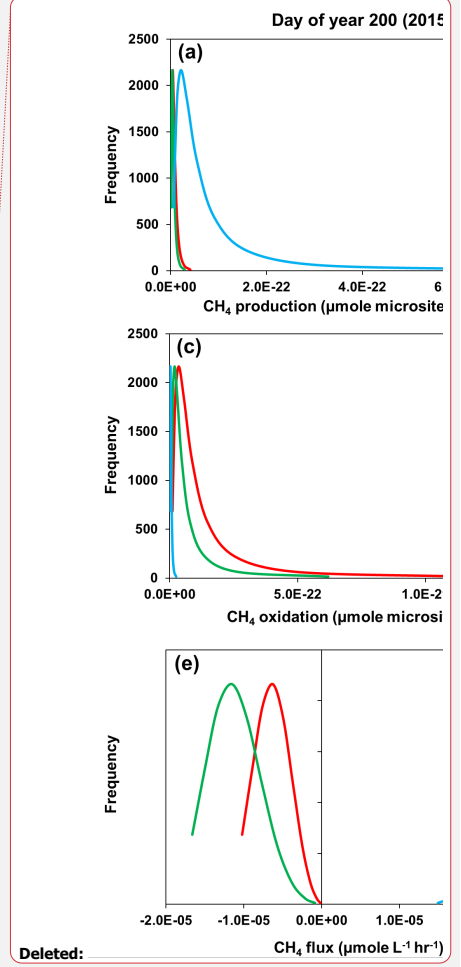
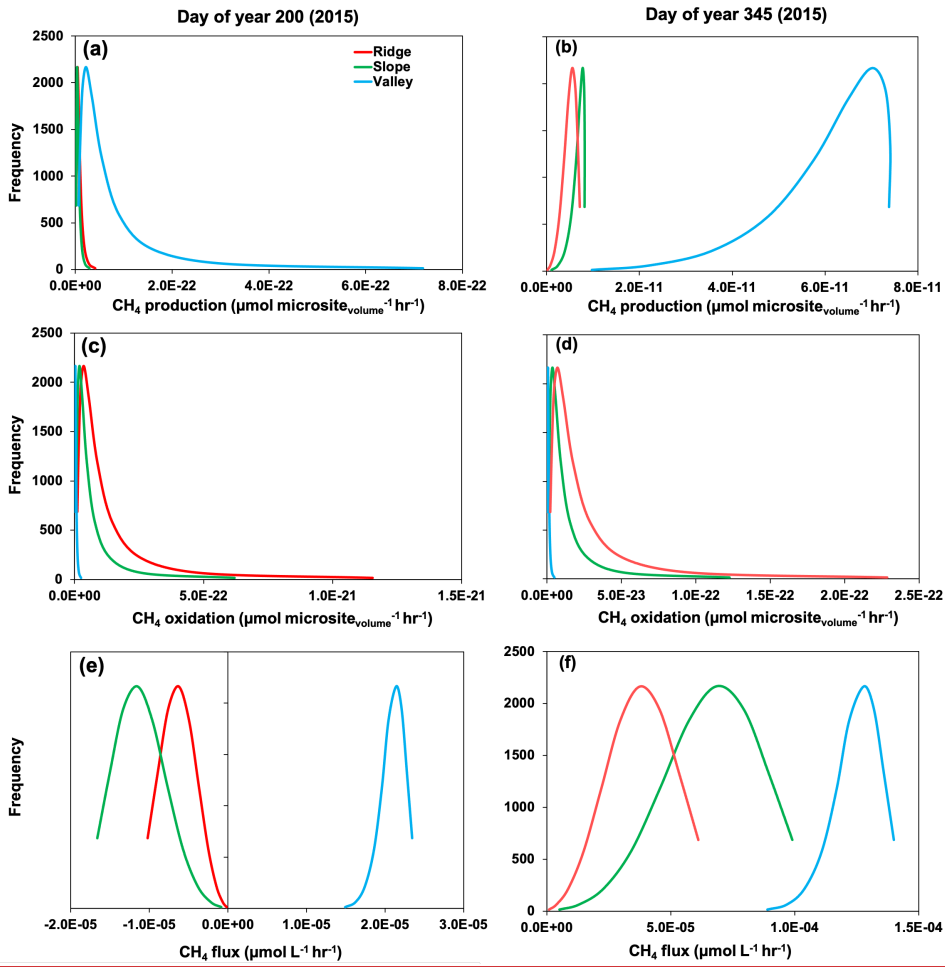


Figure 7: Rates of gross methane (CH_4) production (a, b), oxidation (c, d), and net flux (e, f) across simulated soil microsites. Day of year 200 and 345 represent drought and post-drought recovery, respectively (see medium gray and white shading in Fig. 3).

106
107
108
109
110

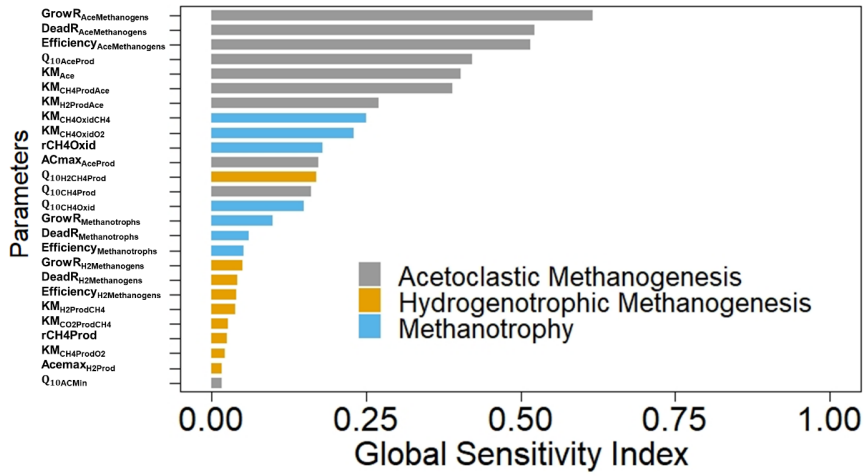


Figure 8: Global sensitivity indices of M3D-DAMM model parameters (defined in Table 1). Gray, yellow, and blue colors represent parameters for acetoclastic methanogenesis, hydrogenotrophic methanogenesis, and methanotrophy, respectively.

Deleted: acetoclastic

112
113
114
115

Page 3: [1] Formatted	Mayes, Melanie A.	11/17/20 8:18:00 PM
Font: (Default) +Body (Times New Roman), 10 pt, Not Italic		
Page 3: [2] Formatted	Mayes, Melanie A.	11/17/20 8:18:00 PM
Font: (Default) +Body (Times New Roman), 10 pt		
Page 4: [3] Formatted	Mayes, Melanie A.	11/17/20 8:18:00 PM
Font: (Default) +Body (Times New Roman), 10 pt, Not Italic		
Page 4: [4] Formatted	Mayes, Melanie A.	11/17/20 8:18:00 PM
Font: (Default) +Body (Times New Roman), 10 pt		
Page 4: [5] Formatted	Mayes, Melanie A.	11/17/20 8:18:00 PM
Font: (Default) +Body (Times New Roman), 10 pt, Not Italic		
Page 4: [6] Formatted	Mayes, Melanie A.	11/17/20 8:18:00 PM
Font: (Default) +Body (Times New Roman), 10 pt		
Page 4: [7] Formatted	Mayes, Melanie A.	11/17/20 8:18:00 PM
Font: (Default) +Body (Times New Roman), 10 pt, Not Italic		
Page 4: [8] Formatted	Mayes, Melanie A.	11/17/20 8:18:00 PM
Font: (Default) +Body (Times New Roman), 10 pt		
Page 4: [9] Formatted	Mayes, Melanie A.	11/17/20 8:18:00 PM
Font: (Default) +Body (Times New Roman), 10 pt, Not Italic		
Page 4: [10] Formatted	Mayes, Melanie A.	11/17/20 8:18:00 PM
Font: (Default) +Body (Times New Roman), 10 pt		
Page 4: [11] Formatted	Mayes, Melanie A.	11/17/20 8:18:00 PM
Font: (Default) +Body (Times New Roman), 10 pt, Not Highlight		
Page 4: [12] Formatted	Mayes, Melanie A.	11/17/20 8:18:00 PM
Font: (Default) +Body (Times New Roman), 10 pt, Not Italic		
Page 4: [13] Formatted	Mayes, Melanie A.	11/17/20 8:18:00 PM
Font: (Default) +Body (Times New Roman), 10 pt		
Page 4: [14] Formatted	Mayes, Melanie A.	11/17/20 8:18:00 PM
Font: (Default) +Body (Times New Roman), 10 pt, Not Italic		
Page 4: [15] Formatted	Mayes, Melanie A.	11/17/20 8:18:00 PM
Font: (Default) +Body (Times New Roman), 10 pt		
Page 4: [16] Formatted	Mayes, Melanie A.	11/17/20 8:18:00 PM
Font: (Default) +Body (Times New Roman), 10 pt, Not Italic		
Page 4: [17] Formatted	Mayes, Melanie A.	11/17/20 8:18:00 PM
Font: (Default) +Body (Times New Roman), 10 pt		
Page 4: [18] Formatted	Mayes, Melanie A.	11/17/20 8:18:00 PM
Font: (Default) +Body (Times New Roman), 10 pt, Not Italic		
Page 4: [19] Formatted	Mayes, Melanie A.	11/17/20 8:18:00 PM
Font: (Default) +Body (Times New Roman), 10 pt, Not Italic, Superscript		
Page 4: [20] Formatted	Mayes, Melanie A.	11/17/20 8:18:00 PM
Font: (Default) +Body (Times New Roman), 10 pt, Not Italic		

Page 4: [21] Formatted	Mayes, Melanie A.	11/17/20 8:18:00 PM
Font: (Default) +Body (Times New Roman), 10 pt		
Page 4: [22] Formatted	Mayes, Melanie A.	11/17/20 8:18:00 PM
Font: (Default) +Body (Times New Roman), 10 pt, Not Italic		
Page 4: [23] Formatted	Mayes, Melanie A.	11/17/20 8:18:00 PM
Font: (Default) +Body (Times New Roman), 10 pt, Not Highlight		
Page 4: [24] Formatted	Mayes, Melanie A.	11/17/20 8:18:00 PM
Font: (Default) +Body (Times New Roman), 10 pt, Not Italic		
Page 4: [25] Formatted	Mayes, Melanie A.	11/17/20 8:18:00 PM
Font: (Default) +Body (Times New Roman), 10 pt		
Page 4: [26] Formatted	Mayes, Melanie A.	11/17/20 8:18:00 PM
Font: (Default) +Body (Times New Roman), 10 pt, Not Italic		
Page 4: [27] Formatted	Mayes, Melanie A.	11/17/20 8:18:00 PM
Font: (Default) +Body (Times New Roman), 10 pt		
Page 4: [28] Formatted	Mayes, Melanie A.	11/17/20 8:18:00 PM
Font: (Default) +Body (Times New Roman), 10 pt, Subscript		
Page 4: [29] Formatted	Mayes, Melanie A.	11/17/20 8:18:00 PM
Font: (Default) +Body (Times New Roman), 10 pt		
Page 4: [30] Formatted	Mayes, Melanie A.	11/17/20 8:18:00 PM
Font: (Default) +Body (Times New Roman), 10 pt		
Page 4: [31] Formatted	Mayes, Melanie A.	11/17/20 8:18:00 PM
Font: (Default) +Body (Times New Roman), 10 pt		
Page 4: [32] Formatted	Mayes, Melanie A.	11/17/20 8:18:00 PM
Font: (Default) +Body (Times New Roman), 10 pt		
Page 5: [33] Formatted	Mayes, Melanie A.	11/17/20 8:18:00 PM
Font: 10 pt		
Page 5: [33] Formatted	Mayes, Melanie A.	11/17/20 8:18:00 PM
Font: 10 pt		
Page 5: [33] Formatted	Mayes, Melanie A.	11/17/20 8:18:00 PM
Font: 10 pt		
Page 5: [33] Formatted	Mayes, Melanie A.	11/17/20 8:18:00 PM
Font: 10 pt		
Page 5: [33] Formatted	Mayes, Melanie A.	11/17/20 8:18:00 PM
Font: 10 pt		
Page 5: [34] Formatted	Mayes, Melanie A.	11/17/20 8:18:00 PM
Font: (Default) +Body (Times New Roman), 10 pt, Not Italic		
Page 5: [34] Formatted	Mayes, Melanie A.	11/17/20 8:18:00 PM
Font: (Default) +Body (Times New Roman), 10 pt, Not Italic		
Page 5: [34] Formatted	Mayes, Melanie A.	11/17/20 8:18:00 PM

▲	Page 5: [36] Formatted	Mayes, Melanie A.	11/17/20 8:18:00 PM
	Font: 10 pt		
▲	Page 5: [36] Formatted	Mayes, Melanie A.	11/17/20 8:18:00 PM
	Font: 10 pt		
▲	Page 6: [37] Formatted	Mayes, Melanie A.	11/17/20 8:18:00 PM
	Font: 10 pt		
▲	Page 6: [37] Formatted	Mayes, Melanie A.	11/17/20 8:18:00 PM
	Font: 10 pt		
▲	Page 6: [37] Formatted	Mayes, Melanie A.	11/17/20 8:18:00 PM
	Font: 10 pt		
▲	Page 6: [37] Formatted	Mayes, Melanie A.	11/17/20 8:18:00 PM
	Font: 10 pt		
▲	Page 6: [38] Formatted	Mayes, Melanie A.	11/17/20 8:18:00 PM
	Font: 10 pt		
▲	Page 6: [38] Formatted	Mayes, Melanie A.	11/17/20 8:18:00 PM
	Font: 10 pt		
▲	Page 6: [38] Formatted	Mayes, Melanie A.	11/17/20 8:18:00 PM
	Font: 10 pt		
▲	Page 6: [38] Formatted	Mayes, Melanie A.	11/17/20 8:18:00 PM
	Font: 10 pt		
▲	Page 6: [39] Deleted	Mayes, Melanie A.	11/17/20 8:29:00 PM
x			
▲	Page 6: [39] Deleted	Mayes, Melanie A.	11/17/20 8:29:00 PM
x			
▲	Page 6: [40] Formatted	Mayes, Melanie A.	11/17/20 8:18:00 PM
	Font: 10 pt		
▲	Page 6: [40] Formatted	Mayes, Melanie A.	11/17/20 8:18:00 PM
	Font: 10 pt		
▲	Page 6: [40] Formatted	Mayes, Melanie A.	11/17/20 8:18:00 PM
	Font: 10 pt		
▲	Page 6: [40] Formatted	Mayes, Melanie A.	11/17/20 8:18:00 PM
	Font: 10 pt		
▲	Page 6: [41] Formatted	Mayes, Melanie A.	11/17/20 8:18:00 PM
	Font: 10 pt		
▲	Page 6: [41] Formatted	Mayes, Melanie A.	11/17/20 8:18:00 PM
	Font: 10 pt		
▲	Page 6: [41] Formatted	Mayes, Melanie A.	11/17/20 8:18:00 PM
	Font: 10 pt		

Page 6: [41] Formatted	Mayes, Melanie A.	11/17/20 8:18:00 PM
Font: 10 pt		
Page 6: [42] Formatted	Mayes, Melanie A.	11/17/20 8:18:00 PM
Font: (Default) +Body (Times New Roman), 10 pt		
Page 6: [43] Formatted	Mayes, Melanie A.	11/17/20 8:18:00 PM
Font: 10 pt		
Page 6: [43] Formatted	Mayes, Melanie A.	11/17/20 8:18:00 PM
Font: 10 pt		
Page 6: [43] Formatted	Mayes, Melanie A.	11/17/20 8:18:00 PM
Font: 10 pt		
Page 6: [43] Formatted	Mayes, Melanie A.	11/17/20 8:18:00 PM
Font: 10 pt		
Page 6: [43] Formatted	Mayes, Melanie A.	11/17/20 8:18:00 PM
Font: 10 pt		
Page 6: [44] Deleted	Mayes, Melanie A.	11/17/20 8:30:00 PM
x		
Page 6: [44] Deleted	Mayes, Melanie A.	11/17/20 8:30:00 PM
x		
Page 6: [45] Formatted	Mayes, Melanie A.	11/17/20 8:18:00 PM
Font: 10 pt		
Page 6: [45] Formatted	Mayes, Melanie A.	11/17/20 8:18:00 PM
Font: 10 pt		
Page 6: [45] Formatted	Mayes, Melanie A.	11/17/20 8:18:00 PM
Font: 10 pt		
Page 6: [45] Formatted	Mayes, Melanie A.	11/17/20 8:18:00 PM
Font: 10 pt		
Page 6: [46] Formatted	Mayes, Melanie A.	11/17/20 8:18:00 PM
Font: 10 pt		
Page 6: [46] Formatted	Mayes, Melanie A.	11/17/20 8:18:00 PM
Font: 10 pt		
Page 6: [46] Formatted	Mayes, Melanie A.	11/17/20 8:18:00 PM
Font: 10 pt		
Page 6: [46] Formatted	Mayes, Melanie A.	11/17/20 8:18:00 PM
Font: 10 pt		
Page 6: [47] Formatted	Mayes, Melanie A.	11/17/20 8:18:00 PM
Font: 10 pt		
Page 6: [47] Formatted	Mayes, Melanie A.	11/17/20 8:18:00 PM
Font: 10 pt		
Page 6: [47] Formatted	Mayes, Melanie A.	11/17/20 8:18:00 PM

Font: 10 pt

▲ **Page 6: [47] Formatted** **Mayes, Melanie A.** **11/17/20 8:18:00 PM**

Font: 10 pt

▲ **Page 6: [48] Formatted** **Mayes, Melanie A.** **11/17/20 8:18:00 PM**

Font: 10 pt

▲ **Page 6: [48] Formatted** **Mayes, Melanie A.** **11/17/20 8:18:00 PM**

Font: 10 pt

▲ **Page 6: [48] Formatted** **Mayes, Melanie A.** **11/17/20 8:18:00 PM**

Font: 10 pt

▲ **Page 6: [48] Formatted** **Mayes, Melanie A.** **11/17/20 8:18:00 PM**

Font: 10 pt

▲ **Page 6: [49] Formatted** **Mayes, Melanie A.** **11/17/20 8:18:00 PM**

Font: 10 pt

▲ **Page 6: [49] Formatted** **Mayes, Melanie A.** **11/17/20 8:18:00 PM**

Font: 10 pt

▲ **Page 6: [49] Formatted** **Mayes, Melanie A.** **11/17/20 8:18:00 PM**

Font: 10 pt

▲ **Page 6: [49] Formatted** **Mayes, Melanie A.** **11/17/20 8:18:00 PM**

Font: 10 pt

▲ **Page 6: [49] Formatted** **Mayes, Melanie A.** **11/17/20 8:18:00 PM**

Font: 10 pt

▲ **Page 6: [49] Formatted** **Mayes, Melanie A.** **11/17/20 8:18:00 PM**

Font: 10 pt

▲ **Page 6: [49] Formatted** **Mayes, Melanie A.** **11/17/20 8:18:00 PM**

Font: 10 pt

▲ **Page 6: [50] Formatted** **Mayes, Melanie A.** **11/17/20 8:18:00 PM**

Font: 10 pt

▲ **Page 6: [50] Formatted** **Mayes, Melanie A.** **11/17/20 8:18:00 PM**

Font: 10 pt

▲ **Page 6: [50] Formatted** **Mayes, Melanie A.** **11/17/20 8:18:00 PM**

Font: 10 pt

▲ **Page 6: [50] Formatted** **Mayes, Melanie A.** **11/17/20 8:18:00 PM**

Font: 10 pt

▲ **Page 6: [50] Formatted** **Mayes, Melanie A.** **11/17/20 8:18:00 PM**

Font: 10 pt

▲ **Page 6: [50] Formatted** **Mayes, Melanie A.** **11/17/20 8:18:00 PM**

Font: 10 pt

▲ **Page 6: [50] Formatted** **Mayes, Melanie A.** **11/17/20 8:18:00 PM**

Font: 10 pt

▲ **Page 6: [50] Formatted** **Mayes, Melanie A.** **11/17/20 8:18:00 PM**

Page 6: [55] Formatted	Mayes, Melanie A.	11/17/20 8:18:00 PM
Font: 10 pt		
Page 6: [55] Formatted	Mayes, Melanie A.	11/17/20 8:18:00 PM
Font: 10 pt		
Page 6: [55] Formatted	Mayes, Melanie A.	11/17/20 8:18:00 PM
Font: 10 pt		
Page 6: [55] Formatted	Mayes, Melanie A.	11/17/20 8:18:00 PM
Font: 10 pt		
Page 6: [56] Formatted	Mayes, Melanie A.	11/17/20 8:18:00 PM
Font: 10 pt		
Page 6: [56] Formatted	Mayes, Melanie A.	11/17/20 8:18:00 PM
Font: 10 pt		
Page 6: [56] Formatted	Mayes, Melanie A.	11/17/20 8:18:00 PM
Font: 10 pt		
Page 6: [56] Formatted	Mayes, Melanie A.	11/17/20 8:18:00 PM
Font: 10 pt		
Page 6: [57] Formatted	Mayes, Melanie A.	11/17/20 8:18:00 PM
Font: 10 pt		
Page 6: [57] Formatted	Mayes, Melanie A.	11/17/20 8:18:00 PM
Font: 10 pt		
Page 6: [57] Formatted	Mayes, Melanie A.	11/17/20 8:18:00 PM
Font: 10 pt		
Page 6: [57] Formatted	Mayes, Melanie A.	11/17/20 8:18:00 PM
Font: 10 pt		
Page 6: [57] Formatted	Mayes, Melanie A.	11/17/20 8:18:00 PM
Font: 10 pt		
Page 6: [57] Formatted	Mayes, Melanie A.	11/17/20 8:18:00 PM
Font: 10 pt		
Page 6: [57] Formatted	Mayes, Melanie A.	11/17/20 8:18:00 PM
Font: 10 pt		
Page 6: [58] Formatted	Mayes, Melanie A.	11/17/20 8:18:00 PM
Font: 10 pt		
Page 6: [58] Formatted	Mayes, Melanie A.	11/17/20 8:18:00 PM
Font: 10 pt		
Page 6: [58] Formatted	Mayes, Melanie A.	11/17/20 8:18:00 PM
Font: 10 pt		
Page 6: [58] Formatted	Mayes, Melanie A.	11/17/20 8:18:00 PM
Font: 10 pt		

Font: 10 pt

▲ **Page 6: [58] Formatted** **Mayes, Melanie A.** **11/17/20 8:18:00 PM**

Font: 10 pt

▲ **Page 6: [59] Formatted** **Mayes, Melanie A.** **11/17/20 8:18:00 PM**

Font: 10 pt

▲ **Page 6: [59] Formatted** **Mayes, Melanie A.** **11/17/20 8:18:00 PM**

Font: 10 pt

▲ **Page 6: [59] Formatted** **Mayes, Melanie A.** **11/17/20 8:18:00 PM**

Font: 10 pt

▲ **Page 6: [59] Formatted** **Mayes, Melanie A.** **11/17/20 8:18:00 PM**

Font: 10 pt

▲ **Page 6: [60] Formatted** **Mayes, Melanie A.** **11/17/20 8:18:00 PM**

Font: 10 pt

▲ **Page 6: [60] Formatted** **Mayes, Melanie A.** **11/17/20 8:18:00 PM**

Font: 10 pt

▲ **Page 6: [60] Formatted** **Mayes, Melanie A.** **11/17/20 8:18:00 PM**

Font: 10 pt

▲ **Page 6: [60] Formatted** **Mayes, Melanie A.** **11/17/20 8:18:00 PM**

Font: 10 pt

▲ **Page 6: [61] Formatted** **Mayes, Melanie A.** **11/17/20 8:18:00 PM**

Font: 10 pt

▲ **Page 6: [62] Formatted** **Mayes, Melanie A.** **11/17/20 8:18:00 PM**

Font: (Default) +Body (Times New Roman), 10 pt

▲ **Page 6: [62] Formatted** **Mayes, Melanie A.** **11/17/20 8:18:00 PM**

Font: (Default) +Body (Times New Roman), 10 pt

▲ **Page 6: [63] Formatted** **Mayes, Melanie A.** **11/17/20 8:18:00 PM**

Font: (Default) +Body (Times New Roman), 10 pt

▲ **Page 6: [64] Formatted** **Mayes, Melanie A.** **11/17/20 8:18:00 PM**

Font: 10 pt

▲ **Page 6: [65] Formatted** **Mayes, Melanie A.** **11/17/20 8:18:00 PM**

Font: 10 pt

▲ **Page 6: [65] Formatted** **Mayes, Melanie A.** **11/17/20 8:18:00 PM**

Font: 10 pt

▲ **Page 6: [65] Formatted** **Mayes, Melanie A.** **11/17/20 8:18:00 PM**

Font: 10 pt

▲ **Page 6: [65] Formatted** **Mayes, Melanie A.** **11/17/20 8:18:00 PM**

Font: 10 pt

▲ **Page 6: [65] Formatted** **Mayes, Melanie A.** **11/17/20 8:18:00 PM**

Font: 10 pt

▲ **Page 6: [65] Formatted** **Mayes, Melanie A.** **11/17/20 8:18:00 PM**

▲	Page 6: [67] Formatted	Mayes, Melanie A.	11/17/20 8:18:00 PM
	Font: 10 pt		
▲	Page 6: [67] Formatted	Mayes, Melanie A.	11/17/20 8:18:00 PM
	Font: 10 pt		
▲	Page 6: [67] Formatted	Mayes, Melanie A.	11/17/20 8:18:00 PM
	Font: 10 pt		
▲	Page 6: [67] Formatted	Mayes, Melanie A.	11/17/20 8:18:00 PM
	Font: 10 pt		
▲	Page 6: [67] Formatted	Mayes, Melanie A.	11/17/20 8:18:00 PM
	Font: 10 pt		
▲	Page 6: [68] Formatted	Mayes, Melanie A.	11/17/20 8:18:00 PM
	Font: 10 pt		
▲	Page 6: [69] Formatted	Mayes, Melanie A.	11/17/20 8:18:00 PM
	Font: 10 pt		
▲	Page 6: [69] Formatted	Mayes, Melanie A.	11/17/20 8:18:00 PM
	Font: 10 pt		
▲	Page 6: [69] Formatted	Mayes, Melanie A.	11/17/20 8:18:00 PM
	Font: 10 pt		
▲	Page 6: [69] Formatted	Mayes, Melanie A.	11/17/20 8:18:00 PM
	Font: 10 pt		
▲	Page 6: [69] Formatted	Mayes, Melanie A.	11/17/20 8:18:00 PM
	Font: 10 pt		
▲	Page 6: [70] Deleted	Mayes, Melanie A.	11/15/20 11:25:00 AM
x			
▲	Page 6: [70] Deleted	Mayes, Melanie A.	11/15/20 11:25:00 AM
x			
▲	Page 6: [71] Formatted	Mayes, Melanie A.	11/17/20 8:18:00 PM
	Font: (Default) +Body (Times New Roman), 10 pt		
▲	Page 6: [72] Formatted	Mayes, Melanie A.	11/17/20 8:18:00 PM
	Font: 10 pt		
▲	Page 6: [72] Formatted	Mayes, Melanie A.	11/17/20 8:18:00 PM
	Font: 10 pt		
▲	Page 6: [72] Formatted	Mayes, Melanie A.	11/17/20 8:18:00 PM
	Font: 10 pt		
▲	Page 6: [72] Formatted	Mayes, Melanie A.	11/17/20 8:18:00 PM
	Font: 10 pt		

Page 6: [72] Formatted	Mayes, Melanie A.	11/17/20 8:18:00 PM
Font: 10 pt		
Page 6: [73] Formatted	Mayes, Melanie A.	11/17/20 8:18:00 PM
Font: 10 pt		
Page 6: [73] Formatted	Mayes, Melanie A.	11/17/20 8:18:00 PM
Font: 10 pt		
Page 6: [73] Formatted	Mayes, Melanie A.	11/17/20 8:18:00 PM
Font: 10 pt		
Page 6: [73] Formatted	Mayes, Melanie A.	11/17/20 8:18:00 PM
Font: 10 pt		
Page 6: [74] Formatted	Mayes, Melanie A.	11/17/20 8:18:00 PM
Font: 10 pt		
Page 6: [74] Formatted	Mayes, Melanie A.	11/17/20 8:18:00 PM
Font: 10 pt		
Page 6: [74] Formatted	Mayes, Melanie A.	11/17/20 8:18:00 PM
Font: 10 pt		
Page 6: [74] Formatted	Mayes, Melanie A.	11/17/20 8:18:00 PM
Font: 10 pt		
Page 6: [75] Formatted	Mayes, Melanie A.	11/17/20 8:18:00 PM
Font: 10 pt		
Page 6: [75] Formatted	Mayes, Melanie A.	11/17/20 8:18:00 PM
Font: 10 pt		
Page 6: [75] Formatted	Mayes, Melanie A.	11/17/20 8:18:00 PM
Font: 10 pt		
Page 6: [75] Formatted	Mayes, Melanie A.	11/17/20 8:18:00 PM
Font: 10 pt		
Page 6: [76] Formatted	Mayes, Melanie A.	11/17/20 8:18:00 PM
Font: 10 pt		
Page 6: [76] Formatted	Mayes, Melanie A.	11/17/20 8:18:00 PM
Font: 10 pt		
Page 6: [76] Formatted	Mayes, Melanie A.	11/17/20 8:18:00 PM
Font: 10 pt		
Page 6: [76] Formatted	Mayes, Melanie A.	11/17/20 8:18:00 PM
Font: 10 pt		
Page 6: [76] Formatted	Mayes, Melanie A.	11/17/20 8:18:00 PM
Font: 10 pt		
Page 6: [77] Formatted	Mayes, Melanie A.	11/17/20 8:18:00 PM
Font: 10 pt		
Page 6: [77] Formatted	Mayes, Melanie A.	11/17/20 8:18:00 PM
Font: 10 pt		

Page 6: [77] Formatted	Mayes, Melanie A.	11/17/20 8:18:00 PM
Font: 10 pt		
Page 7: [78] Formatted	Mayes, Melanie A.	11/17/20 8:18:00 PM
Font: 10 pt		
Page 7: [78] Formatted	Mayes, Melanie A.	11/17/20 8:18:00 PM
Font: 10 pt		
Page 7: [78] Formatted	Mayes, Melanie A.	11/17/20 8:18:00 PM
Font: 10 pt		
Page 7: [78] Formatted	Mayes, Melanie A.	11/17/20 8:18:00 PM
Font: 10 pt		
Page 7: [79] Formatted	Mayes, Melanie A.	11/17/20 8:18:00 PM
Font: (Default) +Body (Times New Roman), 10 pt		
Page 7: [80] Formatted	Mayes, Melanie A.	11/17/20 8:18:00 PM
Font: 10 pt		
Page 7: [80] Formatted	Mayes, Melanie A.	11/17/20 8:18:00 PM
Font: 10 pt		
Page 7: [80] Formatted	Mayes, Melanie A.	11/17/20 8:18:00 PM
Font: 10 pt		
Page 7: [81] Formatted	Mayes, Melanie A.	11/17/20 8:18:00 PM
Font: 10 pt		
Page 7: [81] Formatted	Mayes, Melanie A.	11/17/20 8:18:00 PM
Font: 10 pt		
Page 7: [81] Formatted	Mayes, Melanie A.	11/17/20 8:18:00 PM
Font: 10 pt		
Page 7: [82] Formatted	Mayes, Melanie A.	11/17/20 8:18:00 PM
Font: 10 pt		
Page 7: [82] Formatted	Mayes, Melanie A.	11/17/20 8:18:00 PM
Font: 10 pt		
Page 7: [82] Formatted	Mayes, Melanie A.	11/17/20 8:18:00 PM
Font: 10 pt		
Page 7: [83] Formatted	Mayes, Melanie A.	11/17/20 8:18:00 PM
Font: 10 pt		
Page 7: [83] Formatted	Mayes, Melanie A.	11/17/20 8:18:00 PM
Font: 10 pt		
Page 7: [83] Formatted	Mayes, Melanie A.	11/17/20 8:18:00 PM
Font: 10 pt		
Page 7: [84] Formatted	Mayes, Melanie A.	11/17/20 8:18:00 PM
Font: 10 pt		
Page 7: [85] Formatted	Mayes, Melanie A.	11/17/20 8:18:00 PM

Font: 10 pt

▲ **Page 7: [85] Formatted** **Mayes, Melanie A.** **11/17/20 8:18:00 PM**

Font: 10 pt

▲ **Page 7: [85] Formatted** **Mayes, Melanie A.** **11/17/20 8:18:00 PM**

Font: 10 pt

▲ **Page 7: [86] Formatted** **Mayes, Melanie A.** **11/17/20 8:18:00 PM**

Font: 10 pt

▲ **Page 7: [86] Formatted** **Mayes, Melanie A.** **11/17/20 8:18:00 PM**

Font: 10 pt

▲ **Page 7: [86] Formatted** **Mayes, Melanie A.** **11/17/20 8:18:00 PM**

Font: 10 pt

▲ **Page 7: [86] Formatted** **Mayes, Melanie A.** **11/17/20 8:18:00 PM**

Font: 10 pt

▲ **Page 7: [86] Formatted** **Mayes, Melanie A.** **11/17/20 8:18:00 PM**

Font: 10 pt

▲ **Page 7: [86] Formatted** **Mayes, Melanie A.** **11/17/20 8:18:00 PM**

Font: 10 pt

▲ **Page 7: [86] Formatted** **Mayes, Melanie A.** **11/17/20 8:18:00 PM**

Font: 10 pt

▲ **Page 7: [86] Formatted** **Mayes, Melanie A.** **11/17/20 8:18:00 PM**

Font: 10 pt

▲ **Page 7: [86] Formatted** **Mayes, Melanie A.** **11/17/20 8:18:00 PM**

Font: 10 pt

▲ **Page 7: [86] Formatted** **Mayes, Melanie A.** **11/17/20 8:18:00 PM**

Font: 10 pt

▲ **Page 7: [86] Formatted** **Mayes, Melanie A.** **11/17/20 8:18:00 PM**

Font: 10 pt

▲ **Page 7: [86] Formatted** **Mayes, Melanie A.** **11/17/20 8:18:00 PM**

Font: 10 pt

▲ **Page 7: [87] Formatted** **Mayes, Melanie A.** **11/17/20 8:18:00 PM**

Font: 10 pt

▲ **Page 7: [87] Formatted** **Mayes, Melanie A.** **11/17/20 8:18:00 PM**

Font: 10 pt

▲ **Page 7: [87] Formatted** **Mayes, Melanie A.** **11/17/20 8:18:00 PM**

Font: 10 pt

▲ **Page 7: [88] Formatted** **Mayes, Melanie A.** **11/17/20 8:18:00 PM**

Font: 10 pt

▲ **Page 7: [88] Formatted** **Mayes, Melanie A.** **11/17/20 8:18:00 PM**

Font: 10 pt

▲

Page 7: [92] Formatted	Mayes, Melanie A.	11/17/20 8:18:00 PM
Font: 10 pt		
Page 7: [93] Formatted	Mayes, Melanie A.	11/17/20 8:18:00 PM
Font: 10 pt		
Page 7: [93] Formatted	Mayes, Melanie A.	11/17/20 8:18:00 PM
Font: 10 pt		
Page 7: [93] Formatted	Mayes, Melanie A.	11/17/20 8:18:00 PM
Font: 10 pt		
Page 7: [93] Formatted	Mayes, Melanie A.	11/17/20 8:18:00 PM
Font: 10 pt		
Page 7: [93] Formatted	Mayes, Melanie A.	11/17/20 8:18:00 PM
Font: 10 pt		
Page 7: [93] Formatted	Mayes, Melanie A.	11/17/20 8:18:00 PM
Font: 10 pt		
Page 7: [94] Formatted	Mayes, Melanie A.	11/17/20 8:18:00 PM
Font: 10 pt		
Page 7: [94] Formatted	Mayes, Melanie A.	11/17/20 8:18:00 PM
Font: 10 pt		
Page 7: [94] Formatted	Mayes, Melanie A.	11/17/20 8:18:00 PM
Font: 10 pt		
Page 7: [95] Formatted	Mayes, Melanie A.	11/17/20 8:18:00 PM
Font: 10 pt		
Page 7: [95] Formatted	Mayes, Melanie A.	11/17/20 8:18:00 PM
Font: 10 pt		
Page 7: [95] Formatted	Mayes, Melanie A.	11/17/20 8:18:00 PM
Font: 10 pt		
Page 7: [95] Formatted	Mayes, Melanie A.	11/17/20 8:18:00 PM
Font: 10 pt		
Page 7: [96] Formatted	Mayes, Melanie A.	11/17/20 8:18:00 PM
Font: 10 pt		
Page 7: [96] Formatted	Mayes, Melanie A.	11/17/20 8:18:00 PM
Font: 10 pt		
Page 7: [96] Formatted	Mayes, Melanie A.	11/17/20 8:18:00 PM
Font: 10 pt		
Page 7: [96] Formatted	Mayes, Melanie A.	11/17/20 8:18:00 PM
Font: 10 pt		
Page 7: [97] Formatted	Mayes, Melanie A.	11/17/20 8:18:00 PM
Font: 10 pt		
Page 7: [97] Formatted	Mayes, Melanie A.	11/17/20 8:18:00 PM

Font: 10 pt

▲ **Page 7: [97] Formatted** **Mayes, Melanie A.** **11/17/20 8:18:00 PM**

Font: 10 pt

▲ **Page 7: [98] Formatted** **Mayes, Melanie A.** **11/17/20 8:18:00 PM**

Font: 10 pt

▲ **Page 7: [98] Formatted** **Mayes, Melanie A.** **11/17/20 8:18:00 PM**

Font: 10 pt

▲ **Page 7: [98] Formatted** **Mayes, Melanie A.** **11/17/20 8:18:00 PM**

Font: 10 pt

▲ **Page 7: [98] Formatted** **Mayes, Melanie A.** **11/17/20 8:18:00 PM**

Font: 10 pt

▲ **Page 7: [98] Formatted** **Mayes, Melanie A.** **11/17/20 8:18:00 PM**

Font: 10 pt

▲ **Page 7: [98] Formatted** **Mayes, Melanie A.** **11/17/20 8:18:00 PM**

Font: 10 pt

▲ **Page 7: [98] Formatted** **Mayes, Melanie A.** **11/17/20 8:18:00 PM**

Font: 10 pt

▲ **Page 7: [98] Formatted** **Mayes, Melanie A.** **11/17/20 8:18:00 PM**

Font: 10 pt

▲ **Page 7: [98] Formatted** **Mayes, Melanie A.** **11/17/20 8:18:00 PM**

Font: 10 pt

▲ **Page 7: [98] Formatted** **Mayes, Melanie A.** **11/17/20 8:18:00 PM**

Font: 10 pt

▲ **Page 7: [98] Formatted** **Mayes, Melanie A.** **11/17/20 8:18:00 PM**

Font: 10 pt

▲ **Page 7: [98] Formatted** **Mayes, Melanie A.** **11/17/20 8:18:00 PM**

Font: 10 pt

▲ **Page 7: [98] Formatted** **Mayes, Melanie A.** **11/17/20 8:18:00 PM**

Font: 10 pt

▲ **Page 7: [98] Formatted** **Mayes, Melanie A.** **11/17/20 8:18:00 PM**

Font: 10 pt

▲ **Page 7: [98] Formatted** **Mayes, Melanie A.** **11/17/20 8:18:00 PM**

Font: 10 pt

▲ **Page 7: [99] Formatted** **Mayes, Melanie A.** **11/17/20 8:18:00 PM**

Font: (Default) +Body (Times New Roman), 10 pt, Not Italic

▲ **Page 7: [100] Formatted** **Mayes, Melanie A.** **11/17/20 8:18:00 PM**

Font: (Default) +Body (Times New Roman), 10 pt

▲ **Page 7: [100] Formatted** **Mayes, Melanie A.** **11/17/20 8:18:00 PM**

Font: (Default) +Body (Times New Roman), 10 pt

▲

Page 7: [101] Formatted	Mayes, Melanie A.	11/17/20 8:18:00 PM
Font: (Default) +Body (Times New Roman), 10 pt		
Page 7: [101] Formatted	Mayes, Melanie A.	11/17/20 8:18:00 PM
Font: (Default) +Body (Times New Roman), 10 pt		
Page 7: [102] Formatted	Mayes, Melanie A.	11/17/20 8:18:00 PM
Font: (Default) +Body (Times New Roman), 10 pt		
Page 7: [103] Formatted	Mayes, Melanie A.	11/17/20 8:18:00 PM
Font: (Default) +Body (Times New Roman), 10 pt		
Page 7: [104] Formatted	Mayes, Melanie A.	11/17/20 8:18:00 PM
Font: (Default) +Body (Times New Roman), 10 pt, Not Italic		
Page 7: [104] Formatted	Mayes, Melanie A.	11/17/20 8:18:00 PM
Font: (Default) +Body (Times New Roman), 10 pt, Not Italic		
Page 7: [104] Formatted	Mayes, Melanie A.	11/17/20 8:18:00 PM
Font: (Default) +Body (Times New Roman), 10 pt, Not Italic		
Page 7: [104] Formatted	Mayes, Melanie A.	11/17/20 8:18:00 PM
Font: (Default) +Body (Times New Roman), 10 pt, Not Italic		
Page 7: [105] Formatted	Mayes, Melanie A.	11/17/20 8:18:00 PM
Font: (Default) +Body (Times New Roman), 10 pt, Not Italic		
Page 7: [105] Formatted	Mayes, Melanie A.	11/17/20 8:18:00 PM
Font: (Default) +Body (Times New Roman), 10 pt, Not Italic		
Page 7: [106] Formatted	Mayes, Melanie A.	11/17/20 8:18:00 PM
Font: (Default) +Body (Times New Roman), 10 pt		
Page 7: [107] Deleted	Mayes, Melanie A.	11/17/20 11:56:00 AM
x.....		
▲.....		
Page 7: [107] Deleted	Mayes, Melanie A.	11/17/20 11:56:00 AM
x.....		
▲.....		
Page 7: [107] Deleted	Mayes, Melanie A.	11/17/20 11:56:00 AM
x.....		
▲.....		
Page 7: [107] Deleted	Mayes, Melanie A.	11/17/20 11:56:00 AM
x.....		
▲.....		
Page 7: [108] Formatted	Mayes, Melanie A.	11/17/20 8:18:00 PM
Font: (Default) +Body (Times New Roman), 10 pt		
Page 7: [108] Formatted	Mayes, Melanie A.	11/17/20 8:18:00 PM
Font: (Default) +Body (Times New Roman), 10 pt		
Page 7: [109] Formatted	Mayes, Melanie A.	11/17/20 8:18:00 PM
Font: (Default) +Body (Times New Roman), 10 pt		

▲	Page 7: [109] Formatted	Mayes, Melanie A.	11/17/20 8:18:00 PM
	Font: (Default) +Body (Times New Roman), 10 pt		
▲	Page 7: [110] Formatted	Mayes, Melanie A.	11/17/20 8:18:00 PM
	Font: (Default) +Body (Times New Roman), 10 pt, Not Italic		
▲	Page 7: [110] Formatted	Mayes, Melanie A.	11/17/20 8:18:00 PM
	Font: (Default) +Body (Times New Roman), 10 pt, Not Italic		
▲	Page 7: [111] Formatted	Mayes, Melanie A.	11/17/20 8:18:00 PM
	Font: (Default) +Body (Times New Roman), 10 pt		
▲	Page 7: [111] Formatted	Mayes, Melanie A.	11/17/20 8:18:00 PM
	Font: (Default) +Body (Times New Roman), 10 pt		
▲	Page 7: [111] Formatted	Mayes, Melanie A.	11/17/20 8:18:00 PM
	Font: (Default) +Body (Times New Roman), 10 pt		
▲	Page 8: [112] Formatted	Mayes, Melanie A.	11/17/20 8:18:00 PM
	Font: (Default) +Body (Times New Roman), 10 pt, Subscript		
▲	Page 8: [112] Formatted	Mayes, Melanie A.	11/17/20 8:18:00 PM
	Font: (Default) +Body (Times New Roman), 10 pt, Subscript		
▲	Page 8: [112] Formatted	Mayes, Melanie A.	11/17/20 8:18:00 PM
	Font: (Default) +Body (Times New Roman), 10 pt, Subscript		
▲	Page 8: [112] Formatted	Mayes, Melanie A.	11/17/20 8:18:00 PM
	Font: (Default) +Body (Times New Roman), 10 pt, Subscript		
▲	Page 8: [112] Formatted	Mayes, Melanie A.	11/17/20 8:18:00 PM
	Font: (Default) +Body (Times New Roman), 10 pt, Subscript		
▲	Page 8: [112] Formatted	Mayes, Melanie A.	11/17/20 8:18:00 PM
	Font: (Default) +Body (Times New Roman), 10 pt, Subscript		
▲	Page 8: [112] Formatted	Mayes, Melanie A.	11/17/20 8:18:00 PM
	Font: (Default) +Body (Times New Roman), 10 pt, Subscript		
▲	Page 8: [113] Deleted	Whendee Silver	11/16/20 9:57:00 PM
x			
▲	Page 8: [113] Deleted	Whendee Silver	11/16/20 9:57:00 PM
x			
▲	Page 8: [114] Formatted	Mayes, Melanie A.	11/17/20 8:18:00 PM
	Font: (Default) +Body (Times New Roman), 10 pt, Not Italic		
▲	Page 8: [114] Formatted	Mayes, Melanie A.	11/17/20 8:18:00 PM
	Font: (Default) +Body (Times New Roman), 10 pt, Not Italic		
▲	Page 8: [114] Formatted	Mayes, Melanie A.	11/17/20 8:18:00 PM
	Font: (Default) +Body (Times New Roman), 10 pt, Not Italic		
▲	Page 8: [114] Formatted	Mayes, Melanie A.	11/17/20 8:18:00 PM
	Font: (Default) +Body (Times New Roman), 10 pt, Not Italic		

Page 8: [114] Formatted	Mayes, Melanie A.	11/17/20 8:18:00 PM
Font: (Default) +Body (Times New Roman), 10 pt, Not Italic		
Page 8: [114] Formatted	Mayes, Melanie A.	11/17/20 8:18:00 PM
Font: (Default) +Body (Times New Roman), 10 pt, Not Italic		
Page 8: [115] Deleted	Mayes, Melanie A.	11/14/20 3:51:00 PM
Page 8: [115] Deleted	Mayes, Melanie A.	11/14/20 3:51:00 PM
Page 8: [116] Formatted	Mayes, Melanie A.	11/17/20 8:18:00 PM
Font: 10 pt		
Page 8: [116] Formatted	Mayes, Melanie A.	11/17/20 8:18:00 PM
Font: 10 pt		
Page 8: [116] Formatted	Mayes, Melanie A.	11/17/20 8:18:00 PM
Font: 10 pt		
Page 8: [116] Formatted	Mayes, Melanie A.	11/17/20 8:18:00 PM
Font: 10 pt		
Page 8: [116] Formatted	Mayes, Melanie A.	11/17/20 8:18:00 PM
Font: 10 pt		
Page 8: [116] Formatted	Mayes, Melanie A.	11/17/20 8:18:00 PM
Font: 10 pt		
Page 8: [116] Formatted	Mayes, Melanie A.	11/17/20 8:18:00 PM
Font: 10 pt		
Page 8: [116] Formatted	Mayes, Melanie A.	11/17/20 8:18:00 PM
Font: 10 pt		
Page 8: [116] Formatted	Mayes, Melanie A.	11/17/20 8:18:00 PM
Font: 10 pt		
Page 8: [116] Formatted	Mayes, Melanie A.	11/17/20 8:18:00 PM
Font: 10 pt		
Page 8: [117] Formatted	Mayes, Melanie A.	11/17/20 8:18:00 PM
Font: 10 pt		
Page 8: [117] Formatted	Mayes, Melanie A.	11/17/20 8:18:00 PM
Font: 10 pt		
Page 8: [117] Formatted	Mayes, Melanie A.	11/17/20 8:18:00 PM
Font: 10 pt		
Page 8: [118] Formatted	Mayes, Melanie A.	11/17/20 8:18:00 PM

Font: (Default) +Body (Times New Roman), 10 pt, Not Italic

▲ **Page 8: [118] Formatted** **Mayes, Melanie A.** **11/17/20 8:18:00 PM**

Font: (Default) +Body (Times New Roman), 10 pt, Not Italic

▲ **Page 8: [118] Formatted** **Mayes, Melanie A.** **11/17/20 8:18:00 PM**

Font: (Default) +Body (Times New Roman), 10 pt, Not Italic

▲ **Page 8: [119] Formatted** **Mayes, Melanie A.** **11/17/20 8:18:00 PM**

Font: (Default) +Body (Times New Roman), 10 pt

▲ **Page 8: [119] Formatted** **Mayes, Melanie A.** **11/17/20 8:18:00 PM**

Font: (Default) +Body (Times New Roman), 10 pt

▲ **Page 8: [119] Formatted** **Mayes, Melanie A.** **11/17/20 8:18:00 PM**

Font: (Default) +Body (Times New Roman), 10 pt

▲ **Page 8: [120] Deleted** **Whendee Silver** **11/16/20 10:05:00 PM**

x

▲ **Page 8: [120] Deleted** **Whendee Silver** **11/16/20 10:05:00 PM**

x

▲ **Page 8: [121] Formatted** **Mayes, Melanie A.** **11/17/20 8:18:00 PM**

Font: (Default) +Body (Times New Roman), 10 pt

▲ **Page 8: [121] Formatted** **Mayes, Melanie A.** **11/17/20 8:18:00 PM**

Font: (Default) +Body (Times New Roman), 10 pt

▲ **Page 8: [121] Formatted** **Mayes, Melanie A.** **11/17/20 8:18:00 PM**

Font: (Default) +Body (Times New Roman), 10 pt

▲ **Page 8: [121] Formatted** **Mayes, Melanie A.** **11/17/20 8:18:00 PM**

Font: (Default) +Body (Times New Roman), 10 pt

▲ **Page 8: [122] Formatted** **Mayes, Melanie A.** **11/17/20 8:18:00 PM**

Font: (Default) +Body (Times New Roman), 10 pt

▲ **Page 8: [122] Formatted** **Mayes, Melanie A.** **11/17/20 8:18:00 PM**

Font: (Default) +Body (Times New Roman), 10 pt

▲ **Page 8: [122] Formatted** **Mayes, Melanie A.** **11/17/20 8:18:00 PM**

Font: (Default) +Body (Times New Roman), 10 pt

▲ **Page 8: [122] Formatted** **Mayes, Melanie A.** **11/17/20 8:18:00 PM**

Font: (Default) +Body (Times New Roman), 10 pt

▲ **Page 8: [122] Formatted** **Mayes, Melanie A.** **11/17/20 8:18:00 PM**

Font: (Default) +Body (Times New Roman), 10 pt

▲ **Page 8: [122] Formatted** **Mayes, Melanie A.** **11/17/20 8:18:00 PM**

Font: (Default) +Body (Times New Roman), 10 pt

▲ **Page 8: [123] Formatted** **Mayes, Melanie A.** **11/17/20 8:18:00 PM**

Font: (Default) +Body (Times New Roman), 10 pt

▲ **Page 8: [123] Formatted** **Mayes, Melanie A.** **11/17/20 8:18:00 PM**

Font: (Default) +Body (Times New Roman), 10 pt

Page 8: [123] Formatted	Mayes, Melanie A.	11/17/20 8:18:00 PM
Font: (Default) +Body (Times New Roman), 10 pt		
Page 8: [124] Formatted	Mayes, Melanie A.	11/17/20 8:18:00 PM
Font: (Default) +Body (Times New Roman), 10 pt		
Page 8: [124] Formatted	Mayes, Melanie A.	11/17/20 8:18:00 PM
Font: (Default) +Body (Times New Roman), 10 pt		
Page 8: [124] Formatted	Mayes, Melanie A.	11/17/20 8:18:00 PM
Font: (Default) +Body (Times New Roman), 10 pt		
Page 8: [124] Formatted	Mayes, Melanie A.	11/17/20 8:18:00 PM
Font: (Default) +Body (Times New Roman), 10 pt		
Page 8: [125] Formatted	Mayes, Melanie A.	11/17/20 8:18:00 PM
Font: (Default) +Body (Times New Roman), 10 pt		
Page 8: [125] Formatted	Mayes, Melanie A.	11/17/20 8:18:00 PM
Font: (Default) +Body (Times New Roman), 10 pt		
Page 8: [126] Formatted	Mayes, Melanie A.	11/17/20 8:18:00 PM
Font: (Default) +Body (Times New Roman), 10 pt, Not Italic		
Page 8: [126] Formatted	Mayes, Melanie A.	11/17/20 8:18:00 PM
Font: (Default) +Body (Times New Roman), 10 pt, Not Italic		
Page 8: [126] Formatted	Mayes, Melanie A.	11/17/20 8:18:00 PM
Font: (Default) +Body (Times New Roman), 10 pt, Not Italic		
Page 8: [126] Formatted	Mayes, Melanie A.	11/17/20 8:18:00 PM
Font: (Default) +Body (Times New Roman), 10 pt, Not Italic		
Page 8: [126] Formatted	Mayes, Melanie A.	11/17/20 8:18:00 PM
Font: (Default) +Body (Times New Roman), 10 pt, Not Italic		
Page 8: [126] Formatted	Mayes, Melanie A.	11/17/20 8:18:00 PM
Font: (Default) +Body (Times New Roman), 10 pt, Not Italic		
Page 8: [126] Formatted	Mayes, Melanie A.	11/17/20 8:18:00 PM
Font: (Default) +Body (Times New Roman), 10 pt, Not Italic		
Page 8: [126] Formatted	Mayes, Melanie A.	11/17/20 8:18:00 PM
Font: (Default) +Body (Times New Roman), 10 pt, Not Italic		
Page 8: [127] Formatted	Mayes, Melanie A.	11/17/20 8:18:00 PM
Font: (Default) +Body (Times New Roman), 10 pt		
Page 8: [127] Formatted	Mayes, Melanie A.	11/17/20 8:18:00 PM

Font: (Default) +Body (Times New Roman), 10 pt

▲ **Page 13: [128] Formatted** **Mayes, Melanie A.** **11/17/20 8:18:00 PM**

Font: (Default) +Body (Times New Roman), 10 pt, Not Highlight

▲ **Page 13: [128] Formatted** **Mayes, Melanie A.** **11/17/20 8:18:00 PM**

Font: (Default) +Body (Times New Roman), 10 pt, Not Highlight

▲ **Page 13: [129] Deleted** **Mayes, Melanie A.** **11/15/20 11:12:00 AM**

x

▲ **Page 13: [129] Deleted** **Mayes, Melanie A.** **11/15/20 11:12:00 AM**

x

▲ **Page 13: [130] Formatted** **Mayes, Melanie A.** **11/17/20 8:18:00 PM**

Font: (Default) +Body (Times New Roman), 10 pt, Not Italic

▲ **Page 13: [130] Formatted** **Mayes, Melanie A.** **11/17/20 8:18:00 PM**

Font: (Default) +Body (Times New Roman), 10 pt, Not Italic

▲ **Page 13: [130] Formatted** **Mayes, Melanie A.** **11/17/20 8:18:00 PM**

Font: (Default) +Body (Times New Roman), 10 pt, Not Italic

▲ **Page 13: [130] Formatted** **Mayes, Melanie A.** **11/17/20 8:18:00 PM**

Font: (Default) +Body (Times New Roman), 10 pt, Not Italic

▲ **Page 13: [130] Formatted** **Mayes, Melanie A.** **11/17/20 8:18:00 PM**

Font: (Default) +Body (Times New Roman), 10 pt, Not Italic

▲ **Page 13: [130] Formatted** **Mayes, Melanie A.** **11/17/20 8:18:00 PM**

Font: (Default) +Body (Times New Roman), 10 pt, Not Italic

▲ **Page 13: [130] Formatted** **Mayes, Melanie A.** **11/17/20 8:18:00 PM**

Font: (Default) +Body (Times New Roman), 10 pt, Not Italic

▲ **Page 13: [130] Formatted** **Mayes, Melanie A.** **11/17/20 8:18:00 PM**

Font: (Default) +Body (Times New Roman), 10 pt, Not Italic

▲ **Page 13: [130] Formatted** **Mayes, Melanie A.** **11/17/20 8:18:00 PM**

Font: (Default) +Body (Times New Roman), 10 pt, Not Italic

▲ **Page 13: [130] Formatted** **Mayes, Melanie A.** **11/17/20 8:18:00 PM**

Font: (Default) +Body (Times New Roman), 10 pt, Not Italic

▲ **Page 13: [130] Formatted** **Mayes, Melanie A.** **11/17/20 8:18:00 PM**

Font: (Default) +Body (Times New Roman), 10 pt, Not Italic

▲ **Page 13: [130] Formatted** **Mayes, Melanie A.** **11/17/20 8:18:00 PM**

Font: (Default) +Body (Times New Roman), 10 pt, Not Italic

▲ **Page 13: [130] Formatted** **Mayes, Melanie A.** **11/17/20 8:18:00 PM**

Font: (Default) +Body (Times New Roman), 10 pt, Not Italic

▲ **Page 13: [130] Formatted** **Mayes, Melanie A.** **11/17/20 8:18:00 PM**

Font: (Default) +Body (Times New Roman), 10 pt, Not Italic

▲ **Page 13: [130] Formatted** **Mayes, Melanie A.** **11/17/20 8:18:00 PM**

Font: (Default) +Body (Times New Roman), 10 pt, Not Italic

Font: (Default) +Body (Times New Roman), 10 pt, Not Italic

▲ **Page 13: [130] Formatted** **Mayes, Melanie A.** **11/17/20 8:18:00 PM**

Font: (Default) +Body (Times New Roman), 10 pt, Not Italic

▲ **Page 13: [130] Formatted** **Mayes, Melanie A.** **11/17/20 8:18:00 PM**

Font: (Default) +Body (Times New Roman), 10 pt, Not Italic

▲ **Page 13: [130] Formatted** **Mayes, Melanie A.** **11/17/20 8:18:00 PM**

Font: (Default) +Body (Times New Roman), 10 pt, Not Italic

▲ **Page 13: [130] Formatted** **Mayes, Melanie A.** **11/17/20 8:18:00 PM**

Font: (Default) +Body (Times New Roman), 10 pt, Not Italic

▲ **Page 13: [130] Formatted** **Mayes, Melanie A.** **11/17/20 8:18:00 PM**

Font: (Default) +Body (Times New Roman), 10 pt, Not Italic

▲ **Page 13: [130] Formatted** **Mayes, Melanie A.** **11/17/20 8:18:00 PM**

Font: (Default) +Body (Times New Roman), 10 pt, Not Italic

▲ **Page 13: [130] Formatted** **Mayes, Melanie A.** **11/17/20 8:18:00 PM**

Font: (Default) +Body (Times New Roman), 10 pt, Not Italic

▲ **Page 13: [130] Formatted** **Mayes, Melanie A.** **11/17/20 8:18:00 PM**

Font: (Default) +Body (Times New Roman), 10 pt, Not Italic

▲ **Page 13: [130] Formatted** **Mayes, Melanie A.** **11/17/20 8:18:00 PM**

Font: (Default) +Body (Times New Roman), 10 pt, Not Italic

▲ **Page 13: [130] Formatted** **Mayes, Melanie A.** **11/17/20 8:18:00 PM**

Font: (Default) +Body (Times New Roman), 10 pt, Not Italic

▲ **Page 13: [130] Formatted** **Mayes, Melanie A.** **11/17/20 8:18:00 PM**

Font: (Default) +Body (Times New Roman), 10 pt, Not Italic

▲ **Page 13: [131] Deleted** **Mayes, Melanie A.** **11/15/20 3:53:00 PM**

✖

▲ **Page 13: [131] Deleted** **Mayes, Melanie A.** **11/15/20 3:53:00 PM**

✖

▲ **Page 13: [131] Deleted** **Mayes, Melanie A.** **11/15/20 3:53:00 PM**

✖

▲ **Page 13: [131] Deleted** **Mayes, Melanie A.** **11/15/20 3:53:00 PM**

✖

▲ **Page 23: [132] Deleted** **Mayes, Melanie A.** **11/10/20 2:17:00 PM**

▼